XI. Slovak Biophysical Symposium

Book of Contributions

June 12 – 14, 2024

High Tatras, Slovakia

Slovak Biophysical Society

Institute of Experimental Physics

Slovak Academy of Sciences

Book of Contributions

11th Slovak Biophysical Symposium

June 12 – 14, 2024

High Tatras, Slovakia

ISBN: 978-80-973719-5-1

Book of Contributions, 11th Slovak Biophysical Symposium, June 12 – 14, 2024, High Tatras, Slovakia

Editors: Z. Gažová, A. Antošová, J. Kubacková
Reviewers: M. Fabián, D. Fedunová, D. Jancura, I. Poliaček, J. Staničová
Number of pages: 131

ORGANIZATION

SCIENTIFIC COMMITTEE

RNDr. Andrea Antošová, PhD. (ÚEF SAV, v. v. i. Košice)

doc. Mgr. Gregor Bánó, PhD. (PF UPJŠ Košice)

RNDr. Michal Cagalinec, PhD. (BMC SAV, v. v. i. Bratislava)

doc. RNDr. Zuzana Gažová, DrSc. (ÚEF SAV, v. v. i. Košice)

prof. Alžbeta Marček Chorvátová, DrSc. (UCM FPV Trnava)

doc. RNDr. Katarína Štroffeková, CSc. (PF UPJŠ Košice)

ORGANIZING COMMITTEE

from the Department of Biophysics, Institute of Experimental Physics,
Slovak Academy of Sciences, Košice

RNDr. Andrea Antošová, PhD.

RNDr. Zuzana Bednáriková, PhD.

RNDr. Miroslav Gančár, PhD.

doc. RNDr. Zuzana Gažová, DrSc.

Hanan Abdul Kareem, M. Tech.

RNDr. Jana Kubacková, PhD.

ACKNOWLEDGEMENTS

The Organizing Committee of the 11th Slovak Biophysical Symposium would like to express appreciation and thanks to the following companies for their generous support.

ABL&E-JASCO Hungary Ltd.
Fehérvári út 132-144
H-1116 Budapest
Hungary
https://www.ablelab.eu/

ANAMET s.r.o.
Kováků 3210/26
150 00 Prague 5 – Smíchov
Czech Republic
https://www.anamet.cz/

BIOTECH s.r.o.
Kresánkova 12
841 05 Bratislava
Slovak Republic
https://www.ibiotech.sk/

Merck LifeScience spol.s r.o.
Dvořákovo nábrežie 4
810 06 Bratislava
Slovakia.
https://www.merckgroup.com/

NanoTemper Technologies Sp.z.o.o.
Bobrzynskiego 14
30-348 Krakow
Poland
https://nanotempertech.com/

SPECION, s.r.o.
Květnového vítězství 332/31
149 00 Prague 4 – Chodov
Czech Republic
https://www.specion.cz/

ProScience Tech s.r.o.
Dobšinského 20
811 05 Bratislava
Slovak Republic
https://www.prosciencetech.sk/

Uni-Export Instruments, s.r.o.
Šultysova 15
169 00 Prague 6
Czech Republic
http://uniexport.co.cz/

CONTENTS

Vážené kolegyne a kolegovia,
milé biofyzičky a biofyzici,

v mene Výboru SKBS a organizátorov sympózia Vás srdečne vítame na 11. ročníku sympózia Slovenskej biofyzikálnej spoločnosti v krásnom prostredí Štrbského Plesa vo Vysokých Tatrách, ktoré sme pre vás tentokrát vybrali.

Biofyzika, ako už názov napovedá, je sama osebe interdisciplinárnou vedou, ktorá umožňuje získať významné poznatky v širokom spektre tejto vednej disciplíny s presahom do medicíny, biológie a farmakológie, biotechnológií či materiálového bioinžinierstva. S potešením konštatujeme, že v rámci tohto sympózia budú prezentované výsledky prostredníctvom 15 prednášok a viac ako 25 posterových prezentácií, ktoré pokrývajú takmer celý rozsah biofyzikálneho výskumu - od štúdia funkcií a vlastností rôznych biomakromolekúl až po výučbu biofyziky na univerzitných pracoviskách.

Sme radi, že opäť máme možnosť oceniť našich aktívnych kolegov, Cena SKBS za prínos k rozvoju biofyziky na Slovensku bude udelená A. Zahradníkovej a Cenu SKBS pre mladého vedca do 35 rokov si prevezme A. Hovan.

Rovnako by sme vás chceli pozvať na zasadanie Valného zhromaždenia SKBS, kde prerokujeme aktuálne otázky fungovania našej spoločnosti. S veľkým potešením Vám oznamujeme, že dôležitou súčasťou tohtoročného sympózia bude krst novej publikácie Rozvoj biofyziky na Slovensku, ktorá vďaka úsiliu a obetavosti autorov vychádza práve pri príležitosti storočnice prudkého rozmachu a rozvoja biofyziky a aplikácie biofyzikálnych prístupov v praxi na Slovensku. Veľká vďaka patrí editorom tejto publikácie A. Marček Chorvátovej, M. Klacsovej a I. Zahradníkovi.

Jazykom zborníka ostáva tak ako po iné roky anglický jazyk, aby naše najnovšie poznatky boli prístupné aj našim zahraničným kolegom. Ako jazyk konferencie sme však ponechali jazyk slovenský, aby sme rozvíjali našu odbornú terminológiu. Domnievame sa, že napriek tejto dvojjazyčnosti, sympózium umožní nadviazanie nových spoluprác, nových výskumných zámerov či nových projektov.

Výbor SKBS poveril organizáciou tohto podujatia Zuzanu Gažovú a jej tím z Ústavu experimentálnej fyziky SAV, v. v . i., ktorým patrí poďakovanie za ich úsilie a voľný čas, ktorý príprave podujatia venovali.

Tak ako sa štíty Vysokých Tatier zrkadlia vo vodách Štrbského plesa, prajeme Vám, aby sa účasť na tomto, veríme príjemnom a inšpiratívnom podujatí, odzrkadlila vo Vašich inovatívnych myšlienkach, tvorivom duchu a nových vedeckých výsledkoch.

Dear colleagues,
Dear biophysicists,

On behalf of the SKBS Committee and the symposium organizers, we warmly welcome you to the 11th Symposium of the Slovak Biophysical Society in the beautiful environment of Štrbské Pleso in the High Tatras, which we have selected for you this time.

Biophysics, as the name suggests, is an interdisciplinary science that enables the acquisition of a wide range of significant knowledge overlapping with medicine, biology, pharmacology, biotechnology, and material bioengineering. We are pleased to note that scientific results will be presented through 15 lectures and more than 25 poster presentations, covering almost the entire range of biophysical research - from studying the functions and properties of various biomacromolecules to teaching biophysics at universities.

We are glad that we once again have the opportunity to honor our active colleagues. The SKBS Award for contributions to the development of biophysics in Slovakia will be awarded to A. Zahradníková, and the SKBS Award for a young scientist under 35 years old will be awarded to A. Hovan.

We would also like to invite you to the SKBS General Assembly meeting, where we will discuss current issues regarding the functioning of our society. It is with great pleasure that we announce that an important part of this year's symposium will be the launch of the new publication "Development of Biophysics in Slovakia," which, thanks to the efforts and dedication of the authors, is published precisely on the occasion of the centenary of the rapid growth and development of biophysics and the application of biophysical approaches in Slovakia. Many thanks to the editors of this publication, A. Marček Horvátová, M. Klacsová, and I. Zahradník.

As in other years, the language of the proceedings remains English so that our latest knowledge is accessible to our foreign colleagues. However, we have kept Slovak as the language of the conference to develop our professional terminology. We believe that despite this bilingualism, the symposium will enable the establishment of new collaborations, research intentions, and projects. The SKBS committee entrusted the organization of this event to Zuzana Gažová and her team from the Institute of Experimental Physics SAS, to whom thanks are due for their efforts and the free time they devoted to preparing this event.

Just as the peaks of the High Tatras are reflected in the waters of Štrbské Pleso, we wish your participation in this event, which we believe will be a pleasant and inspiring experience, to be reflected in your innovative ideas, creative spirit, and new scientific results.

SCIENTIFIC PROGRAM

SKBS 2024 PROGRAM

Wednesday, June 12, 2024

12:10 - 14:00	Registration/Lunch	
14:00 - 14:10	Conference opening	
	Chair – M. Cagalinec	
14:10 - 14:55	PL1	G. Žoldák *Frustrations in multidomain proteins*
14:55 - 15:15	CP1	Company presentation, Uniexport – M. Černík *Cutting-edge 3D Raman Imaging in Life Sciences*
15:15 - 15:45	Coffee break	
	Chair - A. Marček Chorvátová	
15:45 - 16:05	CP2	Company presentation, Biotech – J. Uskoba, N. Mirza and R. Marrabini *PROTEIN OLIGOMERIZATION: Characterization of oligomeric state under varying conditions using the same assay in plasma and buffer*
16:05 - 16:45	Flash posters	
16:45 - 18:00	Poster Session I (posters 1 – 15)	
18:10 - 18:15	Welcome drink	
18:15 - 20:00	Dinner	

Thursday, June 13, 2024

7:30 - 9:00	Breakfast	
	Chair - M. Klacsová	
9:00 -9:20	SC1	M. Šimera, M. Veterník, L. Martvoň and I. Poliaček *Relationship between stimulus strength and a magnitude of cough response*
9:20 - 9:40	SC2	D. Beriková, M. Šimera, O.J. Hovengen, M. Veterník, L. Martvoň and I. Poliaček *Limited effect of codeine in the pontine respiratory group*
9:40 - 10:00	SC3	M. Gaburjáková and J. Gaburjáková *Inhibition of a charge-compensating countercurrent during Ca2+ release in the treatment of stress-induced cardiac arrhythmias*
10:00 - 10:20	SC4	K. Ondáčová, K. Polčicová, A. Mišák and Z. Ševčíková Tomášková *Mitochondrial chloride channel: a CLIC or not a CLIC?*
10:20 - 10:50	Coffee break	
	Chair - K. Štroffeková	
10:50 - 11:10	SC5	V. Hovanová, A. Hovan, M.Humeník and E. Sedlák *Analysis of fibrillization mechanism of the recombinant core spidroin eADF4(C16) from Araneus diadematus*
11:10 - 11:30	SC6	A. Antošová, M. Gančár, J. Marek, Z. Gažová *α-lactalbumin amyloid fibrillization in the presence of Hofmeister anions*
11:30 - 11:50	SC7	E. E. Barrera

		In silico peptide design to disable the p53 pathway
11:50 – 12:10	CP3	Company presentation – Nanotemper – P. Wardega and P. Kania *Unlocking Membrane Proteins: Insights into Structure and Interactions with NanoTemper Technologies platforms*
12:10 - 14:00	Lunch	
14:00 - 14:10	SKBS Awards Ceremony	
14:10 - 14:55	AW1	SKBS Awardees' presentation (senior): A. Zahradníková *David and Goliath: the power of small ions to regulate the large channel*
14:55 - 15:15	AW2	SKBS Awardees' presentation (young): A. Hovan, K. Felčíková, Gregor Bánó and E. Sedlák *LOV-domains as genetically encoded photosensitizers and flavin carriers*
15:15 - 15:45	Coffee break	
15:45 - 16:45	General assembly of the SKBS/photo	
16:45 - 18:00	Poster Session II (posters 16 – 30)	
18:10 - 18:15	Book launch (Rozvoj biofyziky na Slovensku)	
19:00 - 22:00	Conference dinner	
	Friday, June 14, 2024	
7:30 - 9:00	Breakfast	
	Chair - D. Jancura	
9:20 - 9:40	SC8	K. Štroffeková and Z. Bednáriková *Comparison of α-synuclein aggregates in non-differentiated and differentiated SH-SY5Y cells treated by rotenone and photobiomodulation*
9:40 - 10:00	SC9	A. Marček Chorvátová, M. Uherek, A. Mateašík and D. Chorvát *Application of microscopy and spectroscopy methods for evaluation of the presence of microplastics in the aquatic environment with living organisms*
10:00 - 10:20	SC10	V. Huntošová, S. Olejárová, C. Slabý, G. Bánó, Z. Jurašeková, T. Vasylyshyn, V. Patsula and D. Horák *Multimodal character of photon-upconverting nanoparticles for bioimaging of glioblastoma*
10:20 - 10:50	Coffee break	
	Chair - G. Bánó	
10:50 - 11:10	SC11	M. Klacsová and D. Uhríková *Effect of Lipid Composition on Interaction of GC376 Antiviral with Membrane Bilayer*
11:10 - 11:30	SC12	J. Staničová, V. Verebová and A. Strejčková *Medical biophysics in the study of medicine and pharmacy*
11:30 - 11:50	SC13	M. Šimera, N. Višňovcová, M. Veterník, J. Misek, O. Králiková, L. Cibulková and I. Poliaček *Teaching of Medical Biophysics at the Jessenius Medical Faculty in Martin*
11:50 - 12:10	Concluding remarks	
12:10 - 14:00	Lunch	

LIST OF AWARDEES' PRESENTATIONS

AW1 **David and Goliath: the power of small ions to regulate the large channel**

A. Zahradníková

Department of Cellular Biophysics, Institute of Experimental Endocrinology, Biomedical Research Center, Slovak Academy of Sciences, Bratislava, Slovakia.

AW2 **LOV-domains as genetically encoded photosensitizers and flavin carriers**

A. Hovan[1], K. Felčíková[1], G. Bánó[1] and E. Sedlák[2]

[1] *Department of Biophysics, Faculty of Science, P. J. Šafárik University in Košice, Slovakia.*

[2] *Center for Interdisciplinary Biosciences, Technology and Innovation Park, P. J. Šafárik University in Košice, Slovakia.*

LIST OF PLENARY LECTURES

PL1 **Frustrations in multidomain proteins**

G. Žoldák

Center for Interdisciplinary Biosciences, Technology and Innovation Park, P. J. Šafárik University in Košice, Slovakia.

LIST OF COMPANY PRESENTATIONS

CP1 **Cutting-edge 3D Raman Imaging in Life Sciences**

I. Lermak[1] and M. Černík[2]

[1] *WITec GmbH, Oxford Instruments Group, Ulm, Germany.*

[2] *Uni-Export Instruments, s.r.o., Prague, Czech Republic.*

CP2 **PROTEIN OLIGOMERIZATION: Characterization of oligomeric state under varying conditions using the same assay in plasma and buffer**

J. Uskoba[1], N. Mirza[2] and R. Marrabini[2]

[1] *BioTech a.s., Prague, Czech Republic.*

[2] *FIDA biosystems ApS, Søborg, Denmark.*

CP3 **Unlocking Membrane Proteins: Insights into Structure and Interactions with NanoTemper Technologies platforms**

P. Wardega and P. Kania

NanoTemper Technologies spzoo, Krakow, Poland.

LIST OF SHORT COMMUNICATIONS

SC1 **Relationship between stimulus strength and a magnitude of cough response**

M. Šimera[1], M. Veterník[1], L. Martvoň[2] and I. Poliaček[1]

[1] *Department of Medical Biophysics, Jessenius Faculty of Medicine in Martin, Comenius University in Bratislava, Slovakia.*

[2] *Medical Education Support Center, Jessenius Faculty of Medicine in Martin, Comenius University in Bratislava, Slovakia.*

SC2 **Limited effect of codeine in the pontine respiratory group**

D. Beriková[1], M. Šimera[1], O.J. Hovengen[1], M. Veterník[1], L. Martvoň[2] and I. Poliaček[1]

[1] *Department of Medical Biophysics, Jessenius Faculty of Medicine in Martin, Comenius University in Bratislava, Slovakia.*

[2] *Medical Education Support Center, Jessenius Faculty of Medicine in Martin, Comenius University in Bratislava, Slovakia.*

SC3 **Inhibition of a charge-compensating countercurrent during Ca^{2+} release in the treatment of stress-induced cardiac arrhythmias**

M. Gaburjáková and J. Gaburjáková

Institute of Molecular Physiology and Genetics, Centre of Biosciences, Slovak Academy of Sciences, Bratislava, Slovakia.

SC4 **Mitochondrial chloride channel: a CLIC or not a CLIC?**

K. Ondáčová[1], K. Polčicová[2], A. Mišák[2] and Z. Ševčíková Tomášková[1]

[1] *Centre of Biosciences, Slovak Academy of Sciences, Bratislava, Slovakia.*

[2] *Biomedical Research Center, Slovak Academy of Sciences, Bratislava, Slovakia.*

SC5 **Analysis of fibrillization mechanism of the recombinant core spidroin eADF4(C16) from Araneus diadematus**

V. Hovanová[1,2], A. Hovan[2], M.Humenik[3] and E. Sedlák[1,4]

[1] *Center for Interdisciplinary Biosciences, Technology and Innovation Park, P. J. Šafárik University in Košice, Slovakia.*

[2] *Department of Biophysics, Faculty of Science, P. J. Šafárik University in Košice, Slovakia.*

[3] *Department of Biomaterials, Faculty of Engineering Science, University of Bayreuth, Germany.*

[4] *Department of Biochemistry, Faculty of Science, P. J. Šafárik University in Košice, Slovakia.*

SC6 **α-lactalbumin amyloid fibrillization in the presence of Hofmeister anions**

A. Antošová, M. Gančár, J. Marek, Z. Gažová

Department of Biophysics, Institute of Experimental Physics, Slovak Academy of Sciences, Košice, Slovakia.

SC7 ***In silico*** **peptide design to disable the p53 pathway**

E. E. Barrera

Institute of Histology and Embryology of Mendoza "Dr. Mario H. Burgos", CONICET – National University of Cuyo, Mendosa, Argentina.

SC8 **Comparison of α-synuclein aggregates in non-differentiated and differentiated SH-SY5Y cells treated by rotenone and photobiomodulation**

K. Štroffeková[1] and Z. Bednáriková[2]

[1] *Department of Biophysics, Institute of Physics, P. J. Šafárik University, Košice, Slovakia.*

[2] *Department of Biophysics, Institute of Experimental Physics, Slovak Academy of Sciences, Košice, Slovakia.*

SC9 **Application of microscopy and spectroscopy methods for evaluation of the presence of microplastics in the aquatic environment with living organisms**

A. Marček Chorvátová[1,2], M. Uherek[1] , A. Mateašík[1] and D. Chorvát[1]

[1] *Department of Biophotonics, International Laser Center SCSTI, Bratislava, Slovakia.*

[2] *Department of Biophysics, FNS, University of Ss Cyril and Methodius in Trnava, Slovakia.*

SC10 **Multimodal character of photon-upconverting nanoparticles for bioimaging of glioblastoma**

V. Huntošová[1,2], S. Olejárová[3], C. Slabý[3], G. Bánó[3], Z. Jurašeková[3], T. Vasylyshyn[4], V. Patsula[4] and D. Horák[4]

[1] *Center for Interdisciplinary Biosciences, Technology and Innovation Park, P. J. Šafárik University in Košice, Slovakia.*

[2] *Institute of Animal Biochemistry and Genetics, Centre of Biosciences, Slovak Academy of Sciences, Bratislava, Slovakia.*

[3] *Department of Biophysics, Faculty of Science, P. J. Šafárik University in Košice, Slovakia.*

[4] *Institute of Macromolecular Chemistry, Czech Academy of Sciences, Prague, Czech Republic.*

SC11 **Effect of Lipid Composition on Interaction of GC376 Antiviral with Membrane Bilayer**

M. Klacsová, D. Uhríková

Department of Physical Chemistry of Drugs, Faculty of Pharmacy, Comenius University in Bratislava, Slovakia.

SC12 **Medical biophysics in the study of medicine and pharmacy**

J. Staničová[1,2], V. Verebová[1] and A. Strejčková[1]

[1] *Department of Chemistry, Biochemistry and Biophysics, University of Veterinary Medicine and Pharmacy, Košice, Slovakia.*

[2] *Institute of Biophysics and Informatics, First Faculty of Medicine, Charles University, Prague, Czech Republic.*

SC13 **Teaching of Medical Biophysics at the Jessenius Medical Faculty in Martin**

M. Šimera, N. Višňovcová, M. Veterník, J. Misek, O. Králiková, L. Cibulková and I. Poliaček

Department of Medical Biophysics, Jessenius Faculty of Medicine in Martin, Comenius University in Bratislava, Slovakia.

LIST OF POSTERS

PO1 **SERS detection of airborne samples**

G. Bánó[1], M. Repovská[2], P. Slepčíková[2], A. Jutková[2], A. Hovan[1] and P. Miškovský[2]

[1] *Department of Biophysics, Faculty of Science, P. J. Šafárik University in Košice, Slovakia.*

[2] *Saftra Photonics s.r.o., Košice Slovakia.*

PO2 **Structural characterization of amyloid fibrils of Tau variants by atomic force microscopy**

Z. Bednáriková[1], O. Cehlár[2], S. Njemoga[2,3] and Z. Gažová[1]

[1] *Department of Biophysics, Institute of Experimental Physics, Slovak Academy of Sciences, Košice, Slovakia.*

[2] *Institute of Neuroimmunology, Slovak Academy of Sciences, Bratislava, Slovakia.*

[3] *Centre of Excellence for Advanced Material Application, Slovak Academy of Sciences, Bratislava, Slovakia.*

PO3 **Cardiac myocyte calcium transient and contractility in treadmill running female Zucker Diabetic Fatty rats**

M. Cagalinec[1,2], I. Baglaeva[1], A. Zahradníková ml.[1], B. Iaparov[1] and A. Zahradníková[1]

[1] *Department of Cellular Cardiology, Institute of Experimental Endocrinology, Biomedical Research Center, Slovak Academy of Sciences, Bratislava, Slovakia.*

[2] *Centre of Excellence for Advanced Material Application, Slovak Academy of Sciences, Bratislava, Slovakia.*

PO4 **Comparison of Mono and Di-gradient Amphiphilic Poly(2-Oxazoline) s as a Drug Delivery System Using Curcumin as a Model Drug**

S. Datta[1], J. Kronek[2], Z. Naďová[3], L. Timuľáková[3], P. Miškovský[1,4]

[1] *Center for Interdisciplinary Biosciences, Technology and Innovation Park, P. J. Šafárik University in Košice, Slovakia.*

[2] *Department for Biomaterials Research, Polymer Institute, Slovak Academy of Sciences, Bratislava, Slovakia.*

[3] *Department of Biophysics, Faculty of Science, P. J. Šafárik University in Košice, Slovakia.*

[4] *SAFTRA Photonics sro., Košice, Slovakia.*

PO5 **Effect of molecular crowding on self-assembly of hybrid protein-DNA conjugates**

V. Fedorová[1], M. Humeník[2] and K. Šipošová[1]

[1] *Department of Biophysics, Institute of Experimental Physics, Slovak Academy of Sciences, Košice, Slovakia.*

[2] *Department of Biomaterials, Faculty of Engineering Science, University of Bayreuth, Germany.*

PO6 **Ionic liquids cations impact on lysozyme properties**

D. Fedunová, V. Vaník and Z. Gažová

Department of Biophysics, Institute of Experimental Physics, Slovak Academy of Sciences, Košice, Slovakia.

PO7 **SERS detection of the herbicide glyphosate in water and milk**

F.B. Fuenzalida[1], D. Jancura[1], P. Miškovský[2,3], S. Sánchez-Cortés[4], Z. Jurašeková[1]

[1] *Department of Biophysics, Faculty of Science, P. J. Šafárik University in Košice, Slovakia.*

[2] *Center for Interdisciplinary Biosciences, Technology and innovation park, P. J. Šafárik University in Košice, Slovakia.*

[3] *SAFTRA Photonics, s.r.o., Košice, Slovakia.*

[4] *Institute of the Structure of Matter, IEM-CSIC, Madrid, Spain.*

PO8 **A strategy to examine 'coupled gating' of cardiac ryanodine receptors by ultrastructural imaging**

J. Gaburjáková, E. Krejčíová, and M. Gaburjáková

Institute of Molecular Physiology and Genetics, Centre of Biosciences, Slovak Academy of Sciences, Bratislava, Slovakia.

PO9 **Interplay of *Origanum vulgare* components in suppressing human insulin amyloid aggregation**

M. Gančár[1], S. Bittner Fialová[2], E. Kurin[2], S. Dokupilová[2], M. Nagy[2], and Z. Gažová[1]

[1] *Department of Biophysics, Institute of Experimental Physics, Slovak Academy of Sciences, Košice, Slovakia.*

[2] *Faculty of Pharmacy, Comenius University in Bratislava, Slovakia.*

PO10 **Antioxidant nanozymes - assessment of ROS absorption potential by CeO2 particles conjugated with activated carbon and magnetite in composite systems**

I. Garčárová[1], M. Drajnová[1,2], Y. Shlapa[3], A. Belous[3], A. Musatov[1], K. Šipošová[1]

[1] *Department of Biophysics, Institute of Experimental Physics, Slovak Academy of Sciences, Košice, Slovakia.*

[2] *Department of Biochemistry, Faculty of Science, P. J. Šafárik University in Košice, Slovakia.*

[3] *V. I. Vernadsky Institute of General & Inorganic Chemistry, NAS of Ukraine, Kyiv, Ukraine.*

PO11 **Involvement of mitochondrial respiratory complexes in hydrogen sulfide utilization**

M. Grman, A. Mišák, K. Ondriáš and L. Tomášová

Biomedical Research Center, Slovak Academy of Sciences, Bratislava, Slovakia.

PO12 **Lithium diminishes the reserve respiratory capacity of cardiac cell line**

M. Grman[1], K. Polčicová[1], K. Ondáčová[2], J. Štepanovský[3], A. Horváth[4], and Z. Ševčíková Tomášková[2]

[1] *Biomedical Research Center, Slovak Academy of Sciences, Bratislava, Slovakia.*

[2] *Centre of Biosciences, Slovak Academy of Sciences, Bratislava, Slovakia.*

[3] *Faculty of Chemical and Food Technology STU, Bratislava, Slovakia.*

[4] *Faculty of Natural Sciences CU, Bratislava, Slovakia.*

PO13 **The impact of ERG6 gene deletion on ergosterol synthesis and phospholipid content in the human pathogen yeast Candida glabrata**

J. Jacko[1], M. Morvová Jr.[1], M. Velísková[1], N. Tóth-Hervay[2], D. Eliaš[2], Y. Gbelská[2], M. Balážová[3] and L. Šikurová[1]

[1] *Department of Nuclear Physics and Biophysics Faculty of Mathematics, Physics and Informatics, Comenius University in Bratislava, Slovakia.*

[2] *Faculty of Natural sciences, Comenius University in Bratislava, Slovakia.*

[3] *Institute of Animal Biochemistry and Genetics, Centre of Biosciences, Slovak Academy of Sciences, Bratislava, Slovakia.*

PO14 **Fabrication of flexible microstructures for biomedical applications**

J. Kubacková[1], C. Slabý[2], Z. Tomori[1] and G. Bánó[2]

[1] *Department of Biophysics, Institute of Experimental Physics, Slovak Academy of Sciences, Košice, Slovakia.*

[2] *Department of Biophysics, Faculty of Science, P. J. Šafárik University in Košice, Slovakia.*

PO15 **Mode of action of quercetin and its derivatives with Ca^{2+}-ATPase – *in silico* study**

M. Májeková, P. Rezbáriková, J. Viskupičová and L. Horáková
Centre of Experimental Medicine, Institute of Experimental Pharmacology and Toxicology, Slovak Academy of Sciences, Bratislava, Slovakia.

PO16 **Determination of tryptophan metabolites in blood and urine of patients with depressive disorder**

D. Masarovičová[1], L. Šikurová[1], I. Mikolášková[2], Ľ. Hunáková[2], B. Kollárik[3] and M. Zvarík[1]
[1] *Department of Nuclear Physics and Biophysics, Faculty of Mathematics, Physics and Informatics, Comenius University in Bratislava, Slovakia.*
[2] *Institute of Immunology, Faculty of Medicine, Comenius University in Bratislava, Slovakia.*
[3] *Department of Urology, Saints Cyril and Methodius Hospital, University Hospital Bratislava, Slovakia.*

PO17 **Allosteric Modulation of 14-3-3 Proteins: Implications for Adipogenesis and Obesity Treatment**

S. Müller[1], L. Rivera[1], L. I. Fontana[1], M. Uhart[1], and D. M. Bustos[1,2]
[1] *Laboratorio de Integración de Señales Celulares, IHEM, CONICET – National University of Cuyo, Mendosa, Argentina.*
[2] *FCEN, National University of Cuyo, Mendoza, Argentina.*

PO18 **Exploration of disordered tau protein's conformational space by metadynamics simulations**

S. Njemoga[1], V. Spiwok[2], E. E. Barrera[3] and O. Cehlár[1]
[1] *Institute of Neuroimmunology, Slovak Academy of Sciences, Bratislava, Slovakia.*
[2] *Department of Biochemistry and Microbiology, University of Chemistry and Technology, Prague, Czech Republic.*
[3] *Institute of Histology and Embryology of Mendoza "Dr. Mario H. Burgos", CONICET – National University of Cuyo, Mendosa, Argentina.*

PO19 **Uncovering the structure of unstructured protein tau and its involvement in aggregation**

A. Polák, S. Njemoga, K. Mešková, O. Cehlár and R. Škrabana
Institute of Neuroimmunology, Slovak Academy of Sciences, Bratislava, Slovakia.

PO20 **Comparison of biophysical properties of selected natural variants of staphylokinase**

M. Štulajterová[1], M. Tomková[2], Ľ. Ambro[2], E. Sedlák[2,3]

[1] *Department of Biophysics, Faculty of Science, P. J. Šafárik University in Košice, Slovakia.*

[2] *Center for Interdisciplinary Biosciences, Technology and Innovation Park, P. J. Šafárik University in Košice, Slovakia.*

[3] *Department of Biochemistry, Faculty of Science, P. J. Šafárik University in Košice,Slovakia.*

PO21 **Multimodal application of polymeric nanoparticles based on poly(2-oxazoline) *in vitro* and *in vivo***

Ľ. Timuľáková[1], S. Datta[2], J. Kronek[3], M. Máčajová[4], J. Levík[4], V. Huntošová[2,4]

[1] *Department of Biophysics, Faculty of Science, P. J. Šafárik University in Košice, Slovakia.*

[2] *Center for Interdisciplinary Biosciences, Technology and Innovation Park, P. J. Šafárik University in Košice, Slovakia.*

[3] *Department for Biomaterials Research, Polymer Institute, Slovak Academy of Sciences, Bratislava, Slovakia.*

[4] *Institute of Animal Biochemistry and Genetics, Centre of Biosciences, Slovak Academy of Sciences, Bratislava, Slovakia.*

PO22 **Determination of the lifetime of radical in the P-type ferryl intermediate of cytochrome c oxidase**

A. Tomková[1], M. Fabián[2], D. Jancura[1]

[1] *Department of Biophysics, Faculty of Science, P. J. Šafárik University in Košice, Slovakia.*

[2] *Center for Interdisciplinary Biosciences, Technology and Innovation Park, P. J. Šafárik University in Košice, Slovakia.*

PO23 **Raman and SERS microspectroscopy studies on DNA and cells**

B. G. Varchol[1], D. Horváth[2], V. Huntošová[2], Z. Jurašeková[1]

[1] *Department of Biophysics, Faculty of Science, P. J. Šafárik University in Košice, Slovakia.*

[2] *Center for Interdisciplinary Biosciences, Technology and Innovation Park, P. J. Šafárik University in Košice, Slovakia.*

PO24 **Incorporation of the conazole fungicide epoxiconazole into the DNA monitored by thermodynamic and hydrodynamic methods**

V. Verebová[1], J. Staničová[1,2]

[1] *Department of Chemistry, Biochemistry and Biophysics, University of Veterinary Medicine and Pharmacy, Košice, Slovakia.*

[2] *Institute of Biophysics and Informatics, First Faculty of Medicine, Charles University, Prague, Czech Republic.*

PO25 **Allosteric inactivation of the ryanodine receptor channel**

I. Zahradník, J. Pavelková, and A. Zahradníková

Department of Cellular Cardiology, Institute of Experimental Endocrinology, Biomedical Research Center, Slovak Academy of Sciences, Bratislava, Slovakia.

PO26 **Application of Raman microspectroscopy for the chemical analysis of fossilized tissues of the gigantic theropod Deinocheirus mirificus**

G. Fabriciová[1], Z. Jurašeková[1] and M. Kundrát[2]

[1] *Department of Biophysics, Faculty of Science, P. J. Šafárik University in Košice, Slovakia.*

[2] *Center for Interdisciplinary Biosciences, Technology and Innovation Park, P. J. Šafárik University in Košice, Slovakia.*

PO27 **Insulin Amyloid Aggregation: Effect of protein concentration**

H. Kareem Abdul, Z. Bednáriková and Z. Gažová

Department of Biophysics, Institute of Experimental Physics, Slovak Academy of Sciences, Košice, Slovakia

PO28 **“Information not provided."**

P. Mydla

Department of Nuclear Physics and Biophysics Faculty of Mathematics, Physics and Informatics, Comenius University in Bratislava, Slovakia.

PO29 ***In silico*** **peptide design to disable the p53 pathway**

E. E. Barrera

Institute of Histology and Embryology of Mendoza “Dr. Mario H. Burgos”, CONICET – National University of Cuyo, Mendosa, Argentina.

AWARDEES' PRESENTATIONS

David and Goliath: the power of small ions to regulate the large channel

A. Zahradníková

Department of Cellular Biophysics, Institute of Experimental Endocrinology, Biomedical Research Center, Slovak Academy of Sciences, Dúbravská cesta 9, 845 05 Bratislava, Slovakia.

e-mail: alexandra.zahradnikova@savba.sk

The ryanodine receptor protein was discovered and hypothesized to play a role in excitation-contraction coupling in 1984 [1]. Its identity with the well-known "junctional feet" of the terminal cisternae of the sarcoplasmic reticulum [2], intensively studied also in our institute [3], was soon confirmed [4] (Fig. 1). From the beginning it was clear that this is an ion channel regulated in a complex fashion by Ca^{2+} and Mg^{2+} ions, with differences between the cardiac muscle RyR2 and the skeletal muscle RyR1 [1]. Soon, when life-threatening RyR mutations were discovered, the importance of the correct function of this channel for life was recognized in RyR1 [5] and somewhat later also in RyR2 [6].

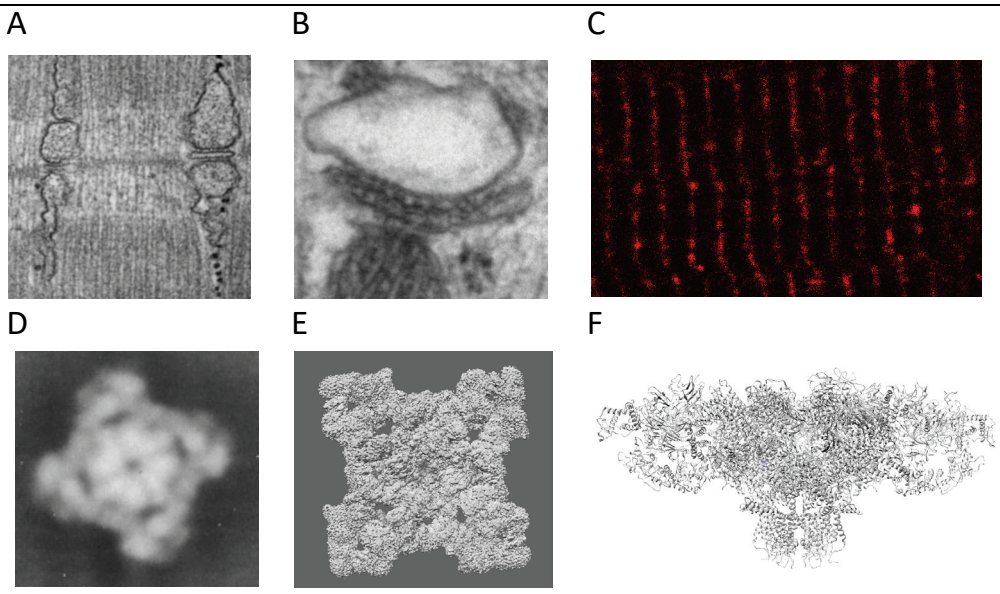

Fig. 1. RyRs *in situ* and their structure. A – Triads of the frog twitch muscle [2]. B – A rat cardiac dyad (M. Novotova, unpublished). C – Immunostaining of RyR2 channels in rat cardiac myocyte (A. Zahradnikova Jr., unpublished). D – Electron micrograph of negatively stained skeletal RyR1 [4]. E – CryoEM map of rabbit RyR1 (EMD-25828). F - Structure of rabbit RyR1 (PDB-7tdg).

My interest in RyR function started in 1989 at UTMB Galveston, where I was entrusted with building a planar lipid bilayer setup for studying RyR single-channel gating. At that time, RyR quickly became a hot topic, studied by different laboratories with many different methods – as its single-channel activity, as calcium fluxes from SR vesicles, biochemically as [^{3}H]-ryanodine binding, and in the cell as calcium transients, sparks and spikes (Fig. 2); however, the results were not fully consistent due to different time scales of measurements and differences in experimental conditions. We showed that part of the problem is in the varying ion conductance in some experiments [7]. Later, we were interested in the regulation of RyRs by Ca^{2+} ions for their key role in cardiac excitation-contraction coupling. This endeavor was demanding due to the coexistence of very slow and very

rapid processes inherent to RyR gating [8-10]. The tetrameric structure of the RyR channel called for 4 calcium activation sites. To confirm it we studied RyR responses to brief changes of Ca^{2+} concentration in the micromolar range, using flash photolysis of a calcium chelator [11]. The results, together with literature data on the activity of RyRs mutated in the calcium-binding region, enabled us to develop the first models of allosteric regulation of RyR2 activation by Ca^{2+} and Mg^{2+} in the isolated channel [12]. We have also shown that activation-enhancing RyR mutations can increase the formation of diastolic Ca sparks and contribute to the formation of arrhythmogenic Ca waves [13, 14].

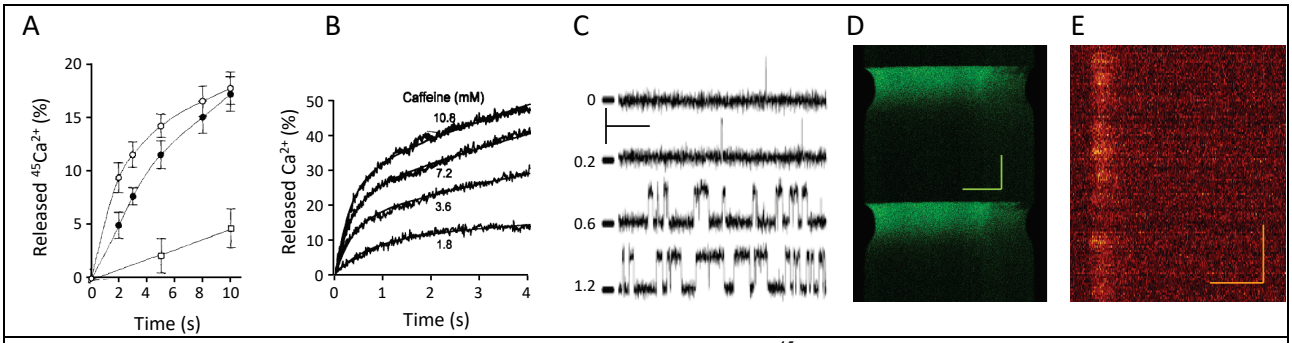

Fig. 2. Direct and indirect measurement of RyR activity. A – Passive ^{45}Ca fluxes through RyR2 [15]. B – Caffeine-induced Ca^{2+} release through RyR1 [16]. C – Single-channel activity of rat RyR2 channels at different ATP concentrations [17], calibration 1pA/250ms. D – Calcium transients in contracting rat cardiac myocyte. I. Baglaeva, unpublished, calibration 250ms/25 µm. E – Calcium spikes in rat cardiac myocytes [18], calibration 5 µm/250ms.

Our studies helped to understand the importance of RyR2 inhibition by cytosolic Mg^{2+} ions in the regulation of RyR activity in health and disease [13, 19, 20]. With the advent of new cryoEM technologies, many structures of RyR1 and RyR2 at a variety of conditions became available. Bioinformatic analysis of these structures [21] allowed us to reveal that: (1) the putative inhibition site has a different structure in RyR1 and RyR2; (2) there is a common allosteric path in the activation/inhibition pathways, which passes through the binding site for the RyR activator ATP. These findings allowed us to postulate a model of RyR regulation by divalent ions and explain the major difference in RyR1 and RyR2 function.

This hypothesis would be difficult to prove experimentally. Therefore, we intend to employ molecular dynamics simulations and combine them with quantitative modelling of RyR function.

Acknowledgment

I would like to acknowledge the colleagues and students without whom this work would not be possible: I. Zahradník, M. Novotová, M. Cagalinec, J. Pavelková, A. Zahradníková Jr. (IMPG and BRC SAS, Bratislava), P. Palade (UTMB Galveston, TX), S. and I. Györke (TTU HSC Lubbock, TX and OSU, Columbus, OH), A. Escobar (TTU HSC Lubbock, TX), L. Mészáros (MCG, Augusta, GA), E. Poláková, M. Dura, I. Valent, E. Cocherová, R. Janíček, M. and J. Gaburjáková, B. Tencerová, A. Faltínová (IMPG SAS, Bratislava), B. Iaparov and I. Baglaeva (BRC SAS, Bratislava), and J. Ševčák, V. Bauerová-Hlinková, J. Bauer, Ľ. Borko, E. Hostinová. and J. Gašperík (IMB SAS, Bratislava).

I am also thankful to all the organizations that contributed to the funding of my research: Howard Hughes Medical Institute, Fulbright Commission, National Institutes of Health, the 6th Framework Program of the European Commission, Slovak Research and Development Agency, The Scientific Grant Agency of the SAS, and the JRP SAS – TUBITAK program.

This work was supported by the project APVV-21-0473 from the Slovak Research and Development Agency.

References

[1] I. N. Pessah, A. L. Waterhouse, J. E. Casida, Biochem. Biophys. Res. Commun., 128 (1984), 449-56.
[2] C. Franzini-Armstrong, J. Cell. Biol., 47 (1970), 488-99.
[3] M. Novotová, B. Uhrík, D. Zacharová, Physiol. Bohemoslov., 33 (1984), 550.
[4] A. Saito; et al, J. Cell. Biol., 107 (1988), 211-9.
[5] J. R. Mickelson; et al, J. Biol. Chem., 263 (1988), 9310-5.
[6] S. G. Priori; et al, Circulation., 103 (2001), 196-200.
[7] A. Zahradníková, I. Zahradník, Biochim. Biophys. Acta., 1418 (1999), 268-84.
[8] A. Zahradníková, I. Zahradník, Biophys. J., 69 (1995), 1780-8.
[9] A. Zahradníková, I. Zahradník, Biophys. J., 71 (1996), 2996-3012.
[10] A. Zahradníková, B. Iaparov, I. Zahradník, Prog. Biophys. Mol. Biol., 157 (2020), 94-106.
[11] A. Zahradníková; et al, J. Gen. Physiol., 114 (1999), 787-98.
[12] I. Zahradník, S. Györke, A. Zahradníková, J. Gen. Physiol., 126 (2005), 515-27.
[13] A. Zahradníková, I. Valent, I. Zahradník, J. Gen. Physiol., 136 (2010), 101-16.
[14] P. Petrovič; et al, J. Gen. Physiol., 145 (2015), 489-511.
[15] A. Zahradníková, J. Bak, L. G. Mészáros. Biochem Biophys Res Commun., 16 (1995), 457-63.
[16] L. G. Mészáros, A. Zahradnikova, P. Volpe., Cell Calcium, 23 (1998), 43-52.
[17] B. Tencerová; et al, J. Gen. Physiol., 140 (2012), 93-108.
[18] A. Zahradníková, Jr.; et al, J. Physiol., 578 (2007), 677-91.
[19] A. Zahradníková; et al, Am. J. Physiol. Cell. Physiol., 285 (2003), C1059-70.
[20] B. Iaparov, et al; Front. Physiol., 12 (2022), 805956.
[21] I. Zahradník, B. Iaparov, A. Zahradníková, this meeting.

11th Slovak Biophysical Symposium, High Tatras, June 12 – 14, 2024

LOV-domains as genetically encoded photosensitizers and flavin carriers

A. Hovan[1], K. Felčíková[1], Gregor Bánó[1] and E. Sedlák[2]

[1] Department of Biophysics, Faculty of Science, P. J. Šafárik University in Košice, Jesenná 5, 041 54 Košice, Slovakia.
[2] Center for Interdisciplinary Biosciences, Technology and Innovation Park, P. J. Šafárik University in Košice, Jesenná 5, 041 54 Košice, Slovakia.

e-mail: andrej.hovan@upjs.sk

Over the last decade, flavin-containing Light-Oxygen-Voltage (LOV) domains have undergone extensive modification and study as singlet oxygen generators [1-6]. Singlet oxygen, the lowest electronic excited state of molecular oxygen, is primarily known for its crucial role in cancer photodynamic therapy, possessing oxidative properties and belonging to the reactive oxygen species. Engineering of LOV domains has led to multiple improvements in singlet oxygen production quantum yield [3], and in some cases, revealed the potential of LOV domains as flavin carriers [7].

Building upon our previous work [7], we aimed to improve LOV-based flavoproteins as flavin carriers with the capability of irradiation-induced release. Reducing amount of light necessary to release a higher amount of flavin, specifically FMN, was the main objective. The primary advantage of flavin carriers over genetically encoded photosensitizers is spatial selectivity. Only in the irradiated space would the flavin cofactor be released, significantly enhancing singlet oxygen production quantum yield and inducing higher levels of oxidative stress.

In our studies, time-resolved singlet oxygen phosphorescence detection, coupled with transient absorption measurements, were employed to study the irradiation dependence of flavin release from the protein matrix. Additionally, fluorescence spectroscopy was used to further elucidate the observed results.

We examined three new mutant variants of AsLOV2 (LOV2 domain from *Avena sativa*) with carefully selected mutation sites (V416C, T418C, V416C/T418C), deducing the amount and rate of flavin release. The efficiency of irradiation-induced FMN dissociation strongly correlated with singlet oxygen production in all cases. Each of the protein variants behaved slightly different, allowing us to examine the effect of individual mutations. The best-performing mutant, in terms of faster flavin release (V416C/T418C) can serve as a new template for further tuning.

Our proof-of-principle study demonstrates the possibility of changing the rate of cofactor release by introducing point mutations in specific regions proximal to the isoalloxazine ring of flavin. This approach enabled us to develop protein variants which release the carried molecule faster to the surrounding media, reducing the amount of light necessary to stimulate this process.

Acknowledgement
This work was supported by the Slovak Research and Development Agency (project APVV-20-0340). Special thanks are given to Carlos Diaz, Veronika Holotová and Ľuboš Ambro for their invaluable contributions to protein expression and purification.

References

[1] J. Torra; et al., Scientific Reports, 9 (2019), 2428.
[2] S. Endres; et al., Scientific Reports, 8 (2018), 15021.
[3] M. Westberg, M. Bregnhoj, M. Etzerodt, and P. R. Ogilby, Journal of Physical Chemistry B, 121(12) (2017), 2561-2574.
[4] F. M. Pimenta, R. L. Jensen, T. Breitenbach, M. Etzerodt, and P. R. Ogilby, Photochemistry and Photobiology, 89(5) (2013), 1116-1126.
[5] R. Ruiz-Gonzalez, A. L. Cortajarena, S. H. Mejias, M. Agut, S. Nonell, and C. Flors, Journal of the American Chemical Society, 135(26) (2013), 9564-9567.
[6] X. K. Shu; et al., Plos. Biology, 9(4) (2011).
[7] M. Petrencakova; et al., Scientific Reports, 10(1) (2020), 4119.

PLENARY LECTURES

11th Slovak Biophysical Symposium, High Tatras, June 12 – 14, 2024

Frustrations in multidomain proteins

G. Žoldák

Centrum interdisciplinárnych biovied, Technologický a inovačný park Univerzita P. J. Šafárika, Trieda SNP 1, 040 11 Košice, Slovensko.

e-mail: gabriel.zoldak@upjs.sk

Certain proteins, such as translation factors, need to function effectively within highly different microenvironments, such as ribosome and cytoplasm in this example. These varying environmental contexts pose unique stability challenges, which are natural part of the evolutionary process. In my recent analysis, I examine the hypothesis that understanding frustration within and among protein domains can shed light on the underlying mechanisms that govern protein stability and functionality across various operational microenvironments. The contact frustration is often overseen due to involvement of other multiple molecular factors and the role, if any, is unclear.

A detailed frustration analysis was performed by implementing the stand-alone frustration analysis R-package (https://github.com/proteinphysiologylab/frustratometeR) [1-3]. This approach classifies individual contacts by their frustration index values, distinguishing between contacts that are comparatively unfavorable ("highly frustrated") and those that are relatively favorable ("minimally frustrated") against the backdrop of potential alternatives within the same locale. Contacts not clearly fitting these extremes are deemed "neutral." Minimally frustrated contacts, characterized by native energy at the lower spectrum of decoy energies, suggest that alternative amino acid pairings in the same position might be less conducive to proper folding. Conversely, highly frustrated contacts, with native energy on the higher end, indicate that most alternative pairings would be more favorable for folding. The "frustration index" (F_{ij}) for a given contact i, j is defined as a Z-score of the energy of the native pair compared to the N generated decoys [1-3]:

$$F_{ij} = \left(H_{ij}^{N} - \langle H_{ij}^{U} \rangle\right) / \sqrt{1/N \sum \left(H_{ij}^{U} - \langle H_{ij}^{U} \rangle\right)^2}$$

where H^N is native energy, H^U is the energy of the decoy. The frustration index measures of how favorable a particular interaction is relative to the set of all possible interactions in that location, normalized using the variance of that distribution.

The presence of highly frustrated contacts between domains can signal potential issues for protein cooperativity and functionality, possibly leading to localized conformational events. By identifying these critical contacts, the analysis deepens our understanding of the structural and functional relationship of several proteins including IF2 [4]. The investigation highlights the significance of frustration analysis, especially for proteins operating in extreme conditions or those designed to function in varied environments. I speculate that this concept can be applied in the misfolding of pathological proteins as the interplay of intrinsic aggregation propensity of the given local sequence.

Acknowledgement
This work was supported by the research grant from the grant provided by the Slovak Grant Agency VEGA No 1/0024/22.

References

[1] M. Jenik, R. G. Parra, L. G. Radusky, A. Turjanski, P. G. Wolynes, D. U. Ferreiro, Nucleic Acids Research, 40 (2012), W348–W351.
[2] R. G. Parra, N. P. Schafer, L. G. Radusky, M. Y. Tsai, A. B. Guzovsky, P. G. Wolynes, D. U. Ferreiro, Nucleic Acids Res., 44 (2016), W356-60.
[3] A. O. Rausch, M. I. Freiberger, C. O. Leonetti, D. M. Luna, L. G. Radusky, P. G. Wolynes, D. U. Ferreiro, R. G. Parra, FrustratometeR: Bioinformatics., 37 (2021), 3038-3040.
[4] V. Džupponová, N. Tomášková, A. Antošová, E. Sedlák, G. Žoldák, Int. J. Mol. Sci., 24 (2023), 6787.

SHORT COMMUNICATIONS

11th Slovak Biophysical Symposium, High Tatras, June 12 – 14, 2024

Relationship between stimulus strength and a magnitude of cough response

M. Simera[1], M. Veternik[1], L. Martvon[2] and I. Poliacek[1]

[1] *Department of Medical Biophysics, Jessenius Faculty of Medicine in Martin, Comenius University in Bratislava, Martin, Slovakia.*
[2] *Medical Education Support Center, Jessenius Faculty of Medicine in Martin, Comenius University in Bratislava, Martin, Slovakia.*

e-mail: michal.simera@uniba.sk

Coughing is an important airway defensive reflex during which, foreign bodies are expelled from the throat, larynx, and trachea through the oral cavity [1]. Vagal afferents play an important role in evoking cough in response to the mechanical and chemical stimulation of the airways [2]. The afferent pathways for cough comprise vagus nerve fibers arising from two main groups of sensory nerve endings [3]: mechano- and acid-sensing cough receptors, represented by Aδ nodose fibers, and chemosensitive nociceptive-like free endings of jugular C-fibers. Impulses travel via the vagus nerve to cough neuronal circuits in the medulla where the central encoding of the cough reflex is executed.

The cough reflex is not immutable rather undergoes plasticity due to changes in the neural pathways regulating cough. The number of active units, the frequency of action potentials, the synaptic efficacy, and the duration of activation all contribute to the integration of the reflex [4].

Our study aimed to investigate the cough characteristics during mechanically stimulated trachea including separate stimulation of the upper and lower part of it employing different speed/strength stimulation techniques.

Experiments were performed on 15 spontaneously breathing male cats anesthetized with sodium pentobarbital. The intrathoracic pressure (esophageal pressure EP) was measured with a soft balloon inserted into the esophagus. Bipolar fine wire hook electrodes were placed in the sternal diaphragm (DIA), bilaterally in the transversus abdominis (ABD), or the external oblique abdominal muscles for EMG recordings. Cough was defined by a large burst of inspiratory-related DIA EMG activity, immediately followed by a burst of expiratory ABD EMG activity, and by a related negative to positive EP swing. During the cough, temporal and spatial cough characteristics were analyzed such as EMG amplitudes, duration of cough cycle; duration of cough inspiratory and expiratory phase etc.

Mechanical stimulation of the trachea was made by back and forth motions lasting approximately 8s with 1) soft catheter - “weak” stimulation by one, “strong” stimulation by 4 penetrations, or 2) the catheter equipped (sealed) across with short fine nylon fibers - “weak” stimulus by 2 penetration using a stimulator with 4 fibers, and “strong” stimulation by 4 penetrations with the stimulator with 8 fibers, and 3) the stimulator with “cross” fibers on upper and separately lower 4 cm part of the trachea - “weak” stimulus vs. stimulation of both segments together - “strong” stimulus.

Our results showed that the “strong” mechanical stimulations resulted in a higher number of coughs and higher inspiratory and expiratory cough efforts. However, the majority of cough temporal characteristics were shortened, in particular the latency to the first cough, the duration of cough inspiratory and expiratory phase, total cough cycle duration, and distance between peak inspiratory and expiratory activity.

Stimulation of tracheal cough mechanoreceptors in cats with different paces, “strengths” and areas of stimulation revealed that stronger stimulus induces stronger cough response with altered cough motor pattern. The changes in spatial and shortening of the temporal cough features are disproportional, however, with some relations among spatial and temporal cough characteristics. The cough reflex can be modified by changing the quantity, intensity, and location of the sensory input that triggers the cough response.

Acknowledgment
This work was supported by VEGA 1/0092/20.

References

[1] Cough and Other Respiratory Reflexes. Korpas and Tomori (Eds.), Kager, Basel (1979).
[2] B. J. Canning, N. Mori, S. B. Mazzone, Respir. Physiol. Neurobiol., 152(3) (2006), 223-242.
[3] J. G. Widdicombe, Eur. Respir. J., 8(7) (1995), 1193-202.
[4] B. J. Canning, Pulm. Pharmacol. Ther., 20(4) (2007), 396-401.

11th Slovak Biophysical Symposium, High Tatras, June 12 – 14, 2024

Limited effect of codeine in the pontine respiratory group

D. Beriková[1], M. Šimera[1], O.J. Hovengen[1], M. Veterník[1], L. Martvoň[2] and I. Poliaček[1]

[1] *Department of medical biophysics, Jessenius faculty of medicine in Martin, Comenius University Bratislava; Malá Hora 4; 036 01 Martin, Slovakia.*
[2] *Medical Education Support Center, Jessenius Faculty of Medicine in Martin, Comenius University in Bratislava, L. Novomeskeho 7A, 03601 Martin, Slovakia.*

e-mail: berikova3@uniba.sk

The Kölliker-Fuse (KF) nuclei and adjacent lateral and medial parabrachial (PB) complex are parts of the pontine respiratory group (PRG) also known as pneumotaxic centre. PRG is composed of a heterogeneous population of respiratory neurons essential for control of respiratory rate, pattern, and rhythm [1, 2]. The lateral PB is responsible for an inspiratory facilitatory influence, and the medial PB and KF control expiratory facilitatory response [3]. The neurons of PRG are functionally connected via excitatory projections to respiratory nuclei in some other parts of the CNS, such as the ventrolateral medulla including the Bötzinger complex, the preBötzinger complex, and the rostral ventral respiratory group [4, 5]. This connection is essential for optimized respiratory output [6, 7] as well as the cough reflex control.

This study aimed to analyze spatio-temporal parameters of mechanically induced tracheobronchial cough after unilateral codeine microinjections in the pontine respiratory group in anesthetized cats.

The experiments were performed on 12 anesthetized non-paralyzed male cats (4.13 ± 0.24 kg). The electromyograms (EMGs) were recorded by bipolar insulated wire hook electrodes bilaterally from the diaphragm (DIA) and expiratory transversus abdominis and/or external oblique abdominal (ABD) muscles. Esophageal pressure (EP), blood pressure (BP), and respiratory parameters were recorded and analyzed as well. Craniectomy and partial cerebellectomy were performed with cats placed in a prone position in a stereotaxic frame. The cough reflex was induced mechanically through the cannula in the trachea. The stimulations were provided by the same person using a soft polyethylene fiber going back and forth 4-5 times in duration of 10 seconds. 24 microinjections of 3 mM codeine (total volume 37 ± 1.2 nl; micro-pipette diameter 26.6 ± 4.5 μm) were injected into the KF and PB complex in 8 anesthetized cats. 18 comparable microinjections of artificial cerebrospinal fluid (aCSF) were performed in 6 cats (59 ± 26.2 nl total volume, tip diameter 36 ± 4.0 μm) as well. The EMGs were filtered, amplified, rectified, and integrated and also recorded along with EP and BP waveforms. The number of cough efforts (CN) induced during tracheal mechanical stimulation (average CN per 10-second duration during trial), the ABD and DIA EMG amplitudes, and the amplitudes of EP during the applicable cough phases were evaluated.

Codeine microinjections into the PRG did not decrease the number of coughs (from 4.5 ± 0.6 to 4.4 ± 0.7; $p > 0.05$), which recovered to 4.8 ± 0.6 after 43 minutes). There were no significant changes in cough temporal parameters. However, we observed a significant reduction of the cough ABD EMG amplitudes and expiratory EP. A slight but statistically significant reduction was found in DIA EMG amplitudes together with a non-significant reduction in inspiratory EP amplitudes during cough. Control microinjections of artificial CSF in 6 cats showed no significant effect on cough data in comparison with those after codeine microinjections.

Our results show that the involvement of PRG neurons in the antitussive activity of codeine is limited and just the excitatory drive to the other parts of the brainstem were suppressed by the codeine microinjections.

Acknowledgement
This work was supported by grants VEGA 1/0072/16; VEGA 1/0275/19; VEGA 1/0092/20.

References

[1] A. A. Navarrete-Opazo, D. R. Cook-Snyder, J. R. Miller, J. J Callison, N. McCarth, B. Palkovic, E. A. E. Stuth, E. J. Zuperku, A. G. Stucke, Respiratory Physiology & Neurobiology, 277 (2020), 1-12.
[2] S. E. Saunders, E. S. Levitt, Respiratory Physiology & Neurobiology, 275 (2020), 1-12.
[3] K. M. Spyer, Experimental physiology, 94.1 (2009), 1-10.
[4] C. F. Yang, E. J. Kim, E. M. Callaway, J. L. Feldman, Frontiers in Neuroanatomy, 14(58) (2020), 1-11.
[5] J. C. Geerling, S. Yokota, I. Rukhadze, D. Roe, N. L. Chamberlin, The Journal of Comparative Neurology (2017), 44-98.
[6] M. Dutschmann, T. E. Dick, Comprehensive Physiology, 2 (2012), 2443-2469.
[7] J. C. Smith, A. P. Abdala, H. Koizumi, I. A. Rybak, J. F. Paton, J. Neurophysiol, 98 (2007), 3370-3387.

Inhibition of a charge-compensating countercurrent during Ca^{2+} release in the treatment of stress-induced cardiac arrhythmias

M. Gaburjáková and J. Gaburjáková

Institute of Molecular Physiology and Genetics, Centre of Biosciences, Slovak Academy of Sciences, Dúbravská cesta 9, 840 05 Bratislava, Slovakia.

e-mail: marta.gaburjakova@savba.sk

In cardiac ventricular muscle, the activated ryanodine receptor (RyR2) plays a fundamental role in the massive release of Ca^{2+} ions from the sarcoplasmic reticulum (SR) into the cytosol that is required to trigger muscle contraction during systole. In diastole, cardiac ventricular muscle relaxes as cytosolic Ca^{2+} falls due to a decline in RyR2 activity and Ca^{2+} pumping back in the SR. Maintaining the RyR2 channel in a low-activity state during diastole is critical because even a small increase in resting cytosolic Ca^{2+} can have major consequences for normal cardiac function. Indeed, it has been suggested that increased diastolic Ca^{2+} leak through the RyR2 channel harboring a heterozygous mutation is mainly implicated in a life-threatening, stress-induced arrhythmogenic disease (CPVT) [1, 2]. In clinical studies, arrhythmias in CPVT patients were effectively suppressed by the class 1C antiarrhythmic agent flecainide when used as a monotherapy or in combination with conventional treatment with β-blockers [3]. While flecainide is regarded as the standard of care for treating CPVT patients, the molecular mechanism underlying its therapeutic action remains controversial [4]. Flecainide is a well-characterized inhibitor of the surface-membrane Na^{+} channel [5]; concurrently, it also possesses the potency to inhibit the RyR2 channel [4, 6, 7, 8, 9]. The collective data, however, indicate that flecainide only inhibits RyR2 activity when the ionic flux via the RyR2 pore is in the opposite direction (from cytosol to lumen) compared to physiological Ca^{2+} release from the SR. Thus, initially, this flecainide`s action was claimed to be not therapeutically relevant [8, 9]. Later, this statement was revisited because it has been proposed that the RyR2 channel is able to carry its own charge-compensating countercurrent in the cytosol-to-lumen direction, and a reduction of this current may indeed result in a compromised Ca^{2+} release [10].

Utilizing a unique experimental approach, we examined whether the primary action of flecainide on the RyR2 channel involves reducing the RyR2-mediated countercurrent in the cytosol-to-lumen direction. In addition, we applied flecainide to the SR Cl^{-} channel because it could also contribute to conducting a charge-compensating countercurrent.

RyR2 and Cl^{-} channels isolated from ventricles of the rat heart [11] were incorporated into planar lipid membranes (BLMs) and examined under voltage-clamp conditions as described in [12]. The RyR2 and Cl^{-} channels were found in the same membrane fraction; therefore, it is reasonable to assume that recorded Cl^{-} channels co-localized with RyR2 channels in the SR membrane. Flecainide was added to the cytosolic face of the ATP-activated RyR2 channel in a dose-dependent manner while Ba^{2+}/Ca^{2+} current flowed via the channel pore from lumen to cytosol, and the countercurrent carried by monovalent cations was in the opposite direction. These conditions more closely mimic the cell situation. In the control group, the countercurrent decreased the amplitude of Ba^{2+}/Ca^{2+} current, leading to decreased RyR2 conductance. When flecainide was added, the countercurrent was reduced,

resulting in an increase in the Ba^{2+}/Ca^{2+} current flowing in the opposite direction. The RyR2 conductance changed in a similar fashion. Notably, overall RyR2 activity analyzed as open probability was not affected by flecainide. In agreement with other studies [6, 8, 9], flecainide did not cause any change in RyR2 activity or the channel conductance when the countercurrent was omitted. Similarly, flecainide did not decrease the activity of the Cl^- channel or change their conducting properties when Cl^- movement via the channel pore was driven by the Cl^- gradient across the BLM.

We demonstrate that flecainide substantially reduced the RyR2-mediated countercurrent without changing the channel activity. Notably, this occurred when the Ba^{2+}/Ca^{2+} current flowing in the physiologically relevant direction was present. The alternative source of the charge-compensating countercurrent, such as the SR Cl^- channel, showed a complete resistance to flecainide. Based on this, it is not unreasonable to propose that the primary intracellular target of flecainide *in vivo* is indeed the RyR2-mediated countercurrent (Fig. 1).

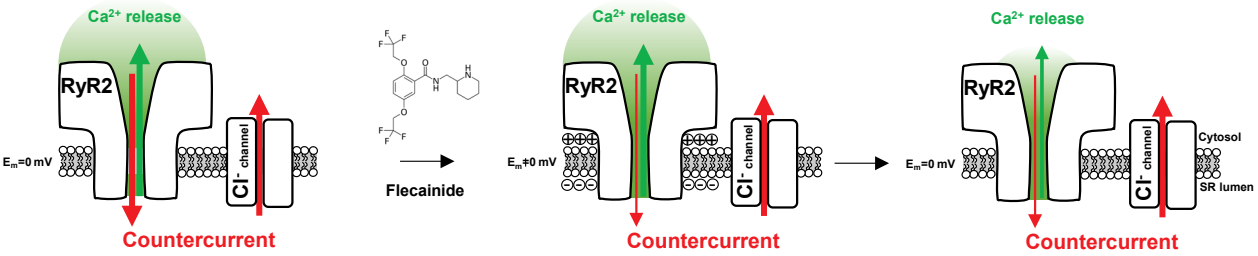

Fig. 1. A schematic illustrating the potential molecular mechanism of flecainide`s action in CPVT with respect to the charge-compensating countercurrent across the SR membrane during Ca^{2+} release.

Acknowledgement
This work was supported by VEGA 2/0018/21 and APVV-22-0061.

References

[1] D. Jiang, B. Xiao, L. Zhang and S. R. W. Chen, Circulation Research, 91 (2002), 218-225.
[2] D. H. MacLennan and S. R. Chen, Journal of Physiology, 587 (2009), 3113-3115.
[3] A. Khoury, I. Marai, M. Suleiman, M. Blich, A. Lorber, L. Gepstein and M. Boulos, Heart Rhythm, 10 (2013), 1671-675.
[4] D. O. Kryshtal, D. J. Blackwell, Ch. L. Egly, A. N. Smith, S. M. Batiste, J. N. Johnston, D. R. Laver and B. C. Knollmann, Circulation Research, 128 (2021), 321-331.
[5] S. C. Salvage, K. H. Chandrasekharan, K. Jeevaratnam, A. F. Dulhunty, A. J. Thompson, A. P. Jackson and Ch. L.-H. Huang, British Journal of Pharmacology, 175 (2018), 1260-1278.
[6] D. Mehra, M. S. Imtiaz, D. F. van Helden, B. C. Knollmann and D. R. Laver, Molecular Pharmacology, 86 (2014), 696-706.
[7] S. C. Salvage, E. M. Gallant, J. A. Fraser, Ch. L.-H. Huang and A. F. Dulhunty, Cells, 10 (2021), 2101.
[8] M. L. Bannister, A. Alvarez-Laviada, N. L. Thomas, S. A. Mason, S. Coleman, C. L. du Plessis, A. T. Moran, D. Neill-Hall, H. Osman, M. C. Bagley, K. T. MacLeod, Ch. H. George and A. J. Williams, British Journal of Pharmacology, 173 (2016), 2446-2459.
[9] M. L. Bannister, N. L. Thomas, M. B. Sikkel, S. Mukherjee, C. Maxwell, K. T. MacLeod, Ch. H. George and A. J. Williams, Circulation Research, 116 (2015), 1324-1335.
[10] M. L. Bannister, T. K. MacLeod and Ch. H. George, British Journal of Pharmacology, 179 (2022), 2558-2563.
[11] J. Gaburjakova and M. Gaburjakova, Bioelectrochemistry,109 (2016), 49-56.
[12] J. Gaburjakova and M. Gaburjakova, Cells, 11 (2022), 868.

11th Slovak Biophysical Symposium, High Tatras, June 12 – 14, 2024

Mitochondrial chloride channel: a CLIC or not a CLIC?

K. Ondacova[1], K. Polcicova[2], A. Misak [2] and Z. Sevcikova Tomaskova[1]

[1] *Centre of Biosciences, Slovak Academy of Sciences, Bratislava, Slovakia.*
[2] *Biomedical Research Center, Slovak Academy of Sciences, Bratislava, Slovakia.*

e-mail: zuzana.tomaskova@savba.sk

Mitochondrial chloride channels were first detected in 1980's. Since then, various information was collected concerning their basic biophysical properties or pharmacological regulation. Despite the vast number of results, the direct assignment of a gene to these channels is still missing. The mitochondrial chloride channels are involved in the regulation of mitochondrial membrane potential $\Delta\Psi_m$. [1-3]. They are responsible for $\Delta\Psi_m$ oscillations under oxidative stress that lead to the development of arrhythmias. The oscillations are spread throughout the cell by reactive oxygen species (ROS) in a process named ROS-induced ROS release (RIRR). The RIRR process can be abolished by application of non-specific anion channel inhibitor 4,4′-diisothiocyano-2,2′-stilbenedisulfonic acid (DIDS) as well as by a specific ligand of translocator protein (TSPO) – 4-chlorodiazepam. TSPO is localized in the outer mitochondrial membrane. It is supposed that TSPO is in direct contact with the chloride channel to achieve the inhibition of the chloride channel by nanomolar concentrations of the ligand. On the other hand, there is a family of proteins named chloride intracellular channels (CLIC) that has several isoforms. Their biophysical properties were described only on recombinant proteins, though these CLIC proteins were detected in many different cellular localizations. Under these artificial conditions, CLIC proteins work as weakly selective anion channels that exhibit several conductive states [4]. Two isoforms - CLIC4 and CLIC5 – were shown to be present in the outer and inner mitochondrial membrane of cardiomyocytes, respectively [5].

Our aim was to show whether the native mitochondrial chloride channel, derived from rat cardiac tissue, are members of CLIC family.

We prepared submitochondrial particles (SMP) from rat cardiac homogenate [6] and measured the native chloride channels by protein reconstitution into bilayer lipid membrane (BLM). The membrane fraction of SMP was also tested for the presence of proteins of interest using western blot analysis. The native chloride channels, measured in 250mM/50mM KCl gradient, had the median value of permeability coefficient ratio $P_{Cl}/P_K = 4.34$ (IQR=2.98). This selectivity is comparable with the reported selectivity of CLIC4 and CLIC5 channels. The mean conductance in 250mM/50mM KCl gradient is 129±3 pS. To better discern the conductive substates, we measured the single-channel currents in 1M/50mM KCl gradient. We detected 4 conductive states: the main state and three substates having uniformly separated conductance values with step of 25% of the maximal conductance. The substates were rarely occupied, which was shown by mean-variance analysis [7]. The number of reported substates of CLIC4 and CLIC5 isoforms varies, but both the number of substates and their respective conductance of the native Cl channels fall within the reported range [8]. The CLIC proteins were purified using their ligand indanyloxyacetic acid IAA-94 [9]. We tested the effect of this ligand on the activity of native Cl channel. At the single-channel level, the activity was inhibited by mechanism of open-channel block, with IC_{50}=380μM. We tested the presence of CLIC4 and CLIC5 in the membrane fraction of submitochondrial particles. We detected the presence of

CLIC5 isoform, but not of the CLIC4 isoform. Subunit IV of cytochrome c oxidase was used as control of the presence of the inner mitochondrial membrane.

The obtained results indicate that the native mitochondrial chloride channels are with high probability members of the CLIC family – the CLIC5 isoform proteins.

Acknowledgement
This work was supported by VEGA 2-0051-23 and APVV-22-0085.

References

[1] M. A. Aon, S. Cortassa, E. Marba, B. O'Rourke, J. Biol. Chem., 278 (2003), 44735-44744.
[2] M. A. Aon, S. Cortassa, B. O'Rourke, Adv. Exp. Med. Biol., 641 (2008), 98-117.
[3] M. A. Aon, S. Cortassa, F. G. Akar, D. A. Brown, L. Zhoua, B. O'Rourke, Int. J. Biochem. Cell Biol., 40 (2009), 1940-1948.
[4] H. Singh, M. A. Cousin, R. H. Ashley, FEBS J., 274 (2007), 6306-6316.
[5] D. Ponnalagu, S. Gururaja Rao, J. Farber, W. Xin, A. T. Hussain, K. Shah, S. Tanda, M. Berryman, J. C. Edwards, H. Singh, Mitochondrion, 27 (2016), 6-14.
[6] A. Misak, M. Grman, L. Malekova, M. Novotova, J. Markova, O. Krizanova, K. Ondrias, Z. Tomaskova, Eur. Biophys. J., 42 (2013), 709-720.
[7] M. Tomasek, A. Misak, M. Grman, Z. Tomaskova, FEBS Lett., 591 (2017), 2251-2260.
[8] K. Mackova, A. Misak, Z. Tomaskova, IntechOpen, London (2018), 175-192.
[9] D. W. Landry, M. Reitman, E. J. Cragoe, Jr., Q. Al-Awqati, J. Gen. Physiol., 90 (1987), 779-798.

11th Slovak Biophysical Symposium, High Tatras, June 12 – 14, 2024

Analysis of fibrillization mechanism of the recombinant core spidroin eADF4(C16) from *Araneus diadematus*

V. Hovanová[1,2], A. Hovan[2], M. Humenik[3] and E. Sedlák[1,4]

[1] *Center for Interdisciplinary Biosciences, Technology and Innovation Park, P. J. Šafárik University, Košice, Slovakia.*
[2] *Department of Biophysics, Faculty of Science, P. J. Šafárik University, Košice, Slovakia.*
[3] *Department of Biomaterials, Faculty of Engineering Science, University Bayreuth, Bayreuth, Germany.*
[4] *Department of Biochemistry, Faculty of Science, P. J. Šafárik University, Košice, Slovakia.*

e-mail: erik.sedlak@upjs.sk

Introduction. Spider silk, especially dragline silk, due to its unusual combination of tensile strength, elasticity, and break resistance as well as biocompatibility, has been used as an inspiration for preparation of protein-based material. The recombinant spider silk protein, eADF4(C16), possesses the ability to form diverse nanostructures based on nanofibrils. The protein structure mimics the core domain of fibroin 4 from the dragline silk of the European garden spider *Araneus diadematus*, containing a 16-times repeating C-module that includes polyalanine and glycine-proline-rich motives.

Aims. Although the molecular mechanism involved in cross-β fibril formation is a subject of broad research interest, there have been limited attempts to elucidate the specific molecular mechanism in case of structural protein forming β-sheet rich fibrils such as eADF4(C16). Our particular goals were: (i) to perform a detailed global analysis of the eADF4(C16) cross-β fibrils formation, using integrated rate law kinetics implemented in the platform AmyloFit [1] and [ii] to investigate the role of cosolvents, represented by Hofmeister anions, and solvent pH on the fibrillization of the recombinant core spidroin eADF4(C16) from *Araneus diadematus*.

Methods. Fibrillization kinetics of eADF4(C16) have been monitored by Thioflavin T (ThT) and 1-anilino-8-naphthalene sulfonate acid (ANS) fluorescence and absorbance at 340 nm. The protein and formed fibrils and aggregates were analyzed by circular dichroism, atomic force microscopy, and transmission electron microscopy. Kinetic datasets of protein eADF4(C16) with or without seeds were fitted using the online platform AmyloFit (www.amylofit.ch.cam.ac.uk) [1]. The entire analysis was performed according to the protocol of Meisl et al. (2016) [1].

Conclusion. The self-assembly of the protein eADF4(C16) was examined by varying the protein concentration and temperatures in the presence or absence of eADF4(C16) seeds. Through this approach, we were to elucidate that the fibril formation process involves not only primary processes, such as primary nucleation and elongation, but also secondary pathways, including secondary nucleation (Fig.1) [2].

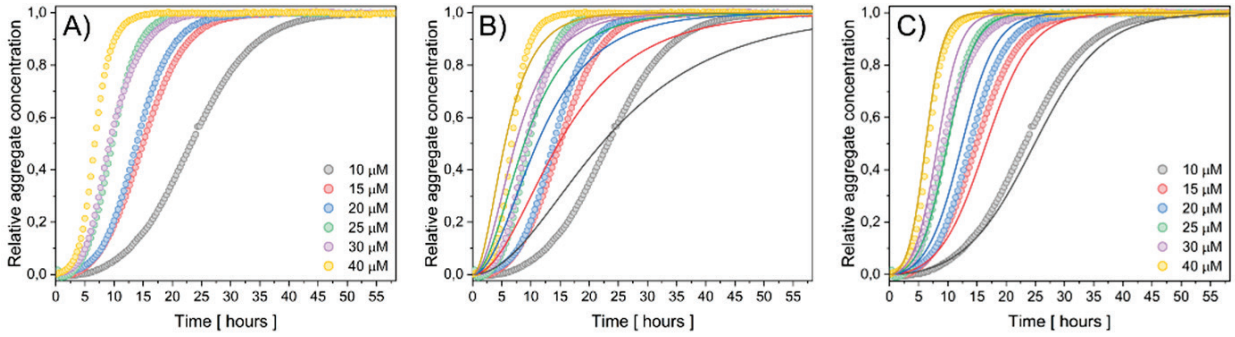

Fig. 1. Self- assembly kinetics of eADF4(C16) protein in the presence of 150 mM KPi, at 20°C. (A) Normalized changes in turbidity at 340 nm upon formation of fibrils from the monomeric protein in the concentrations range 10–40 μM. (B) Data fitting the nucleation-elongation model. The global fit function did not adequately describe the kinetic. (C) Data fitting with the global model including the secondary nucleation revealed a higher accuracy to (B).

We showed that similarly to phosphate anions, other kosmotropic anions such as sulfate and fluoride also trigger the fibrillization of the protein, and secondary nucleation plays an important role in the self-assembly process. This result is likely achieved through the stabilization of fibrillization-prone conformers of eADF4(C16) by anion hydration intermediates, in accordance with the Hofmeister effect. In contrast, chaotropic anions stabilize water-soluble conformers that are unable to form fibrils, likely due to direct interaction with the polypeptide chain of eADF4(C16). Reported results further suggest that a hydrated cosolvent, for example, osmolytes, or crowding agents, may accelerate protein fibrillization (Fig. 2) [3].

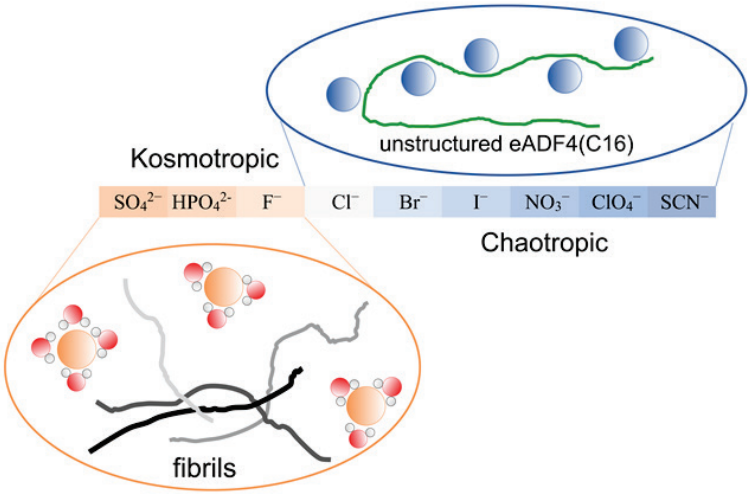

Fig. 2. A schematic overview of the presented research illustrates the influence of kosmotropic and chaotropic anions, according to the Hofmeister order, on the self-assembly of the protein eADF4(C16). The water molecules form a structured arrangement around the kosmotropic anions, leading to the self-assembly of the protein. In contrast, chaotropic anions stabilize the protein, possibly by binding to the protein structure, and it remains dissolved in the solution.

Acknowledgement
This work was supported by the Slovak Research and Development Agency (project APVV-20-0340) and Agency of Ministry of education, research, development and youth of the Slovak republic (VEGA 2/0034/22).

References

[1] G. Meisl, J. B. Kirkegaard, P. Arosio, T. C. T. Michaels, M. Vendruscolo, C. M. Dobson; et al., Nat. Protoc. 11 (2016), 252-272.
[2] V. Hovanová, A. Hovan, G. Žoldák, E. Sedlák, M. Humenik., Protein Sci. 32 (2023), e4722.
[3] V. Hovanová, A. Hovan, M. Humenik, E. Sedlák., Protein Sci. 32 (2023), e4832.

11th Slovak Biophysical Symposium, High Tatras, June 12 – 14, 2024

α-Lactalbumin amyloid fibrillization in the presence of Hofmeister anions

A. Antošová, M. Gančár, J. Marek, Z. Gažová

Institute of Experimental Physics, Slovak Academy of Sciences, Watsonova 47, 040 01 Kosice, Slovakia

e-mail: antosova@saske.sk

The effect of salt ions from the Hofmeister series (HS) on protein properties has been known for more than a century [1]. However, its influence on the process of protein amyloid fibrillization is little explored. The α-Lactalbumin (α-LA), a 123- amino acids (14.2 kDa) protein, a component of milk whey, gained attention in drug, vitamin, and bioactive compound delivery [2]. We have studied the influence of selected anions (SO_4^{2-}, CH_3COO^-, $H_2PO_4^-$, Br^-, NO_3^-, ClO_4^-) in the form of sodium salts on the α-LA amyloid aggregation, aiming to prepare amyloid fibrils with specific properties suitable for biotechnological applications.

The aggregation kinetics, morphology and secondary/tertiary structures of native α-LA and its amyloid fibrils have been studied using ThT fluorescence, ATR-FTIR, CD spectroscopy, and AFM. We have observed selected anions affecting the characteristics mentioned above of α-LA fibrils differently. The effect of studied anions on kinetic parameters of α-LA amyloid formation (lag phase time t_{LAG}, half-time of elongation phases t_{HALF}) strongly correlates to their position in the HS with the exception of large and strongly hydrated anions $H_2PO_4^{2-}$ and CH_3COO^-. Distinctly shortest lag and half-time phases were observed for strongly hydrated anion SO_4^{2-}. Using ATR-FTIR, it was found that fibrils formed in the presence of CH_3COONa have the highest β-sheets content and the least amount of random secondary structure (Fig. 1). Except for Na_2SO_4, the fibril β-sheets content decreases, corresponding to the position of the anions in HS - from CH_3COONa to $NaClO_4$. α-LA aggregates formed in the presence of studied salts were visualised using AFM. The presence of CH_3COONa (Fig. 1), NaH_2PO_4 and NaBr resulted in many long fibrils, while a smaller number of short fibrils formed in the presence of Na_2SO_4, $NaNO_3$ and $NaClO_4$ (Fig. 1). This may be related to the fact that the tertiary structure of α-LA was intensively altered in the presence of these anions, as near-UV CD results have shown.

These findings are essential to clarify the mechanism of α-LA amyloid assembly and the possible application of its fibrils in biotechnology.

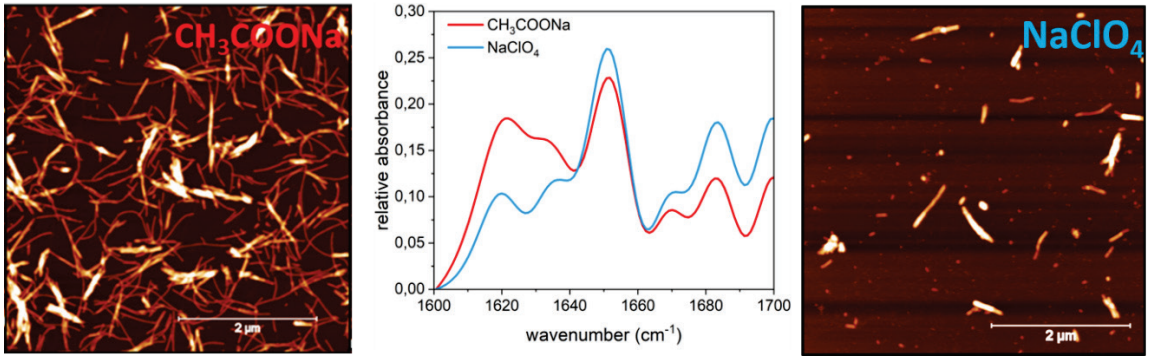

Fig. 1. AFM images of α-LA fibrils prepared in the presence of CH_3COONa and $NaClO_4$. ATR-FTIR spectra α-LA amyloid fibrils prepared in the presence of 300 mM salts: CH_3COONa (red line) and $NaClO_4$ (blue line) at pH 2.0 (in the middle).

Acknowledgement

This work was supported by research grants from the Slovak Research and Development Agency under the Contract no. APVV-18-0284, APVV-22-0598 and Slovak Grant Agency VEGA 2/0176/21, 02/0164/22.

References

[1] F. Hofmeister, Arch. Exp. Pathol. Pharmacol., 24 (1888), 247-260.
[2] E. A. Permyakov, Biomolecules, 10 (2020), 1210.

11th Slovak Biophysical Symposium, High Tatras, June 12 – 14, 2024

In silico peptide design to disable the p53 pathway.

Exequiel E. Barrera

Instituto de Histología y Embriología Mendoza (CONICET), Av. Del Libertador 80, Mendoza, Argentina.

e-mail: ebarrera@mendoza-conicet.gob.ar

Introduction and aims:

The nuclear transcription factor p53 is a protein with a pro-apoptotic function that accumulates in the cell nucleus in response to DNA damage. Since p53 mutations represent an early event in carcinogenesis, big efforts have been directed in recovering its activity to treat and prevent different types of cancer. But this is not our case.

Our objective consists on transiently disable the p53 activity, in the context of CRISPR-Cas9 genomic engineering. DNA modifications, like the ones induced by this technique, normally activates the p53 pathway, inducing a partial apoptosis that leads to an unwanted p53-deficient clonal selection. P53 exerts its activity by interacting with DNA, increasing its binding affinity under its tetrameric form. This oligomerization is conducted by its interaction with 14-3-3, a family of dimeric adapter proteins that through protein-protein interactions modulate a wide range of physiological and pathological processes, including apoptosis. 14-3-3 possess an amphipathic binding groove in its structure that binds protein partners containing phosphorylated threonine or serine residues, included on disordered regions. For the case of p53 this corresponds to its C-terminal region. In this work we combined different molecular modelling techniques to propose peptide candidates capable of inhibit its interaction with 14-3-3 and consequently prevent its association into tetrameric active forms.

Methods:

We propose inhibitory peptide candidates by exploring all the possible combinations of the variation of three residues from the sequence of the C-terminal region of p53 (^{382}KLMFK-pT-**E**GPD**SD**^{393}) and generate input files for 8 thousand peptides (variations with repetition = M^n; being M the number of natural aminoacids and N the number of positions to vary). Additionally, to confer cell penetrating properties, we included to each peptide an N-terminal poly-Arg tail.

The first selection criteria consisted on the capacity of the peptides to adopt the conformation of p53 when interacting with 14-3-3. This consists of a unique turn induced by G389 and P390 and its determining for its binding affinity as shown by diverse biophysical techniques[1]. To explore the conformational landscape of each peptide we performed 1 microsecond molecular dynamics simulations of single peptides in solution, employing the SIRAH Coarse-grained force field[2]. Complementary we employed a machine-learning-based framework to predict if our candidates present cell-penetrating characteristics[3].

On a second step we assessed the binding capacity of these peptides to the 14-3-3 binding groove, modelling the peptide/14-3-3 complexes with the Haddock docking software[4].

Results and Discussion:

By means of in-house scripts we analysed our 8000 **MD simulations**. To select peptides with the highest structural similarities to those of the turned p53 X-ray structure and discard conformers with unwanted poly-Arg/C-terminal interactions we employed a root mean square deviation (RMSD) cutoff of 3.5 Å and End-to-End distances larger than 15 Å. We selected 20 peptides to continue with the next screening step.

Then, we employed two docking strategies: 1) **Blind docking** space search, allowing the peptide to explore the full surface of 14-3-3. By this, we evaluated if the peptide candidates presented unspecific interactions in regions outside the 14-3-3's binding groove. And 2) **Position-restrained docking**, forcing the peptides to interact in the binding groove. By restraining the search surface and including in our model's peptide flexibility and solvation, we energy-minimized the docking solutions, and evaluated them with an RMSD and energetic criteria. Results from one of the selected peptides are displayed in Fig. 1 and analysis of the top candidates are summarized in the Table 1.

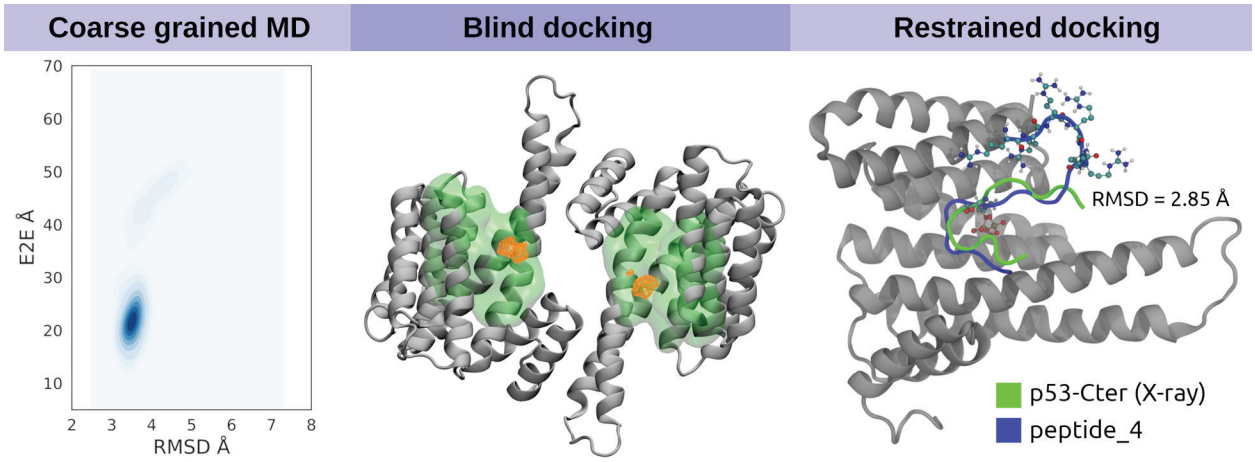

Fig. 1. Analysis example of peptide candidate #4. (Left) 2D density plot showing end-to-end distances and RMSD values through 1μs MD simulations. (Center) Cartoon representation of the 14-3-3 dimer; transparent green surfaces correspond to its binding groove and orange meshes indicate the occupancy of the phospho-threonine of peptide 4. (Right) Cartoon representation showing the complex between peptide 4 (blue ribbon) and 14-3-3. A green ribbon shows the structural overlapping of the X-ray p53 structure.

Summarizing, a virtual screening campaign was held, to select peptide candidates able to compete with p53 from binding to 14-3-3. We trimmed the list from 8000 to 5 candidates for further experimental evaluation. According to our *in silico* approach, each of these peptides were characterized for desired folding behavior in solution and to present cell-penetrating properties. They also showed specific interactions in the 14-3-3's binding groove, displaying the lowest binding energies.

Table 1. Structural and energetic descriptors for the top 5 peptide candidates.

	MD simulations	Blind docking		Restrained docking	CPP pred
	E2E / RMSD (ranking)[a]	Binding specificity[b]	RMSD[c]	Docking score (a.u.)[d]	Probability (%)[e]
pep_1	57.32 (#2)	medium	3.06	-159.86	97.21
pep_2	19.16 (#20)	high	2.95	-149.15	96.69
pep_3	22.30 (#17)	medium	3.12	-148.49	97.19
pep_4	38.70 (#6)	high	2.85	-139.19	97.64
pep_5	20.68 (#18)	medium	3.33	-135.25	97.5

[a] Percentage time satisfying E2E & RMSD cutoff values. [b]Top 20 energetic complexes locating exclusively at the binding groove (high), binding groove +1 site (medium) and binding groove +2 or more sites (low). [c]Root mean square deviation of the backbone atoms using as a reference the X-ray structure of p53 (PDBid: 5MHC) [d]According to the Haddock scoring function. More negative values correspond to greater binding affinities. [e]According to the BchemRF-CPPred tool.

Acknowledgement
This work was supported by the former Ministry of Science and Technology. (PICT-2021-GRF-TI-00278).

References
[1] A. Kuusk; et al, ACS Chem. Biol., 15 (2020), 262-271.
[2] M. R. Machado; et al, J. Chem. Theory Comput., 15 (2019), 2719-2733.
[3] de Oliveira; et al, Sci. Rep., 11 (2021), 1-15.
[4] G. C. P. Van Zundert; et al, J. Mol. Biol., 428 (2016), 720-725.

11th Slovak Biophysical Symposium, High Tatras, June 12 – 14, 2024

Comparison of α-synuclein aggregates in non-differentiated and differentiated SH-SY5Y cells treated by rotenone and photobiomodulation

K. Stroffekova[1] and Z. Bednarikova[2]

[1] *Department of Biophysics, Institute of Physics, P. J. Safarik University, Kosice, Slovakia.*
[2] *Institute of Experimental Physics, Slovak Academy of Sciences, Kosice, Slovakia.*

e-mail: katarina.stroffekova@upjs.sk

According to the WHO, the population older than 60 years will nearly double from 12% to 23% by 2050. Significant aging correlates with an increase of the neurodegenerations in population, including Parkinson's (PD), Alzheimer (AD) diseases and ALS (amyotrophic lateral sclerosis). PD is a progressive neurodegenerative disorder characterized by the loss of dopaminergic neurons in the *substantia nigra pars compacta* (SNc) and accumulation of insoluble cytoplasmic protein inclusions, including α-synuclein (αSNC). The present work compares the levels of α-synuclein (αSNC) monomers and aggregates in non-differentiated and differentiated SH-SY5Y cells treated with rotenone and photobiomodulation (PBM). Photobiomodulation (PBM) by low-level near infrared (NiR) radiation was shown to have positive effects in cell repair processes and proliferation, in wound healing, muscle repair, and angiogenesis. We have established the 2D model of PD by using human neuroblastoma cell line SH-SY5Y and ROT treatment and PBM (200nM Rot for 48hr, NiR 1J/cm^2). We have investigated αSNC species with specifically designed antibodies to recognize monomer and aggregated form. In non-differentiated SH-SY5Y cells, control cells displayed a low level of αSNC monomer and appreciably higher level of αSNC aggregates. Treatment with ROT increased αSNC level of both species, monomers and aggregates, respectively. These findings were confirmed further by the AFM analysis and Thioflavin T (ThT) assay, which showed that ROT treated cells have higher load of amyloid species based on the significantly higher ThT fluorescence intensity compared to non-treated cells and media. PBM treatment increased αSNC monomer level in both, control and ROT cells. In contrast, PBM notably decreased αSNC aggregates level in both, control and ROT cells. In the next step, we have differentiated SH-SY5Y cells by incubation with 1% FBS media and 10mM retinoic acid (RA) for 10-14 days. Differentiation media was changed every 72 hr. The SH-SY5Y differentiation was confirmed by expression of neuronal markers microtubule-associated protein 2 (MAP2) and tyrosine hydroxylase (TH). In differentiated SH-SY5Y cells (D9–D17), we have found noticeably higher load of αSNC aggregates in comparison with non-differentiated cells. The load of αSNC aggregates increased with the length of cultivation. In following steps, we will investigate effects of ROT and PBM in differentiated SH-SY5Y. Comparison of ROT and PBM effects in non-differentiated and differentiated SH-SY5Y cells will give us better understanding of PD mechanisms at the cellular level. These results can be the groundwork for PD research in more complex systems such as 3D organoids, or in the animal model *in vivo*.

Acknowledgement
This work was supported by the EU ERDF grant OPENMED (ITMS2014+: 313011V455), by the Slovak Grant Agency VEGA 1/0421/18;1/0557/20 and 1/0187/23; and by the Slovak Research and Development Agency APVV-21-0333 and APVV-22-0598.

11th Slovak Biophysical Symposium, High Tatras, June 12 – 14, 2024

Application of microscopy and spectroscopy methods for evaluation of the presence of microplastics in the aquatic environment with living organisms

A. Marček Chorvátová[1,2] , M. Uherek[1] , A. Mateašík[1] and D. Chorvát[1]

[1] *Department of Biophotonics, International Laser Center SCSTI, Ilkovičova 3, 814 04 Bratislava, Slovakia.*
[2] *Department of Biophysics, FNS, Univ. Ss Cyril and Methodius, J Herdu 1, 917 02 Trnava, Slovakia.*

e-mail: Alzbeta.Marcek.Chorvatova@ucm.sk

Microplastics (MPs) have strong contribution to environmental pollution and impact several diseases. Inappropriate disposal and low biodegradability lead to accumulation of small plastic fragments in aquatic environment, including fresh water reservoirs. Evaluation of the presence of MPs is therefore crucial in order to establish their presence in the natural conditions and evaluate potential risks. However, their identification in aquatic environment in the presence of microorganisms such as algae, or moss is still complex. Our aim is to apply advanced biophotonics methods to determine the presence of MPs in the aquatics environment in the presence of living organisms. We previously applied fluorescence spectroscopy and microscopy methods to test chosen environmental stressors on endogenous fluorescence in algae and moss [1-3].

In this work, we evaluate the advantages and limitations of microscopy and spectroscopy methods to determine the presence of MPs in aquatic environment where sweet water algae *Chlorella sp.* or moss *Fontinalis antipyretica* are located. MPs were purchased commercially as a FluoSpheres® size kit #2 (F8888, Invitrogen by Thermo Fisher Scientific), carboxylate coupling surface, labelled with yellow-green fluorescence (Ex/Em 505/515). Six sizes were used with nominal bead diameters of 0.02, 0.1, 0.2, 0.5, 1.0, 2.0 μm. MPs were added to cells in concentration 0.5 or 2 μL/mL (2% solids in the original solution).

Laser scanning confocal microscopy (LSCM) imaging with Axiovert 200 LSM 510 Meta (Carl Zeiss, Germany) equipped with objective C-Apochromat 40x, 1.2 NA was employed. Fluorescence of living algae and moss was excited with the 458 nm laser-line (Kvant, Slovakia) and detected using a 16 channel META detector. Fluorescence lifetime imaging microscopy (FLIM) images were gathered by time-correlated single photon counting (TCSPC) technique equipped with a 445 nm picosecond laser diode (BDS-SM-445-FBC, Becker&Hickl, Germany). The laser beam was reflected to the sample through an epifluorescence path of the LSCM. The emitted fluorescence was separated from laser excitation using BP 700±20 nm and detected by PMC-100-20 photomultiplier (Becker&Hickl, Germany) with an SPC-830 TCSPC board.

Algae *Chlorella sp.* were gathered from the University of Ss. Cyril and Methodius in Trnava, Faculty of Natural Sciences collection of green algae (previously isolated from the main drinking water supply) and cultivated in the Hoagland cultivation medium. Water bryophyte green moss species *Fontinalis antipyretica* was gathered commercially from aquashop (Aquasymbioza, Bratislava, Slovakia) and grown under ambient light.

Performed experiments demonstrated that confocal microscopy methods are useful for evaluation of the effect of MPs on endogenous fluorescence of living organisms down to nanometric

sizes. At the same time, measurement of fluorescence lifetimes of chlorophylls at emission around 700 nm by FLIM revealed an additional possibility to visualize the MPs of micrometric size near the individual algae cell (Fig. 1 middle and right). Further work is necessary to determine the best experimental approaches in order to identify the presence of MPs in aquatic environment in the presence of algae and moss using advanced microscopy and spectroscopy methods. Performed research is crucial in order to propose the best approaches for monitoring of MPs and their effects in the real and thus eventual removal of this environmental pollution from water sources.

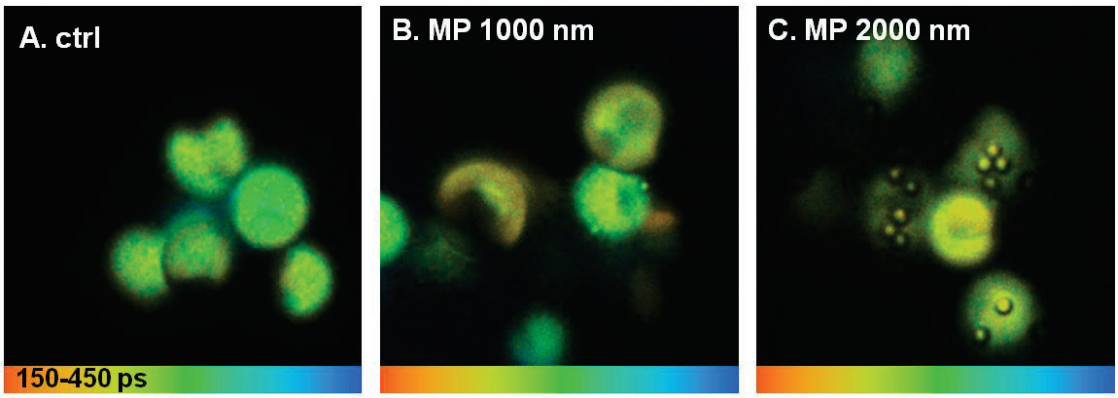

Fig. 1. FLIM images of algae *Chlorella sp.* gathered following excitation by 445 nm ps laser, 700±20 nm; the lifetime distribution is shown in the range of 150-450 ps (red-blue) in control conditions (left) and in the presence MPs of the size 1000 nm (middle) and 2000 nm (right).

Acknowledgement

This work is supported by VEGA No. 2/0040/24, as well as the LASERLAB-EUROPE (grant agreement no. 871124, European Union's Horizon 2020 research and innovation programme) and Operational program integrated infrastructure project BIOFOTO "New methods of integrated nano-bio-photonics for early diagnosis of biological and environmental factors", ITMS 313011T458, co-financed from the resources of the European Regional Development Fund.

References

[1] A. Marcek Chorvatova, M. Uherek, A. Mateasik, D. Bondarev, F. Ariese, D. Chorvat Jr., Proc. SPIE 12394, Nanoscale Imaging, Sensing and Actuation for Biomedical Applications XX, the International Society for Optical Engineering, 1239407 (2023).

[2] A. Marcek Chorvatova, M. Uherek, A. Mateasik, D. Chorvat Jr., Frontiers in Physics, 9 (2021), 634324: 1-9.

[3] A. Marcek Chorvatova, M. Uherek, A. Mateasik, D. Chorvat Jr., Methods and Applications in Fluorescence, 8 (2020), 024007.

11th Slovak Biophysical Symposium, High Tatras, June 12 – 14, 2024

Multimodal character of photon-upconverting nanoparticles for bioimaging of glioblastoma

V. Huntošová[1,2], S. Olejárová[3], C. Slabý[3], G. Bánó[3], Z. Jurašeková[3], T. Vasylyshyn[4], V. Patsula[4] and D. Horák[4]

[1] *Center for Interdisciplinary Biosciences, Technology and Innovation Park, P. J. Šafárik University in Košice, Jesenná 5, SK-041 54 Košice, Slovak Republic.*
[2] *Institute of Animal Biochemistry and Genetics, Centre of Biosciences, Slovak Academy of Sciences, Dubravska cesta 9, Bratislava 840 05, Slovak Republic.*
[3] *Department of Biophysics, Institute of Physics, Faculty of Science, P. J. Šafárik University in Košice, Jesenná 5, SK-041 54 Košice, Slovak Republic.*
[4] *Institute of Macromolecular Chemistry, Czech Academy of Sciences, Heyrovského nám. 2, 162 06 Prague, Czech Republic.*

e-mail: veronika.huntosova@upjs.sk

Nanotechnology is one of the most highly developed fields of research. Structures ranging in size from μm to nm are used in various fields, including bioimaging. The functionalisation of nanoparticles makes it possible to attach ligands in order to bring the particles specifically into the cells. On the other hand, the porous structure of the nanoparticles makes it possible to bind fluorescent molecules to the particle. Fluorescence imaging uses fluorophores that are clearly defined by the excitation and emission wavelength of photons. In one particular case, these molecules can interact with the environment from their triplet state and trigger a photoreaction that leads to photodestruction. When these molecules interact with molecular oxygen, the oxidative stress in the cells can increase dramatically and trigger cell death. The interaction times are very short. Therefore, the correct localisation and stability of fluorophores in cells and tissue is very important.

Unfortunately, the biggest limitation of fluorescence bioimaging (in the visible range of light) is the thickness of the sample. For this reason, we have developed photon upconverting nanoparticles based on ($NaYF_4$:Yb^{3+}, Er^{3+}@$NaYF_4$:Nd^{3+}), which enable the conversion of infrared (IR) light into light in the visible range. In addition, IR light can penetrate deeper into the tissue than visible light. These particles have been conjugated with hypericin, a well-known photosensitiser. Hypericin has an orange/red fluorescence after excitation at 560-590 nm and can be used as a contrast agent in fluorescence bioimaging of glioblastomas.

Cells were grown in spheroids or immobilised in photoresist microstructures and incubated with upconverting nanoparticles conjugated with hypericin and detected using three different imaging techniques: i) IR imaging at 976 nm excitation, ii) confocal fluorescence imaging at 555 nm excitation and iii) Raman microspectroscopy at 785 nm. The upconverting nanoparticles were identified by IR imaging in the cells as specific foci that could correspond to intracellular vesicles. This observation suggests that the particles enter the cells by endocytosis, which was confirmed by flow cytometry of individual cells. The distribution of hypericin in the cells was observed by confocal fluorescence imaging. A homogeneous distribution of hypericin was observed in the cells, with the exception of the nuclei. However, intense fluorescence of hypericin was observed in subcellular vesicular structures, confirming the hypothesis of endocytosis of hypericin-conjugated particles. Raman microspectroscopy confirmed the unique properties of the upconverting particles, which were only identified in cells exposed to these particles.

In summary, the multimodality of high-converting nanoparticles for bioimaging of glioblastomas was demonstrated. The lanthanide composition of the particles makes them promising for other imaging techniques such as optical coherence tomography and X-ray imaging.

Acknowledgement
This work was supported by APVV-21-0333, APVV-20-0340, vvgs-2023-2556 and GAČR 24-10125S.

11th Slovak Biophysical Symposium, High Tatras, June 12 – 14, 2024

Effect of Lipid Composition on Interaction of GC376 Antiviral with Membrane Bilayer

M. Klacsová, D. Uhríková

Department of Physical Chemistry of Drugs, Faculty of Pharmacy, Comenius University Bratislava, Odbojárov 10, 832 32 Bratislava, Slovakia.

e-mail: klacsova@fpharm.uniba.sk

Pathogens such as coronaviruses (CoVs) are considered to be the major agents of emerging respiratory disease outbreaks. Lipids were suggested to play an essential role during viral infection involving membrane fusion of virus to host cell, viral internalization through receptor-mediated or lipid-microdomain mediated endocytosis, viral replication and viral exocytosis [1]. CoVs bud from the endoplasmic reticulum/Golgi intermediate complex and exit via lysosomal secretion, thus the composition of the virion envelope significantly differs from plasma membrane. Lipidomic analysis of viral lipids extracted following infection of VeroE6 and A459 cells detected ~260 lipid species. The most abundant were phosphatidylcholines (PCs), phosphatidylethanolamines (PEs) and phosphatidylinositols (PIs) with fatty acid composition predominantly 16:0, 18:0, 18:1 [1]. These lipids are not affected by mutation of the virus, therefore might be used as potential targets for antiviral approaches.

GC376 is a dipeptide-based bisulfide antiviral prodrug showed to be potent against a number of CoVs, including SARS-CoV-2 [2]. The primary site of action of GC376 is CoVs main protease M^{pro}. Within the concept of dual mechanism of antiviral action, GC376 is assumed to affect also properties of lipid bilayer of virion envelope. One of the factors controlling the stability of the bilayer are lateral interactions between the lipid molecules. The distribution of forces acting in different planes across the bilayer is given by the lateral pressure profile.

The ratio of excimer-to-monomer emission intensities of bispyrenyl fluorescent probes (Pyr*n*PC) was used as a measure of bilayer lateral pressure (η) at the level of n = 4 and 10 carbons, respectively [3]. The effect of GC376 on η was studied in three types of lipid bilayers differing by composition of polar headgroup and/or acyl chains: bilayer forming dioleoylphosphatidylcholine (DOPC) and egg-yolk phosphatidylcholine (EYPC), and inverse hexagonal phase H_{II}-prone egg-yolk phosphatidylethanolamine (EYPE). Lipid, probe and antiviral in respective organic solutions were mixed at Pyr*n*PC:lipid = 1:1500 and GC376:lipid = 0 – 0.3 mole ratios. After removal of the organic solvent, samples were hydrated by 150 mmol/l NaCl solution and homogenized. Measurements were performed using a fluorimeter FluoroMax-4 (HORIBA Jobin Yvon, France). The fluorescence intensity, after excitation at λ_{ex} = 345 nm, was monitored during 120 s at emission wavelengths of monomer λ_{em} = 376 nm and excimer λ_{em} = 481 nm. Sample temperature was regulated to within ± 0.01 °C by a Peltier thermocouple drive.

Lateral pressure was found to nonlinearly increase with GC376: lipid mole ratio in DOPC, however decrease for EYPC and EYPE, at both monitored depths of the fluid bilayers (Fig. 1 left). This difference suggests that the lipid acyl chain composition plays the crucial role in lateral pressure distribution across the bilayer. Assuming that the intramolecular excimer formation is a two-state process, activation energy E_a of excimer formation was evaluated from the slope of Arrhenius plots

ln(η/T) = f(1/T) for each membrane composition. Upon binding of GC376, E_a subtly decreases in DOPC and more pronouncedly in EYPC bilayers. In EYPE bilayer a dramatic increase of E_a is seen already at low GC376: lipid mole ratios (Fig. 1 right). These trends were obtained both for Pyr4PC and Pyr10PC probes (not shown). The increase in activation energy is assumed to reflect decreased excimer formation rate *k*. Factors determining the rate *k* are the geometrical and the dynamical factor [4]. As E_a was evaluated within a 5°C temperature interval in the lamellar phase, the main contributing effect should be the change in geometry of lipid packing. It follows that binding of GC376 into EYPE bilayers significantly increases defects in the hydrophobic region of a membrane. Thus, the number of conformational states of pyrene is increased and formation of pyrene-excimers becomes less probable, what correlates with the observed decrease in η.

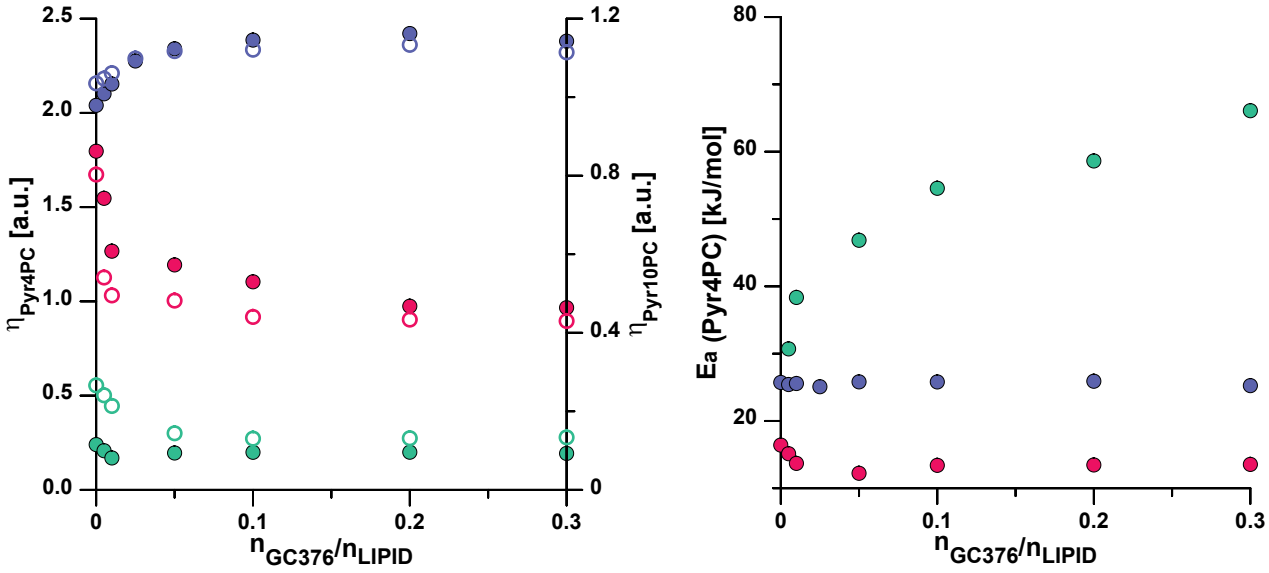

Fig. 1. Lateral pressure η (left) determined by Pyr4PC (dots) and Pyr10PC (circles) and activation energy of excimer formation E_a (right) in DOPC (blue), EYPC (red) and EYPE (green) bilayer, respectively, as a function of GC376: lipid mole ratio at 40°C.

The opposite assumption is valid for DOPC bilayers, where preferential binding of GC376 in the polar region of the bilayer was suggested [5]. Increased attraction at the headgroup region induced by GC376 leads to reduction of the area per DOPC molecule. Consequently, the average distance between two acyl chains in Pyr*n*PC probes is shortened and the collision frequency of the two intramolecular pyrene moieties increases. As a result, an increase of η is observed. In EYPC bilayers the correlation between E_a and η is not so straightforward. This is likely due to counteracting effects described for acyl chains of EYPE and polar region of DOPC.

Acknowledgement
This work was supported by VEGA 1/0305/24 and APVV 21-0108 grants.

References
[1] Z. Saud, V.J. Tyrrell, R.J. Stanton; et al, J. Lipid Res., 63 (2022), 100208.
[2] W. Vuong, M.B. Khan, M.J. Lemieux; et al, Nat. Commun., 11 (2020), 4282.

[3] S. J. Cowsley, R. H. Templer and D. R. Klug, J. Fluoresc., 3 (1993), 149-152.
[4] P. Butko and K. H. Cheng, Chem. Phys. Lipids, 62 (1992), 39-43.
[5] M. Klacsová, A. Čelková, A. Búcsi, J. C. Martínez and D. Uhríková, Coll. Surf. B: Biointerfaces, 220 (2022), 112918.

11th Slovak Biophysical Symposium, High Tatras, June 12 – 14, 2024

Medical biophysics in the study of medicine and pharmacy

J. Staničová[1,2], V. Verebová[1] and A. Strejčková[1]

[1] *Department of Chemistry, Biochemistry and Biophysics, University of Veterinary Medicine and Pharmacy, Komenského 73 Košice, Slovakia.*
[2] *Institute of Biophysics and Informatics, First Faculty of Medicine, Charles University, Salmovská 1 Prague, Czech Republic.*

e-mail: jana.stanicova@uvlf.sk

Medical biophysics, which includes selected parts of biophysics aimed at the practical application of biophysical knowledge in medicine, forms a connecting link between mathematics, physics and physical chemistry on the one hand and biological sciences on the other in the education program of physicians and pharmacists. Study of medical biophysics provides students of medicine and pharmacy with the necessary theoretical knowledge needed to understand physical laws, phenomena and processes in living organisms at different levels of the organism, but also no less important information about experimental methods used in the diagnosis and treatment of diseases as well as in scientific research.

In the presented lecture, the author will present several observations and ideas on how to modernize and improve the teaching of medical biophysics, which she has been authorizing to do by her long-term experience and lifelong effort to make this otherwise not very popular subject attractive to medical students. Above all, it is necessary to show students that this subject is not about memorizing physical formulas or describing the construction of devices, but about searching for physical phenomena and processes in a living organism. It should bring students as many connections as possible with medicine and their future practice. The subject should be a pre-requisite for the following pre-clinical disciplines such as medicinal chemistry and biochemistry, cell biology, histology, physiology, pharmacology and clinical disciplines such as nuclear medicine, radio diagnostics, ophthalmology, orthopaedics, rehabilitation medicine and others. Not to focus on high school subjects, but to explain biophysical phenomena in living systems (from the level of the atom, small molecules, bio macromolecules, through cellular components, cells, tissues, organs, organism, population) so that it is clear that the above subjects they will continue to build on these phenomena and processes. There should be connections and successions between individual parts of the curriculum (lectures). It is more interesting for students to follow the curriculum when they know that it has based on previous facts. It is not easy to find these connections, since the subject is subsidized by a small number of hours, but in some chapters, it is possible.

In the sciences of living organisms today, there is a huge amount of knowledge that is interconnected and many of them have a physical explanation. Interdisciplinarity in scientific research also translates into applied disciplines taught at universities and should definitely help students to have a comprehensive perception of living organisms.

11th Slovak Biophysical Symposium, High Tatras, June 12 – 14, 2024

Teaching of Medical Biophysics at the Jessenius Medical Faculty in Martin

M. Simera, N. Visnovcova, M. Veternik, J. Misek, O. Kralikova, L. Cibulkova and I. Poliacek

Department of Medical Biophysics, Jessenius Faculty of Medicine in Martin, Comenius University in Bratislava, Martin, Slovakia.

e-mail: michal.simera@uniba.sk

The teaching of the subject of Medical Biophysics has recently undergone significant changes, especially in terms of the organization of practical courses. The Institute provides teaching on the subject of Medical Biophysics for first-year students of general and dental medicine in Slovak and general medicine in English. For non-medical disciplines, the Institute provides teaching of the subject of Biophysics and Radiology.

The basic idea of teaching the subject of Medical Biophysics at our workplace is the application of physical phenomena to medical theory and practice. In teaching, we use modern models to demonstrate physical laws in a living organism, as well as clinical devices to demonstrate the use of a given physical phenomenon in diagnostics. The practical teaching of biophysics is complemented by high-quality teaching texts and lectures, which are also available online.

In 2014, the institute's teachers participated in an international training on medical education (An International Association for Medical Education - AMEE) in Milan, Italy. Following this training, we change some tasks in practical teaching with a focus on greater student activity. The current concept and philosophy of teaching are as follows: the content, form, and scope of medical biophysics teaching at JLF UK in Martin will be (or must be) comparable to domestic and foreign workplaces of the same focus. The content of the subject emphasizes the needs of real medical theory and practice and connects to other related subjects. Lectures and practical sessions are primarily oriented to issues of medical biophysics and instrumentation. Emphasis is placed on knowing the principles of the most important diagnostic and treatment methods used in medicine.

Based on the knowledge gained from the AMEE conference, we proposed several trial alternative methods of teaching practical exercises, considering the following pedagogical procedures: creative teaching, limited ability to simply hand the knowledge to students, stimulation to acquire knowledge by students themselves, stimulation to think and ask questions. Knowledge is acquired through active cognition through motor and intellectual activities.

Changing the teaching based on this concept, we followed:

- Provide several individual cases (case studies), to which the use of the relevant biophysics' terms corresponds,
- to enable students to independently and correctly apply the given concept to medical cases,
- to point out the most common mistakes in the application of knowledge,
- to create a new and modern textbook [1, 2].

Student remember 10% of what he hears, 15% of what he sees, 20% of what he sees and hears, 40% of what he discusses, 80% of what he directly experiences or does, and 90% percent of what he teaches others.

Acknowledgment
This work was supported by KEGA 072UK-4/2017, 057UK-4/2021.

References

[1] Vybrané kapitoly z lekárskej biofyziky s praktickými úlohami: vysokoškolské skriptá. M. Šimera, J. Jakuš, I. Poliaček a kol. (Eds.), JLF UK, Martin (2018).
[2] Medical Biophysics with practical course. J. Míšek, M. Vetrník, J. Jakuš a kol. (Eds.), JLF UK, Martin (2022).

COMPANY PRESENTATIONS

11th Slovak Biophysical Symposium, High Tatras, June 12 – 14, 2024

Cutting-edge 3D Raman Imaging in Life Sciences

I. Lermak[1] and M. Černík[2]

[1] *WITec GmbH, Oxford Instruments Group, Lise-Meitner-Str. 6, Ulm, Germany.*
[2] *Uni-Export Instruments, s.r.o., Šultysova 15, Praha 6, Czech Republic.*

e-mail: uniexport@uniexport.co.cz

Raman imaging is very powerful method of analyzing chemical composition of various kinds of samples. Raman spectroscopy detects vibrational states of molecules excited by different laser sources. In combination with confocal microscope this method enables creating 2D or 3D images with diffraction limited (or some techniques even better) spatial resolution and its spectral resolution reveals not only different chemical compounds but even different crystallinity or differences caused by mechanical stress. The presentation introduces basic principles and applications of confocal Raman imaging. On several application examples is demonstrated performance and sensitivity of Witec confocal Raman microscopic systems.

Fig.1. Family of WITec Raman microscopes.

PROTEIN OLIGOMERIZATION: Characterization of oligomeric state under varying conditions using the same assay in plasma and buffer

J. Uskoba[1], N. Mirza[2] and R. Marrabini[2]

[1] BioTech a.s., Služeb 4, Praha 10, 108 00.
[2] FIDA biosystems ApS, Generatorvej 6, 2860 Søborg.

e-mail: uskoba@ibiotech.cz

The active state of many proteins, including many drug targets, primarily exists as dimers or oligomers. Understanding the conditions under which oligomerization happens is paramount in drug development, formulation, and bioprocessing. In this work, we have analyzed an injectable therapeutic protein which can appear as monomer, dimer and tetramer; of which only the latter binds to its target receptor. As the protein is active in the bloodstream, we also performed experiments in 90% plasma to simulate physiological conditions. All the experiments were conducted, using a Fida 1 instrument, enabling accurate detection of protein size and size changes under different conditions. A distinctive feature of the Fida 1, is the possibility of analyzing directly in crude matrices such as plasma and serum.

Materials and Methods:

Fida 1 instrument with 480 nm ex LED fluorescence detection for binding experiments. Fidabio standard capillary (i.d.: 75 µm, LT: 100 cm, Leff: 84 cm). Flow-Induced-Dispersion-Analysis was performed by filling the capillary with the analyte (buffer or unlabeled POI), followed by an injection of 40nL of POI-alexa488 or preincubated POI alexa488+POI, which was mobilized towards the detector at 400 mbar.

I. Effect of ionic strength:
   Acetate phosphate buffer, 0.03% Pluronic Acid F127, pH 5,0. NaCl was titrated from 0,5 to 150 mM. Protein of interest (POI) was used as the indicator at 25 nM, labeled with Alexa Fluor® 488 Protein Labeling Kit from ThermoFisher Scientific.
II. Effect of pH:
   Acetate phosphate buffer, 0.03% Pluronic Acid F127, 100 mM NaCl. pH was varied from 3.5 to 7.2 in the pH titrations. Protein of interest (POI) was used as the indicator at 25 nM, labeled with Alexa Fluor® 488 Protein Labeling Kit from ThermoFisher Scientific.
III. Sample matrix: Buffer & 90 % plasma:
   Acetate phosphate buffer, 0.03% Pluronic Acid F127, 100 mM NaCl, pH 5,0. POI- Alexa488 was kept constant at 10 nM, and unlabeled-POI was titrated from 10nM to 16µM, using standard buffer or plasma as matrix.

Results and discussion:

Effect of ionic strength

Fig. 1A reveals the impact on size with variation in NaCl concentration. Below 10 uM, the size corresponds to that of a monomer. From 10 uM NaCl upwards, the Rh increases from the monomeric size of 3 nm as more and more multimeric forms assemble. The 10 different titration points have an average error of only ±0.077nm, which is between 1-1.5% of the measured Rh.

Effect of pH

Acetate phosphate buffer, 0.03% Pluronic Acid F127, 100 mM NaCl. pH was varied from 3.5 to 7.2 in the pH titrations. Protein of interest (POI) was used as the indicator at 25 nM, labeled with Alexa Fluor® 488 Protein Labeling Kit from ThermoFisher Scientific.

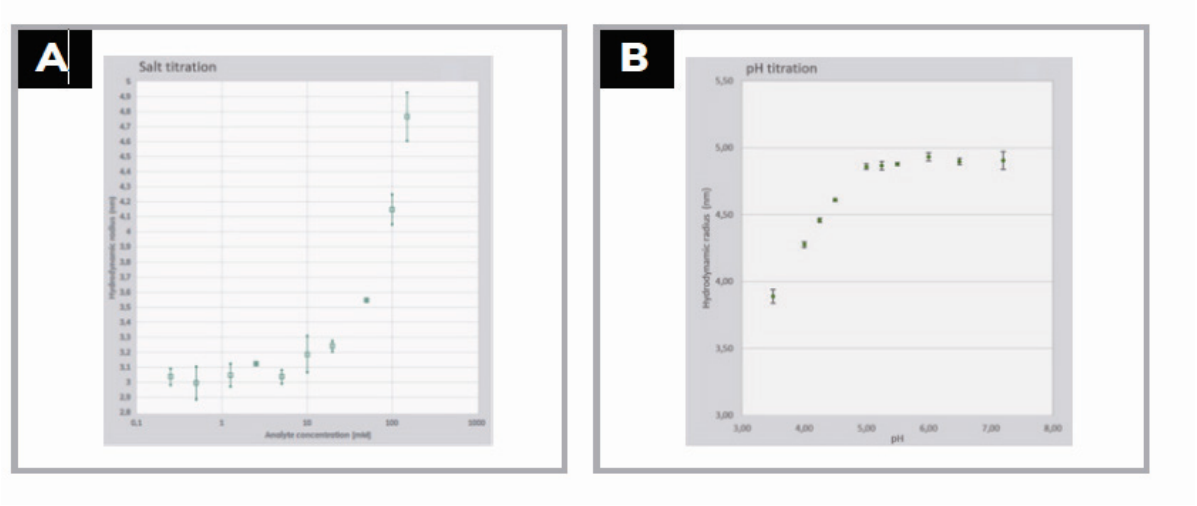

Fig. 1. (A) Rh of POI-Alexa488 at 25nM, pH 5 Acetate phosphate buffer, NaCl was titrated from 0.5 to 150 mM at 25°C. (B) pH titration where the Rh of POI-Alexa488 was measured from pH 3.5 to 7.2.

Sample matrix: Buffer & 90 % plasma

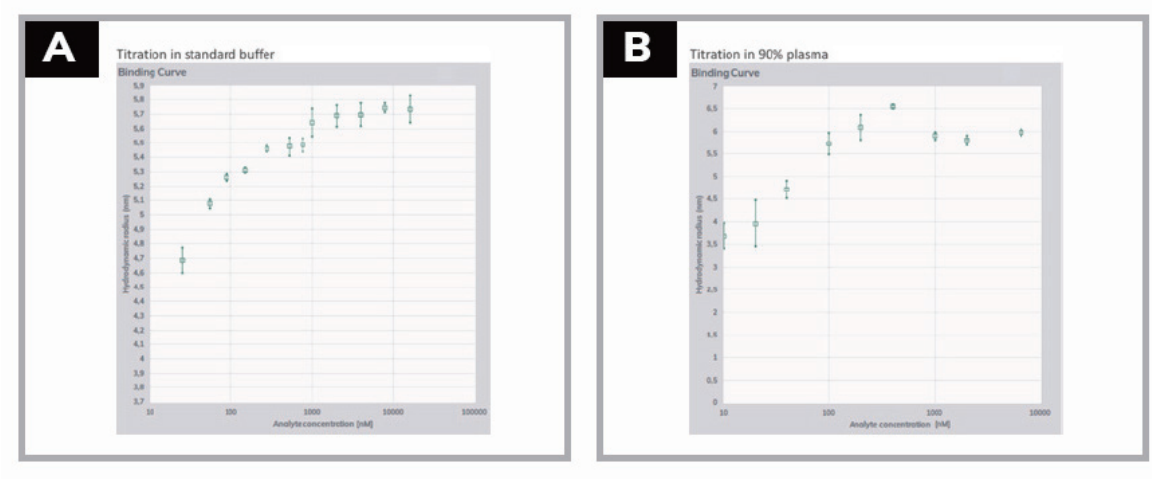

Fig. 2. (A) POI titration from 0-16 µM in buffer; (B) POI titration in 90% plasma.

Conclusions

Oligomerization of proteins is known to occur for many systems. However, the impact of environmental parameters such as Ionic strength, pH and sample matrix is notoriously hard to assess using a single methodology. The FIDA technology enables easy and reliable assessment of the oligomeric state of protein drug targets in varying assay conditions. In addition, it can confirm the oligo- meric state of the protein in crude matrices such as plasma thus providing important information on protein's confirmation in near physiological conditions. Fida 1 therefore can be used to conveniently optimize protein condition for example in formulation studies and bioprocessing routines.

Acknowledgement
This work was supported by FIDA Biosystems for internal purpose.

POSTER PRESENTATIONS

SERS detection of airborne samples

G. Bánó[1], M. Repovská[2], P. Slepčíková[2], A. Jutková[2], A. Hovan[1] and P. Miškovský[2]

[1] *Department of Biophysics, P. J. Šafárik University in Košice, Jesenná 5, Košice, Slovakia.*
[2] *Saftra Photonics s.r.o., Moldavská cesta 51, Košice, Slovakia.*

e-mail: gregor.bano@upjs.sk

Gas-phase samples containing volatile compounds and/or aerosol droplets are critical in a wide range of healthcare, agricultural and food-related applications. As examples, we can mention the detection of microorganisms in air, vapors arising from rotten fruits and vegetables for food quality control, or the problems of harmful airborne aerosol droplets during pesticide spraying in the fields.

Surface-enhanced Raman Spectroscopy (SERS) is a sensitive analytical tool for detecting low levels of molecules adsorbed on or near structured metal surfaces. SERS is usually used to detect molecules in liquid phase solutions or on solid samples. Until now, much less has been done in SERS detection of airborne samples [1, 2].

The current work aims to analyze gas-phase samples by SERS detection. The proposed solution is based on a tabletop Raman spectrometer (Ramascope) that has been adapted for SERS detection on 5x5 mm SERS active silicon chips. The chip surface is functionalized with metal nanoparticles to provide the required SERS enhancement and is exposed to gas phase samples. The SERS spectra of adsorbed molecules are detected.

The method was tested with samples of volatile organic compounds including rotten vegetables (garlic), fruits (apples) and cereals (wheat). The preliminary results proved the high sensitivity of the proposed method.

Acknowledgement
This work was supported by the Slovak Research and Development Agency, grant APVV-19-0580 and by the Horizon Europe, call HORIZON-CL6-2021-FARM2FORK-01, type of action HORIZON RIA, proposal acronym PURPEST, No. 101060634 (by P. M.).

References

[1] J. Choi, J. Lee and J. H. Jung, Biosensors and Bioelectronics, 169 (2020), 112611.
[2] E-C. Lin, J. Fang, S-C. Park, F. Johnson and H. Jacob, Nature Communications, 4 (2013), 1636.

Structural characterization of amyloid fibrils of Tau variants by atomic force microscopy

Z. Bednáriková[1], O. Cehlár[2], S. Njemoga[2,3] and Z. Gažová[1]

[1] *Institute of Experimental Physics Slovak Academy of Sciences, Kosice, Slovakia.*
[2] *Institute of Neuroimmunology, Slovak Academy of Sciences, Bratislava, Slovakia.*
[3] *Faculty of Natural Sciences, Comenius University, Bratislava, Slovakia.*

e-mail: bednarikova@saske.sk

The formation and accumulation of amyloid fibrils represent key pathological features in over 50 human disorders, including neurodegenerative diseases and systemic amyloidoses. Despite significant research, much remains unknown regarding the relationship between the structural elements of fibrils and the pathology of amyloid-related diseases. While techniques such as cryo-EM and solid-state NMR offer high-resolution structural characterization of amyloid fibrils, they generally provide structural information of the average fibril ensembles in the sample under study. In this study, we present a structural characterization of individual populations of Tau variant amyloid fibrils using atomic force microscopy (AFM). The amyloid fibrils were formed in vitro from five fragments of tau (297–391, 306-391, 316-391, 321-391, 326-391). The fibrils formation was monitored using Thioflavin T assay, and resulting fibrils were visualized using NTegra atomic force microscope equipped with SNL-10 cantilever in air. Our data reveal that truncation of the tau sequence leads to the formation of fibrils with distinct morphologies and characteristics, with one tau variant failing to form amyloid fibrils altogether. Interestingly, one tau variant formed ThT-negative amyloid fibrils. These findings underscore the utility of individual particle structural analysis using AFM in providing valuable insights into the polymorphism of amyloid fibrils. Overall, our study sheds light on the diverse structural features of Tau variants amyloid fibrils.

Acknowledgement

This work was supported by the Slovak Research and Development Agency under the Contract no. APVV-22-0598; Slovak Grant Agency VEGA 02/0176/21; and COST Action ML4NGP and MVTS grant ML4NGP Slovakia.

Cardiac myocyte calcium transient and contractility in treadmill running female Zucker Diabetic Fatty rats

M. Cagalinec[1,2], I. Baglaeva[1], A. Zahradníková ml[1], B. Iaparov[1] and A. Zahradníková[1]

[1] *Dept. of Cellular Cardiology, Institute of Experimental Endocrinology, Biomedical Research Center, Slovak Academy of Sciences, Dúbravská cesta 9, 845 05 Bratislava, Slovakia.*
[2] *Centre of Excellence for Advanced Material Application, Slovak Academy of Sciences, Dúbravská cesta 9, 845 11 Bratislava, Slovakia.*

e-mail: michal.cagalinec@savba.sk

Introduction: Cardiovascular diseases represent the most common cause of death worldwide where sexual dimorphism seems to play an important role in the development of hypertrophic and dilated cardiomyopathy [1]. Obesity is one of the important risk factors of high blood pressure that may lead to cardiac hypertrophy and subsequent heart failure. In this regard, the Zucker Diabetic Fatty (ZDF) rat model represents a suitable model of obesity-induced cardiomyopathy. However, the vast majority of existing knowledge has been established in males [2, 3]. Independently, physical exercise is a well-known factor to improve cardiac performance under physiological and pathological conditions including obesity [1]. Focusing specifically on the ZDF model, it has been recently demonstrated that in males, treadmill running exercise increases the calcium sensitivity of myofilaments [4].

Aim: To analyze the parameters of calcium transients and contractility in left ventricular myocytes isolated from female ZDF rats after six weeks of forced running.

Methods: Lean (fa/+) and obese (fa/fa) female ZDF rats at the age of 12 weeks were divided into lean sedentary (LS, n=5), lean running (LR, n=5), obese sedentary (OS, n=6), and obese running (OR, n=4) groups. Treadmill exercise was performed 5 days/week, gradually increasing from 15 minutes at 9m/min, to 30 minutes at 18m/min for the first four weeks and then maintained at 30 minutes at 18m/min for two weeks. After six weeks, left ventricular myocytes were isolated by retrograde perfusion of the heart with Tyrode solution containing collagenase/protease [5]. To record the calcium transients, myocytes were loaded with the fluorescent calcium indicator Fluo-3/AM at a concentration of 2.5 μmol/l at room temperature for 15 min. The cells were then gently centrifuged at 300 RPM for 1 min and the supernatant was gradually replaced with a modified Tyrode solution containing 1.2 mmol/l $CaCl_2$. Myocytes were perfused with the same solution at a rate of 1 ml/min and electrically stimulated using the Myopacer current pulse generator at a rate of 1 Hz. Fluo-3 fluorescence (excitation at 488 nm, emission at 505 - 560 nm) was recorded by Zeiss LSM510 META inverted confocal microscope equipped with a 63×/1.4 NA Plan-Apochromat oil immersion objective. The signal was acquired using a line-scan protocol at a rate of 518 Hz [5]. The confocal data were transferred to an in-house developed automatic software [6] for the determination of the basal signal level, signal amplitude, signal duration at half-amplitude (*FDHM*), time to peak, 10-90% rise time and 90-10% decay time. The data were processed in a Python Notebook and statistically analyzed using a Linear Mixed Model (LMM) implemented in the lme4 library [7].

Results: Fig. 1 depicts calcium transient and myocyte shortening linescans recorded simultaneously (upper panel) and the corresponding derived traces (lower panel). The analysis showed clustering of the calcium transient amplitude and the myocyte maximal shortening

corresponding to individual animals, thus justifying the use of LMM for including the random effect of the animal into the statistical model. The p-values obtained using Kenward-Roger's approximation indicated that the effects of obesity and exercise on the parameters were not statistically significant, with all p-values > 0.05.

Conclusions: Neither exercise nor obesity had a significant effect on calcium signalling and contractility in isolated myocytes of female ZDF rats after six weeks of treadmill running.

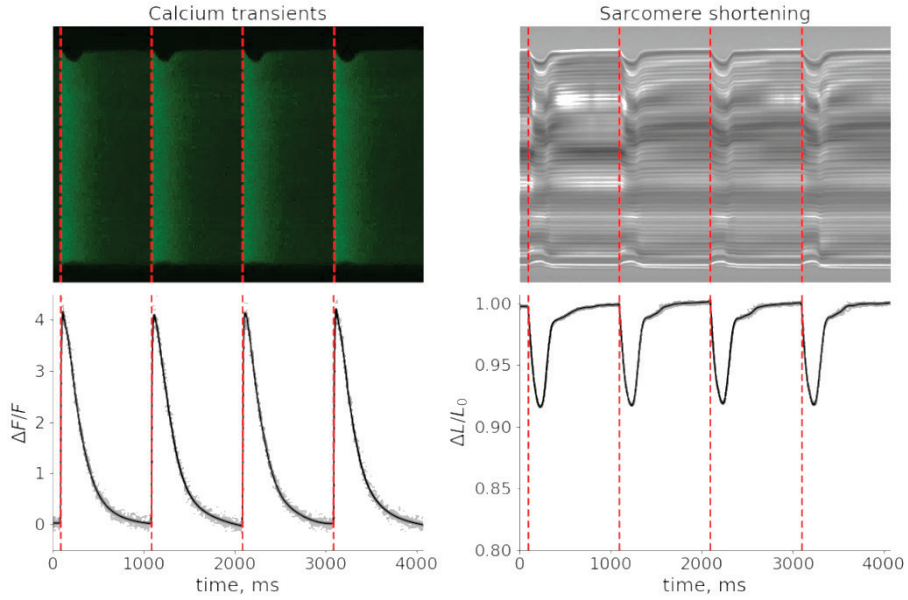

Fig. 1. Linescan images of stimulated myocyte contraction: left panel - Fluo-3 fluorescence, right panel – transmitted light intensity. Bottom graphs: left - calcium transients, right – myocyte shortening. The fitted traces (lines) are overlaid on the acquired data (points). Red dashed traces indicate individual stimulation pulses.

Acknowledgement
This work was supported by the projects VEGA 2/0182/21 from the Scientific Grant Agency of the Slovak Academy of Sciences and APVV-21-0473 from the Slovak Research and Development Agency of the Ministry of Education, Research, Development and Youth of the Slovak Republic. This work was performed during the implementation of the projects Building-up Centre for advanced materials application of the Slovak Academy of Sciences, ITMS: 313021T081 supported by the Integrated Infrastructure Operational Programme of the ERDF.

References
[1] A. Pellicia; et al, Rev. Esp. Cardiol., 74(6) (2021).
[2] L. J. Daniels; et al, Cardiovasc. Diabetol., 17(1) (2018).
[3] C. E. van den Brom; et al, Cardiovasc. Diabetol., 8(39) (2009).
[4] A. C. Greenman; et al, J. Appl. Physiol., 132(6) (1985) (2022).
[5] M. Cagalinec; et al, Front. Physiol. 172 (2019).
[6] I. Baglaeva; et al, Biophys. J., 122(3) (2023).
[7] https://cran.r-project.org/web/packages/lme4/index.html.

Comparison of Mono and Di-gradient Amphiphilic Poly(2-Oxazoline) s as a Drug Delivery System Using Curcumin as a Model Drug

S. Datta[1], J. Kronek[2], Z. Naďová[3], L. Timuľáková[3], P. Miškovský[1, 4]

[1]Center for Interdisciplinary Biosciences, Technology and innovation park, P. J. Safarik University in Košice, Jesenná 5, 041 54 Kosice, Slovakia.
[2]Department for Biomaterials Research, Polymer Institute of the Slovak Academy of Sciences, Dúbravska cesta 9, 845 41 Bratislava, Slovakia.
[3]Department of Biophysics, Faculty of Science, P. J. Safarik University in Košice, Jesenná 5, 041 54 Košice, Slovakia.
[4]SAFTRA Photonics sro., Moldavská cesta 51, 04011 Košice, Slovakia.

e-mail: pavol.miskovsky@upjs.sk

Polymeric nanoparticles (NPs) made up of amphiphilic copolymers and cancer therapeutics are increasingly applied as colloidal drug delivery systems [1]. For many years polyethylene glycol (PEG) remained as a gold standard for the preparation of polymeric NPs for drug delivery [2]. Recently the discovery of anti-PEG antibodies in some patients and so called ABC (accelerated blood clearance) effect of PEG-based formulation forced researchers to develop alternative next generation polymer therapeutics to overcome such medical restriction [3]. In the last decade Poly(2-oxazoline)s (POx) appeared as a viable alternative to PEG as an biomaterials for drug delivery due to their unique hemo and crypto compatibility [4]. Amphiphilic block copoly(2-oxazoline)s have been widely used to encapsulate and deliver drugs at the tumor site [5]. However, their multistep synthetic procedure may become the obstacle for potential application. Now a days gradient copoly(2-oxazoline)s are gaining more research interests [6]. The advantage of gradient copolymers is, that they can be synthesized in a single step in a straightforward way and thus could become an attractive alternative.

Efficient translation of polymeric NPs into clinical products requires strict control over the physicochemical properties of the engineered colloids, including NP size, drug loading and stability. In this study we investigated the influence of polymer architecture on the properties of drug formulation. Two different architectures of amphiphilic gradient copoly(2-oxazoline)s: hydrophilic-grad-hydrophobic (mono-gradient) and hydrophobic-grad-hydrophilic-grad-hydrophobic (di-gradient) were synthesized with varying content of hydrophobicity. Both architecture contains 2-ethyl-2-oxazoline (EtOx) as a hydrophilic monomer and 2-phenyl-2- oxazoline (PhOx) as a hydrophobic monomer. The drug solubilization ability of the synthesized copolymers were investigated using curcumin as a model drug. The negligible water solubility of curcumin (< 8μg mL^{-1}) makes it an ideal system for the encapsulation study which is focused to enhance the solubility of the hydrophobic drugs. Size and stability of self-assembled nanoparticles, loading of hydrophobic drug curcumin, as well as cytotoxicities of the prepared nanoformulations are thoroughly examined here.

Acknowledgements

This work has been supported by the Slovak Research and Development Agency under the contract APVV-19-0580 and APVV-20-0202 and by the Research Agency of the Slovak Republic, Operational program for Integrated infrastructure funder by ERDF, project BioPickMol, code: ITMS2014+: 313011AUW6.

References

[1] N. Kamaly; et al., Chem. Soc. Rev., 41 (2012), 2971-3010.
[2] K. Knop; in drug delivery, Angew. Chem. Int. Ed., 49 (2010), 6288-6308.
[3] G. Kozma; et al., Adv. Drug Deliv. Rev., 154 (2020), 163-175.
[4] R. Luxenhofer; et al., J. Control. Release, 153 (2011), 73-82.
[5] R. Luxenhofer; et al., Biomaterials, 31 (2010), 4972-4979.
[6] A. Zahoranová; et al., Adv. Health Mater., 10 (2021), 2001382.

Effect of molecular crowding on self-assembly of hybrid protein-DNA conjugates

V. Fedorová[1], M. Humenik[2] and K. Šipošová[1]

[1]*Department of Biophysics, Institute of Experimental Physics, SAS, Watsonova 47, 040 01 Kosice, Slovak Republic.*
[2]*Department of Biomaterials, University Bayreuth, Prof.-Rüdiger- Bormann-Str.1, D-95447 Bayreuth, Germany.*

e-mail: fedorova@saske.sk

In nature, remarkable for its spontaneity and low energy requirements, process called "self-assembly" was discovered. This process leads to the formation of ordered nanostructures, playing more or less important roles in living organisms [1]. Beside pathological proteins, associated with neurodegeneration, such as amyloid β peptide [2], many proteins are known to be responsible for the significant vital functions, i.e., forming of biofilms, spider webs or cell movement [3]. These insights inspire current biotechnological and biomedical research for processing of bio-inspired nanomaterials with additional features.

As initial aims of this work, synthesis of negatively charged conjugates consisting of recombinant spider protein eADF4(C16) and DNA oligonucleotides and subsequent experiments to verify the preserved ability of protein to form higher organized structures, were established. To achieve successful self-assembly, the eADF4(C16)-DNA conjugates were incubated in experimental conditions where kosmotropic ions, such as KPi, were added [4]. In order to obtain more complex view on self-assembly process of spider-DNA conjugates, the effect of molecular crowding has been evaluated, using different compounds, such as polyethylenglycol, chobimalt or dextran, for both protein and protein-DNA bioconjugates.

To achieve the results set, divergent biophysical and biochemical methods were used, including MALDI-TOF, HPLC and electrophoresis for the processing of synthesized conjugates. Further experiments consisted of kinetic absorbance measurements, circular dichroism and atomic force microscopy.

In agreement with previous research, our analysis shows that recombinant spider silk protein, even modified and conjugated with DNA, retains the unique natural capability to undergo spontaneous self-assembly and form highly organized fibrillar structures, with characteristic secondary structure motif. Moreover, we demonstrate that self-assembly process of bioconjugates used can be altered with respect to the kinetic rate and morphology of emerged structures with the use experimental conditions, e.g., temperature or adding of organic large molecules.

In conclusion, our study shows the potential of recombinant spider silk protein-DNA bioconjugates to form sophisticated, functional, highly programmable bio-nanomaterials with remarkable features via hybridization of the designed nucleic acids sequences and optimized conditions for aimed application, for example in biomedicine.

Acknowledgement
This work was supported by the grants VEGA 2/0034/22, SK-DAAD 2024-2025, Preveda OZ and SAIA n.o.

References

[1] N. H. Kim, H. Choi, Z. M. Shahzad, H. Ki, J. Lee, H. Chae & Y. H. Kim, Nano Convergence, 9 (2022), 1-17.
[2] F. Chiti & C. M. Dobson, Annual Review of Biochemistry, 86(1) (2017), 27-68.
[3] A. Bleem & V. Daggett, Biotechnology and Bioengineering, 114(1) (2017), 7-20.
[4] M. Humenik, A. M. Smith, S. Arndt & T. Scheibel, Journal of Structural Biology, 191(2) (2015), 130-138.

11th Slovak Biophysical Symposium, High Tatras, June 12 – 14, 2024

Ionic liquids cations impact on lysozyme properties

D. Fedunová, V. Vaník and Z. Gažová

[1] *Institute of Experimental Physics, Slovak Academy of Sciences, Watsonova 47, 040 01 Kosice, Slovakia.*

e-mail: fedunova@saske.sk

Ionic liquids (ILs) are novel solvents with increasing applications in biochemistry, biophysics, and biotechnology, particularly as stabilizers of proteins and protein-based products. ILs are organic salts that consists of an organic cation paired with an organic or inorganic anion. They are called "designer solvents" since the numerous possible anion and cation combinations are responsible for the extensive variation in their physicochemical properties (melting temperature, polarity, hydrophobicity, density, viscosity, solubility, and more) [1].

The aim of this work is to characterize ILs containing aliphatic and aromatic imidazolium-bound side chains with different geometries and hydrophobicities, in combination with the chloride anion, on the stability and activity of lysozyme (Lys). The main goal is to assess the mechanism of protein de/stabilization for biotechnological applications. In addition to being a model protein, Lys is used as an antibacterial and anti-inflammatory agent in medicine and the food industry [2]. The calorimetric measurement and bacteriolytic turbidity assay (*Micrococcus Lysodeikticus*) showed that

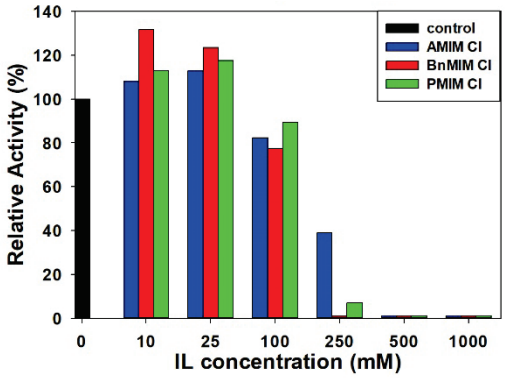

Fig. 1. Bacteriolytic activity of Lys at the presence of ILs with allyl (AMIM), propyl (PMIM) and benzyl (BnMIM) side chains.

all ILs up to 25 mM concentration enhanced the thermal stability and activity of Lys in order of benzyl > propyl > allyl. However, a decline in thermal stability and activity is observed at higher concentrations. Spectroscopic techniques (CD, FTIR) and fluorescence quenching revealed that at lower ILs concentrations, the native structure is maintained, but with increasing concentrations, the tertiary structure is altered. The interactions between selected ILs and Lys are not very strong. ILs mainly affected the microenvironment around Trp62 or Trp108, which are located in the active site of Lys.

In conclusion, selected ILs are capable of preserving the native state of Lys and enhancing its activity depending on the concentration. These findings underline the potential of selected ILs for further study in biotechnological applications.

Acknowledgement
This work was supported by the Slovak Research and Development Agency under the Contract no. APVV-22-0598; Slovak Grant Agency VEGA 02/0164/22 and 2/0176/21 and the Operational Programme Integrated Infrastructure, the project "NANOVIR ", ITMS: 313011AUW7, co-funded by ERDF.

References
[1] H. D. B. Jenkins, Sci. Prog., 94 (2011), 265–297.
[2] L. P. Dang, W. Z. Fang, Y. Li, Q. Wang, H. Z. Xiao and Z. Z. Wang, Appl Biochem Biotechnol., 169 (2013), 290-300.

SERS detection of the herbicide glyphosate in water and milk

F. Belén Fuenzalida[1], D. Jancura[1], P. Miškovský[2,3], S. Sanchez-Cortes[4], Z. Jurašeková[1]

[1] *Department of Biophysics, Faculty of Science, P. J. Šafárik University, Jesenná 5, 040 01 Košice, Slovakia.*
[2] *Technology and Innovation Park, P. J. Šafárik University, Jesenná 5, 040 01 Košice, Slovakia.*
[3] *SAFTRA Photonics, s.r.o., Moldavská cesta 51, 040 11 Košice, Slovakia.*
[4] *Institute of the Structure of Matter, IEM-CSIC, Serrano 121, 28006 Madrid, Spain.*

e-mail: zuzana.jurasekova@upjs.sk

Glyphosate (GPH), an amino-phosphonic analogue of the amino acid glycine, is a broad-spectrum systemic herbicide known especially under its trade name Roundup®. It was introduced for weed control in agricultural production fields in 1974 [1], and in the 20th century, its use increased dramatically due to the introduction of genetically modified glyphosate-resistant crops [2]. GPH was originally considered to be of low toxicity to microorganisms, animals, and humans [3]. However, in recent years, a large number of publications indicate possible harmful effects of GPH (and its metabolites) on the quality of soil and water and thus on the health of plants and animals [4-9] and have linked the consumption of GPH with possible harmful effects on human health. Toxicological studies indicate that chronic exposure to this herbicide is potentially carcinogenic [10-12] and can induce different diseases such as gluten intolerance, diabetes, heart disease, multiple sclerosis, Alzheimer's disease, autism, and birth defects [2, 4, 13, 14]. Besides, numerous studies on its harmfulness are still ongoing [7, 8, 10, 15-17].

Although the use of GPH is not banned currently (it is likely just a matter of time), its monitoring is becoming increasingly important [17-19]. For that, it is crucial to have a simple, fast, low-cost detection and quantification method on hand [4]. Raman spectroscopy, and especially surface-enhanced Raman spectroscopy (SERS), is a very potential analytical tool since it is highly sensitive, requires minimum sample preparation, can be used *in situ*, and provides very specific structural information [20-23]. In this context, SERS has already been used as both a powerful tool for ultrasensitive chemical analysis and an accessible and fast screening method, which makes it an appropriate technique to detect GPH molecules. Nevertheless, GPH SERS spectra show rather weak signals, leading to a relatively high limit of detection of GPH by a direct SERS method [4, 22, 23]. The reason is a high polarity of GPH molecules, which seriously hinders the approach of the molecules to the surface of metallic nanostructures.

In this work, we present an innovative method for the selective and sensitive detection of the GPH molecules which is based on the previous chemical modification of the GPH molecules to obtain molecules which demonstrates a significantly higher affinity towards nanoparticles, and thus can be detected even at low concentrations, since the corresponding final products are recognized by specific SERS spectra* [24]. On the base of the obtained results, we have proposed and described in details the mechanism of the chemical modification and subsequent detection of the GPH molecules by SERS. In addition, the relative intensity of the recorded SERS spectra allows us to use this method to assess the concentration range of the herbicide present in the analysed sample, or even to determine its quantity. We have also shown that the proposed method can be also used for glyphosate *on-site*

detection by using a portable Raman spectrometer (PickMol™ Ramascope developed by SAFTRA Photonics). Moreover, there are preliminary indications that the method can be even improved using nano-optical chips (PickMol™ Sensing chips developed and fabricated by SAFTRA Photonics). The method was already tested and successfully employed as a fast and soft screening method to analyze real water and milk samples.

*The developed method is the subject of the international application no. PCT/SK2023/050012 (Slovak patent application no. PP50028-2023) of the applicant SAFTRA photonics Inc.

Acknowledgement
This work was supported by the Ministry of Education, Science, Research and Sport of the Slovak Republic project APVV-19-0580.

References

[1] M. R. Jan, J. Shah, M. Muhammad, B. Ara, J. Hazard. Mater., 169 (2009), 742-745.
[2] S. O. Duke, Pest. Manag. Sci., 74 (2018), 1027-1034.
[3] H. J. Beckie, K. C. Flower, M. B. Ashworth, Plants, 9 (2020), 96.
[4] F. E. Belbin, G. J. Hall, A. B. Jackson, F. E. Schanschieff, G. Archibald, C. Formstone, A. N. Dodd, Nat. Commun. 10 (2019), 1-11.
[5] A. H. C. van Bruggen, M. M. He, K. Shin, V. Mai, K. C. Jeong, M. R. Finckh, J. G. Morris, Sci. Total Environ., 616–617 (2018), 255-268.
[6] S. O. Duke, B. Powles, Pest. Manag. Sci., 64 (2008), 319-325.
[7] M. Watts, P. Clausing, A. Lyssimachou, G. Schutte, R. Guadagnini, E. Marquez, (2016) https://pan-international.org/wp-content/uploads/Glyphosate-monograph.pdf.
[8] M. Mertens, S. Höss, G. Neumann, J. Afzal, W. Reichenbecher, Environ. Sci. Pollut. Res. Int., 25 (2018), 5298-5317.
[9] J. Li, R. J. Smeda, B. A. Sellers, W. G. Johnson, Weed Sci., 53 (2005), 153-159.
[10] K. Barnor, J. Caton, D. Miljkovic, J. Policy Model., 45 (2023), 103-120.
[11] Q. L. Zhang, X. Liu, M. T. Gao, X. Li, Y. F. Wang, Y. Y. Chang, X. M. Zhang, Z. L. Huo, L. Zhang, J. J. Shan, F. Zhang, B. L. Zhu, W. F. Yao, Chemosphere, 298 (2022), 134308.
[12] K. Gandhi, S. Khan, M. Patrikar, A. Markad, N. Kumar, A. Choudhari, P. Sagar, S. Indurkar, Environ. Challenges, 4 (2021), 100149.
[13] L. Zhang, I. Rana, R. M. Shaffer, E. Taioli, L. Sheppard, Mutat. Res. Mutat. Res., 781 (2019), 186-206.
[14] F. Zhang, Q. Zhang, X. Liu, M. Gao, X. Li, Y. Wang, Y. Chang, X. Zhang, Z. Huo, L. Zhang, J. Shan, B. Zhu, W. Yao, Environ. Int., 171 (2023), 107682.
[15] J. O. Ighalo, O. J. Ajala, A. G. Adeniyi, E. O. Babatunde, M. A. Ajala, Environ. Sci. Pollut. Res., 28 (2021), 2655-2668.
[16] N. de Castilhos Ghisi, N. R. Zuanazzi, T. M. C. Fabrin, E. C. Oliveira, Sci. Total Environ., 733 (2020), 139359.
[17] G. R. Group, https://www.glyphosate.eu/useful-information/environment-biodiversity/environmental-monitoring-of-glyphosate-ampa-metabolite-in-the-eu/.
[18] H. Greim, D. Saltmiras, V. Mostert, C. Strupp, Crit. Rev. Toxicol. 45 (2015), 185-208.
[19] S. Rani, M. T. Sørensen, J. Estellé, S. J. Noel, N. Nørskov, U. Krogh, L. Foldager, O. Højberg, Microbiol. Spectr., 11 (2023), e0061523.
[20] J. Xu, S. Smith, G. Smith, W. Wang, Y. Li, Food Control, 106 (2019), 106710.
[21] K. Kocadal, F. B. Alkas, D. Battal, S. A. Saygi, Arch. Environ. Prot., 48 (2022), 89-98.
[22] A. Feis, C. Gellini, M. Ricci, L. Tognaccini, M. Becucci, G. Smulevich, Vib. Spectrosc., 108 (2020), 103061.
[23] F. B. Fuenzalida, P. Mškovský, S. Sánchez-Cortés, Z. Jurašeková, Molecules, (Submitted).
[24] F. Belén Fuenzalida, P. Slepčíková, M. Repovská, A. Jutková, M. V. Cañamares, P. Miškovský, Z. Jurašeková, S. Sánchez-Cortés, ACS Applied Nano Materials, (Under revision).

11th Slovak Biophysical Symposium, High Tatras, June 12 – 14, 2024

A strategy to examine 'coupled gating' of cardiac ryanodine receptors by ultrastructural imaging

J. Gaburjáková , E. Krejčíová, and M. Gaburjáková

Institute of Molecular Physiology and Genetics, Centre of Biosciences, Slovak Academy of Sciences, Dúbravská cesta 9, 840 05 Bratislava, Slovakia.

e-mail: jana.gaburjakova@savba.sk

A common feature for ion channels is their ability to aggregate into dense clusters, enabling them to achieve a hierarchically higher level of functioning and regulation [1]. Numerous studies demonstrated the existence of 'coupled gating' when two or more clustered ion channels open and close in a synchronized fashion. Information about the functional state of one ion channel is likely allosterically transmitted to nearby channels via direct physical interactions, which are strongly facilitated by the aggregation of ion channels into clusters [2, 3]. Electrophysiological experiments, in combination with mathematical modelling and advanced imaging techniques, have shown that coupled gating of ion channels is a universal phenomenon that can influence all levels of bioelectrical signalling, rather than independent gating [4]. At the single-channel level, coupled gating has also been documented for cardiac ryanodine receptors (RyR2) [5, 6]. These intracellular Ca^{2+} channels are critically involved in cardiac Ca^{2+} signalling. They mediate a massive release of Ca^{2+} from the sarcoplasmic reticulum, leading to activation of cardiac contraction. *In vivo* as well *in vitro*, RyR2 channels self-organize into larger clusters, constituting 'release units' [2, 3, 7]. Small regions within these clusters exhibit a 'checkerboard-like' pattern, wherein approximately square-shaped RyR2 channels appear to be in proximity at the corners, thus supporting the concept of allosteric interactions [7].

To link the coupled gating phenomenon with a specific RyR2 arrangement, we attempted to develop a protocol for processing RyR2 channels incorporated into a planar lipid membrane for ultrastructure imaging by electron microscopy (EM).

The RyR2 channels were isolated from rat cardiac ventricles by differential centrifugation and yielded microsomes were fused with a planar lipid membrane (BLM) painted across a small aperture within the wall of a polystyrene cup. After a successful reconstitution, we tested RyR2 response to known cytosolic regulators such as caffeine, Ca^{2+} or ATP. To process the BLM for imaging by EM, the integrity of lipid membrane with embedded RyR2 channels has to be preserved. For this purpose, we perfused the cytosolic side of channels with a fixing solution for 5 minutes, followed by a 10-15 minute break. During this period, we continuously monitored the presence of the BLM in the aperture by ion current recording. Subsequently, the BLM still present was exposed to the same fixing solution from the luminal side of RyR2 channels for an additional 10-15 minutes. After this, the polystyrene cup was allowed to dry and visually checked for the presence of the BLM. Since the BLM setup cannot be moved to the fume hood, we used non-toxic or, at least, less harmful fixators to avoid exposure to their toxic vapors. Particularly, we tested a 2.5% glyoxal solution and 9% sucrose dissolved in PBS. While the glyoxal solution caused rupture of the BLMs after 5 minutes of incubation, sucrose fixation was successful. We stored polystyrene cups with sucrose-coated BLMs at 4−8°C for over 2 weeks without any visible damage.

From our results, it is evident that sucrose fixation provides sufficient long-term stability for the BLM painted across a small aperture within the wall of a polystyrene cup. In the future, we plan to test trehalose, a non-reducing disaccharide that has been used for the optimal fixation of lipid monolayers enriched in proteins for electron crystallographic analysis. The biggest challenge, however, is to mount the fixed BLM with RyR2 channels onto a carbon-coated copper grid covered with formvar and safely transport it to the EM facility for ultrastructural analysis.

Acknowledgement
This work was supported by VEGA 2/0010/24 and APVV-22-0061.

References

[1] R. E. Dixon, M. F. Navedo, M. D. Binder, L. F. Santana, Physiological Reviews, 102 (2022), 1159-1210.
[2] D. Sato, G. Hernández-Hernández, C. Matsumoto, S. Tajada, C. M. Moreno, R. E. Dixon, S. O'Dwyer, M. F. Navedo, J. S. Trimmer, C. E. Clancy, M. D. Binder, L. F. Santana, Journal of General Physiology, 151 (2019), 1116-1134.
[3] P. Pfeiffer, A. V. Egorov, F. Lorenz, J.-H. Schleimer, A. Draguhn, S. Schreiberet, eLife, 9 (2020), e49974.
[4] M. Levin, Cell, 184 (2021), 1971-1989.
[5] S. O. Marx, J. Gaburjakova, M. Gaburjakova, C. Henrikson, K. Ondrias, A. R. Marks, Circulation Research, 88 (2001), 1151-1158.
[6] J. Gaburjakova, M. Gaburjakova, Biochimica et Biophysica Acta, 1838 (2014), 867-73.
[7] Ch.-Ch. Yin, H. Han, R. Wei, F. A. Lai, Journal of Structural Biology, 149 (2005), 219-224.

11th Slovak Biophysical Symposium, High Tatras, June 12 – 14, 2024

Interplay of *Origanum vulgare* components in suppressing human insulin amyloid aggregation

M. Gančár[1], S. Bittner Fialová[2], E. Kurin[2], S. Dokupilová[2], M. Nagy[2], and Z. Gažová[1]

[1]*Institute of Experimental Physics, Slovak Academy of Sciences, Watsonova 47, 040 01 Kosice, Slovakia*
[2]*Faculty of Pharmacy, Comenius University Bratislava, Odbojarov 10, 832 32 Bratislava, Slovakia*

e-mail: gancar@saske.sk

Exogenous insulin, employed therapeutically for diabetes management, has been observed to precipitate into insoluble amyloid deposits proximal to the site of administration [1]. A promising approach in therapeutic intervention entails the inhibition of amyloidogenesis and/or facilitation of amyloid clearance. Certain bioactive compounds inherent in medicinal herbs, particularly small natural molecules, have demonstrated potential as amyloid formation inhibitors [2].

Origanum vulgare extracts, abundant in flavonoids and phenolic compounds, have exhibited a spectrum of pharmacological activities encompassing antimicrobial, antiparasitic, antioxidant, anti-inflammatory, and antispasmodic properties both *in vitro* and *in vivo* [3]. This study assessed the anti-amyloidogenic properties of the *Origanum vulgare* aqueous extract lyophilizate (referred to as LYO), its principal constituents (lithospermic acid (LA), rosmarinic acid (RA), luteolin-7-diglucuronide (L7dG), oreganol A (OA)), and their equimolar mixtures as identified via LC-MS/MS, against human insulin. The efficacy of anti-amyloid activity was quantified using Thioflavin T fluorescence (IC_{50} values), and formation of amyloid aggregates has been described through kinetic parameters. Furthermore, atomic force microscopy (AFM) was employed to visually inspect the studied samples (Fig. 1), while molecular docking was conducted to interpret the observed synergistic or antagonistic interactions.

Notably, LA and L7dG emerged as the most potent standalone inhibitors and their mixture, LA:L7dG, retained the inhibitory potential of its individual constituents. Intriguingly, a mixture of LA and OA (LA:OA) exhibited significant synergism, whereas OA demonstrated negligible efficacy when assessed independently and, furthermore, displayed antagonism in mixture with L7dG. Noteworthy, none of the compounds or mixtures studied approached the anti-amyloidogenic efficacy of LYO in terms of kinetics inhibition.

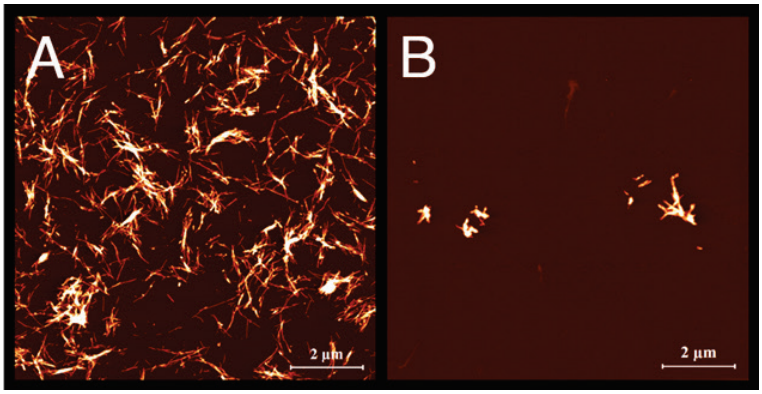

Fig. 1. AFM images of (A) human insulin amyloid aggregates without treatment and (B) aggregates formed in the presence of 1mM LYO (*Origanum vulgare* water extract lyophilizate). The images are unfiltered, 10x10 µm, and contain a scale representing 2 µm.

Acknowledgement

This work was supported by the Slovak Research and Development Agency under Contract no. APVV-22-0598 and Slovak Grant Agency VEGA 2/0176/21, 02/0164/22, 1/0170/24 and BIOVID-19 (ITMS2014+ 313011AVG3) supported by OPII and funded by the ERDF.

References

[1] P. Alam; et al., Arch. Biochem. Biophys., 621 (2017), 54-62.
[2] K. Vus; et al., J. Mol. Liq., 276 (2019), 541-552.
[3] R. Pezzani; et al., Phytochem. Rev., 16 (2017), 1253-1268.

11th Slovak Biophysical Symposium, High Tatras, June 12 – 14, 2024

Antioxidant nanozymes - assessment of ROS absorption potential by CeO_2 particles conjugated with activated carbon and magnetite in composite systems

I. Garčárova[1], M. Drajnová[1,2], Y. Shlapa[3], A. Belous[3], A. Musatov[1], K. Šipošová[1]

[1] *Department of Biophysics, Institute of Experimental Physics, SAS, Kosice, Slovak Republic.*
[2] *Department of Biochemistry, Institute of Chemistry, Faculty of Science, P. J. Safarik University in Kosice, Slovakia.*
[3] *V. I. Vernadsky Institute of General & Inorganic Chemistry of the NAS of Ukraine, Kyiv, Ukraine.*

e-mail: garcarova@saske.sk

In a biological context, reactive oxygen species (ROS) are formed as a natural by-product of cellular aerobic metabolism. Oxidative stress reflects the imbalance between reactive oxygen species formation and cellular antioxidant capacity due to enhanced ROS generation and/or dysfunction of the antioxidant system. Because of their highly reactive nature, ROS can modify other oxygen species, proteins, nucleic acids, lipids, and other molecules. Their ability to be scavenged is important in combating serious oxidative stress-related diseases, such as aging, cancer, diabetes mellitus, or neurodegenerative diseases, including Alzheimer's. Antioxidants are widely preferred to combat oxidative stress and can play an important role in delaying the onset as well as reducing the progression of neurodegeneration. However, despite decades of intensive study, highly successful treatment of both oxidative stress and protein misfolding in neurodegenerative diseases is still missing. This opens the door for nanomaterials with unique physicochemical properties, tenability, and multifunctionality to improve the understanding and treatment of diseases. Additionally, composite nanomaterials are being developed to improve therapeutic/theranostic techniques, that appear to be forging a path toward a multifaceted approach to the pathologies of age-related diseases [1, 2].

Our attention was focused on the evaluation of the anti-oxidant properties of redox-active particles/composites, those consisting of magnetic magnetite (Fe_3O_4) core, activated carbon, and cerium dioxide particles as well. The antioxidant activity of particles and composites NPs, i.e. the ability to scavenge reactive oxygen species, was tested *in vitro*, paying special attention to the pseudo-enzymatic activities such as catalase-, oxidase- and superoxide dismutase (SOD)-like activity. The intrinsic ability of CeO_2 particles, carbon@CeO_2, and Fe_3O_4@CeO_2 composites to decompose hydrogen peroxide has been evaluated using a colorimetric method based on monitoring of chromogenic substrate DPD oxidation. To assess the impact of the composition of carbon@CeO_2 and Fe_3O_4@CeO_2 particles on SOD mimetic activity, the newly prepared composites have been tested using a commercial colorimetric SOD kit, where the generation of superoxide radical anions was initiated by adding xanthine oxidase. The nascent superoxide radicals reduced a water-soluble tetrazolium salt to formazan. The SOD-mimicking particles catalyse the dismutation of the superoxide anion into hydrogen peroxide and molecular oxygen, resulting in decreased WST-1 reduction as monitored by absorbance at 450 nm.

Our results demonstrate well-defined valence- and size-dependent catalase- and SOD-like activity. The obtained results suggest that the main catalytic activity arises from the CeO_2 part of composites. These data allow us to hypothesize that catalase-like activity is a result of the interplay

between carbon or Fe_3O_4 and CeO_2 particles and can be connected with Ox-Red chemical processes during the synthesis of the composites. We can assume that the major catalytic activity arises from the shell of NCPs; however, the involvement of carbon or magnetite core cannot be excluded. Additionally, the CeO_2 "shell" is probably not completely uniform. The coupling of both carbon or Fe_3O_4 and CeO_2 led to higher catalytic activity than any of individual particles, probably due to synergistic catalytic mechanism. Analysis of the published and current results allows us to predict the anti-oxidant of CeO_2-containing composites based on size and surface chemistry which can be manipulated/controlled by the adjustment of synthesis conditions [3-5].

Acknowledgement
This work was supported by the grants VEGA 2/0034/22 and APPV 19-324.

References
[1] M. Pichla; et al., Oxid. Med. Cell. Longev, (2020), 3534570.
[2] A. Kakinen; et al., Nanoscale Horiz, 6 (2021), 95-119.
[3] Y. Shlapa; et al., Colloids Surf. B, 220 (2022), 112960.
[4] K. Siposova; et al., Biomedicines, 10(5) (2022), 942.
[5] Y. Shlapa; et al., ACS Appl. Mater. Interfaces, 15(42) (2023), 49346-49361.

Involvement of mitochondrial respiratory complexes in hydrogen sulfide utilization

M. Grman, A. Misak, K. Ondrias and L. Tomasova

Biomedical Research Center of the Slovak Academy of Sciences, Dubravska cesta 9, 845 05 Bratislava, Slovakia.

e-mail: marian.grman@savba.sk

Hydrogen sulfide (H_2S) belongs to the family of gaseous signalling molecules together with nitric oxide and carbon monoxide. For eight decades it has been known that hydrogen sulfide inhibits mitochondrial respiration by the reversible inhibition of cytochrome *c* oxidase [1, 2]. Recent studies have also demonstrated its role in the modulation of mitochondrial bioenergetics, where it could serve as a potential inorganic substrate for energy production through sulfide: quinone oxidoreductase (SQR) [3, 4]. However, the involvement of individual respiratory complexes was not studied.

In the present work, we therefore decided to investigate the effect of H_2S and also polysulfides (Na_2S_n, n = 2-4) on the respiration of mitochondria in the presence of respiratory complexes inhibitors.

Mitochondria were isolated from the liver of adult male Wistar rats by differential centrifugation. Mitochondrial respiration was measured polarographically using the Clark-type oxygen electrode with a Strathkelvin Mitocell MT 200A system and analyzed by the home-made template.

We found that complexes II, III and IV are most involved in the utilization of sulfides by mitochondria. After their blocking there was a gradual decrease in oxygen consumption after the addition of sulfides. In conclusion, our results thus suggest that sulfide species may serve as inorganic substrate not only through SQR, but also through the other parts of mitochondrial respiratory chain.

Acknowledgement
This work was supported by the Slovak Research and Development Agency, grant no. APVV-19-0154 and the Scientific Grant Agency of the Ministry of Education, Science, Research and Sport of the Slovak Republic and the Slovak Academy of Sciences, grant no. VEGA/2/0091/21 and VEGA/2/0066/23.

References

[1] B. C. Hill, T. C. Woon, P. Nicholls, J. Peterson, C. Greenwood and A. J. Thomson, Biochemical Journal, 24 (1984), 591-600.
[2] P. Nicholls, D. C. Marshall, C. E. Cooper and M. T. Wilson, Biochem. Society Transactions, 41 (2013), 1312-1316.
[3] A. P. Landry, D. Ballou and R. Banerjee, ChemBioChem, 22 (2021), 949-960.
[4] F. Bouillaud, Biomolecules, 12(361) (2022).

11th Slovak Biophysical Symposium, High Tatras, June 12 – 14, 2024

Lithium diminishes the reserve respiratory capacity of cardiac cell line

M. Grman[1], K. Polcicova[1], K. Ondacova[2], J. Stepanovsky[3], A. Horvath[4], and Z. Sevcikova Tomaskova[2]

[1] *Biomedical Research Center SAS, Bratislava, Slovakia.*
[2] *Centre of Biosciences SAS, Bratislava, Slovakia.*
[3] *Faculty of Chemical and Food Technology STU, Bratislava, Slovakia.*
[4] *Faculty of Natural Sciences CU, Bratislava, Slovakia.*

e-mail: virukava@savba.sk

Lithium is used for the treatment of bipolar disorder to stabilize the mood changes. Lithium has a narrow therapeutic index and its serum level should be kept within the range of 0.4 to 1.2mM. The treatment with lithium is associated with low incidence of adverse effects on the cardiac function, which may lead to severe cardiac condition. The increased reactive oxygen species level and altered metabolic activity (activity of dehydrogenases) were observed in isolated cardiomyocytes after up to 3 hours of incubation in the therapeutic level of lithium. The adverse effects are reported in patients that have higher than the therapeutic concentration of lithium in blood (1.5 - 3mM).

We aimed to determine the effect of the exposition to 2mM lithium during 48 hours on the cardiomyoblasts (h9c2) cell line, which is a commonly used model of cardiac cells. We focused on the mitochondrial bioenergetics and morphology of the mitochondrial network, which reflects the function of mitochondria.

We measured the oxygen consumption rate of the intact cells using Clark electrode. The mitochondrial network was visualized using 25nM TMRM fluorescent dye by confocal imaging. The mitochondrial network morphology was analyzed using Mitochondria analyzer plugin in ImageJ [1]. The level of reactive oxygen species was determined using MitoSOX fluorescent dye and confocal image analysis. The protein level of succinate dehydrogenase was determined using western blot and qPCR analysis, its activity was quantified using absorption spectroscopy.

At first, we measured the oxygen consumption rate of intact cells using different modulators of the mitochondrial respiratory chain. We determined the maximal respiratory capacity that comprises different types of oxygen-consuming reactions: ATP-linked respiration, reserve respiratory capacity (RRC), proton leak, and non-mitochondrial respiration. We found that the cells treated with lithium had compromised biophysical parameters of respiration: the cells exhibited significantly decreased RRC to 51% of the control cells (in absolute values of oxygen consumption rate per 10^6 cells). The maximal respiratory capacity itself was lowered in lithium-treated cells to 78% of control. The ATP-linked respiration, which reflects the cells' energetic needs, remained unchanged. Altered mitochondrial function is often reflected in the plasticity of the mitochondrial network [2, 3]. Therefore, we analyzed the mitochondrial network morphology – number of junctions, the mitochondrial area per cell, the number of isolated mitochondria, and mitochondrial morphological factors. Though the mitochondrial network in the presence of lithium was unaltered in comparison to control cells, the unhealthy state of the mitochondrial energetics was indicated by the increased level of superoxide radicals in mitochondria. The RRC is mainly regulated by succinate dehydrogenase

(SDH) activity [4, 5]. The drop of RRC in the presence of lithium was, however, not mediated by direct inhibition of SDH activity, nor did lithium affect the expression of SDH on the protein level. Thus, the marked drop in RRC must be mediated by other components of the electron transport chain or substrates that are needed for the building of RRC.

Our results indicate that the increased level of lithium can make the cardiac cells prone to failure, as the cells do not have the reserve to meet higher energetic demands. It can be the reason for the severity of the adverse effects of lithium.

Acknowledgement
The work was supported by VEGA 2-0051-23.

References

[1] A. Chaudhry, R. Shi, D. S. Luciani, Am. J. Physiol. Endocrinol. Metab., 318 (2020), E87-E101.
[2] G. Benard, N. Bellance, D. James, P. Parrone, H. Fernandez, T. Letellier, R. Rossignol, J. Cell Sci., 120 (2007), 838-848.
[3] L. L. Xie, F. Shi, Z. Tan, Y. Li, A. M. Bode, Y. Cao, Cancer Sci., 109 (2018), 3686-3694
[4] P. Marchetti, Q. Fovez, N. Germain, R. Khamari, J. Kluza, FASEB J., 34 (2020), 13106-13124.
[5] J. Pfleger, M. He, M. Abdellatif, Cell Death Dis., 6 (2015), e1835.

11th Slovak Biophysical Symposium, High Tatras, June 12 – 14, 2024

The impact of *ERG6* gene deletion on ergosterol synthesis and phospholipid content in the human pathogen yeast *Candida glabrata*

J. Jacko[1], M. Morvová Jr.[1], M. Velísková[1], N. Toth-Hervay[2], D. Eliaš[2], Y. Gbelská[2], M. Balážová[3] L. Šikurová[1]

[1] *Faculty of Mathematics, Physics and Informatics, Comenius University, Mlynská dolina F1, 842 48 Bratislava, Slovakia.*
[2] *Faculty of Natural sciences, Comenius University, Ilkovičova 6, 842 48 Bratislava, Slovakia.*
[3] *Institute of Animal Biochemistry and Genetics, Centre of Biosciences SAS, Dúbravská cesta 9, P.O.BOX 63, Slovakia.*

email: juraj.jacko@fmph.uniba.sk

Candida glabrata is human opportunistic pathogen. It´s yeast known for its ability to cause infections in humans, especially in individuals with weakened immune system. One of the characteristic features of *Candida glabrata* is its natural resistance to many antifungal agents, making it a serious health concern, particularly in the treatment of invasive yeast infections. *Candida glabrata* exhibits resistance to antifungal agents for various reasons. One of the main factors is its ability for rapid adaptation and development of drug resistance. Another factor may be the high expression of its own enzymes, which can metabolize or inactivate antifungal agents, thereby reducing their effectiveness. Additionally, *Candida glabrata* can modify its cell membranes to make them less permeable to drugs, leading to a limitation of their effect [1]. The plasma membrane is important cell organelle and it plays a notable role in drug resistance mechanisms. Its properties depend on the lipid and protein composition. Changes in membrane composition leads to changes in azole antifungals susceptibility [2]. It has been shown that altered plasma membrane phospholipid and sterol composition can influence the membrane barrier function [3].

The aim of our study is to determine the impact of *ERG6* gene deletion on the membrane properties of *Candida glabrata*. The *ERG6* gene is a key enzyme in the synthesis of ergosterol, an important component of yeast cell membranes. Investigating its role and influence on membrane characteristics can provide valuable insights into resistance mechanisms and potential therapeutic targets. In our study we focused on the synthesis of ergosterol, its precursors, and the phospholipid composition. High-performance liquid chromatography (HPLC) was used to analyze the composition of selected sterols in cell membranes, while thin-layer chromatography (TLC) was utilized to determine the phospholipid profile of the membranes.

The results of our study suggest that deletion of the *ERG6* gene leads to significant changes in the membrane properties of *Candida glabrata*, which may affect its resistance to antifungal agents and overall pathogenicity. Understanding these changes could lead to the identification of new therapeutic targets and the development of more effective treatment strategies for infections caused by *Candida glabrata*. Further research in this area is necessary for a comprehensive understanding of resistance mechanisms and the optimization of treatment for these infections.

Acknowledgement
This work was supported by grants: UK/126/2022, UK/28/2023, SAS-NSTC-JRP-2023-04.

References

[1] Candida albicans: Cellular and molecular biology [online], 2nd, RAHENDRA Prasad, Springer, (2017).
[2] H.Van den Hazel; et al., J. of Biological Chemistry, 274(4) (1999), 1934-1941.
[3] J. Loffler, H. Einsele, H. Hebart, U. Schumacher, C. Hrastnik and G. Daum, FEMS Microbiology Letters, 185(1) (2000), 59-63.

Fabrication of flexible microstructures for biomedical applications

J. Kubacková[1], C. Slabý[2], Z. Tomori[1] and Gregor Bánó[2]

[1] *Institute of Experimental Physics, Slovak Academy of Sciences, Watsonova 47, 040 01 Košice, Slovakia.*
[2] *Department of Biophysics, Faculty of Science, P. J. Šafárik University in Košice, Jesenná 5, 041 54 Košice, Slovakia.*

e-mail: kubackova@saske.sk

Two-photon polymerization direct laser writing (TPP-DLW) is a highly-precise nano and micro scale 3D printing technology of CAD-designed objects. It is a non-linear optical process based on the simultaneous absorption of two photons in a photosensitive material (photoresist). Microstructures are fabricated by direct laser writing as the laser focus is scanned along a pre-defined trajectory inside the microstructure volume. The potential of this technique consists in fabrication of microstructures of arbitrary shape customizable for every experiment. Such type of microstructures prepared by TPP-DLW can be easily manipulated by optical tweezer.

We currently focused on light driven microtools developed for live cell experiments. A special container was designed (Fig. 1) to facilitate intercellular signalization and drug transport studies of non-adherent cell lines. Inside the container, the cells are arranged in a row. In general, the container can be filled with different cell types to see their mutual interactions. Because live cells may be harmed during manipulation by extensive photon flux of optical tweezer, we have developed various versions of optically trapped micro-robots equipped with end-effectors to trap cells and manipulate them subsequently (not shown). After transporting cells to the vicinity of the measuring container, another optical trap opens a flexible "gate" of a container before the first and closes it after the last cell enters the container (Fig. 1B). In such a way we prevent the cell at the end of the container from releasing itself spontaneously under the influence of Brownian motion.

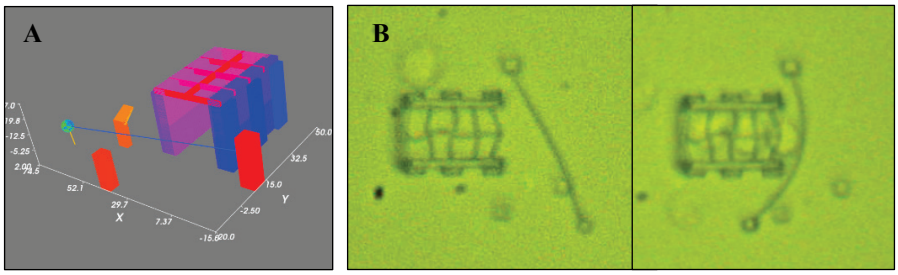

Fig. 1. Proof of concept of container with a flexible barrier (manual control). (A) CAD model. (B) Process of micromanipulation with optical tweezer: gate open (left); gate closed; three live cells placed to the container (right).

Acknowledgement
This work was supported by the Slovak Research and Development Agency (project APVV-21-0333) and VEGA 2-0101-22.

Mode of action of quercetin and its derivatives with Ca^{2+}-ATPase – *in silico* study

M. Majekova, P. Rezbarikova, J. Viskupicova and L. Horakova

Centre of Experimental Medicine, Institute of Experimental Pharmacology and Toxicology, Slovak Academy of Sciences, Bratislava, Slovakia.

e-mail: magdalena.majekova@savba.sk

Sarcoplasmic reticulum Ca^{2+}-ATPases (SERCAs) are crucial in regulating calcium homeostasis in cells. Decreased SERCA expression or activity is an important therapeutic target for managing various age-related diseases. We investigated the impact of quercetin and its two derivatives, monochloropivaloylquercetin (CPQ) and 2-chloro-1,4-naphthoquinonequercetin (CHNQ), on SERCA1a, specific to adult fast-twitch skeletal muscle [1]. Although the compounds had similarities in their effects on enzyme activity and kinetics, they had diverse effects on ATP binding on SERCA1a. This diversity was elucidated by the results of a molecular modelling study.

SERCA1 activity was measured by NADH-coupled assay. Sarcoplasmic reticulum vesicles (0.1 mg/ml) were incubated with compounds (25-250 μM) at 37°C for 2 min SERCA1a. In order to model the SERCA1a interactions with quercetin, CPQ, and CHNQ, we used the crystal structures PDB ID 4xou and 3w5c for the E1 and E2 states, respectively. The software Yasara (www.yasara.org) was used with the AMBER14 force field and the AutodockLGA method for docking calculations. Complexes with the best score were fully optimized using the Energy Minimization protocol, which consists of the combination of gradient optimization, molecular dynamics, and simulated annealing.

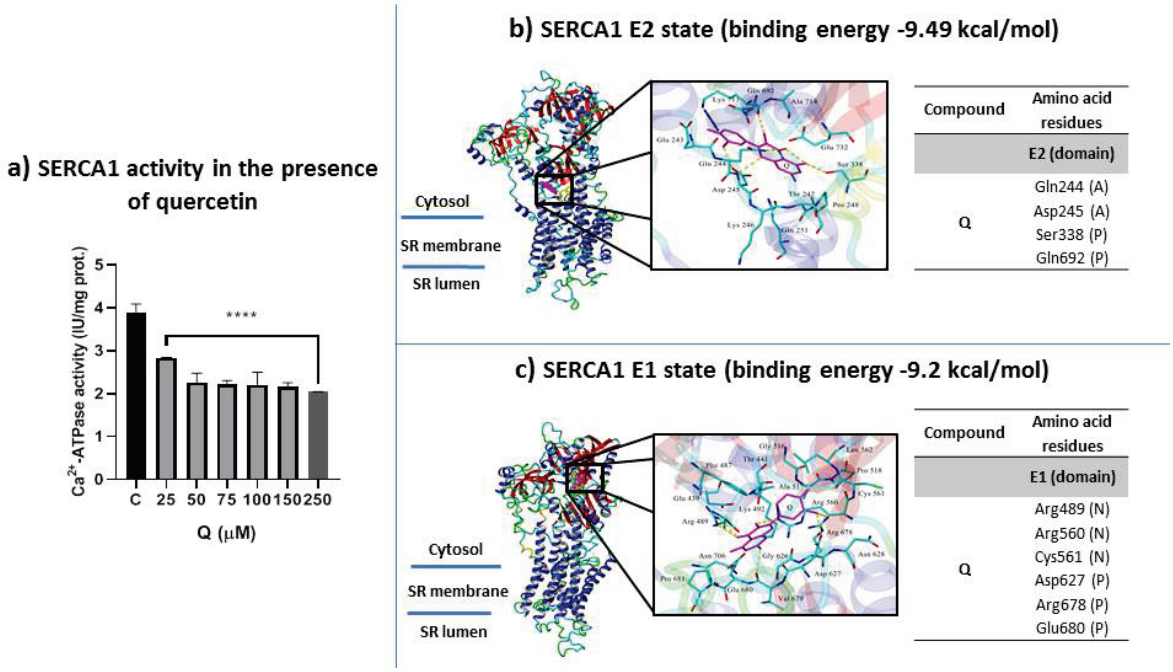

Fig. 1. Effect of quercetin (Q) on Ca^{2+}-ATPase from the sarcoplasmic reticulum (SERCA1). a) SERCA1 activity. b) Structural arrangement of the SERCA1 in E2 (PDB code 3w5c) with bound Q. c) Structural arrangement of the SERCA1 in E1 state (PDB code 4xou) with bound Q. Yellow lines represent H-bonds between Q and amino acids.

Quercetin was found to decrease SERCA1a activity by binding near the ATP-binding sites. This was confirmed through changes in the kinetic parameters, molecular modelling, and previously reported decreased thiol content and FITC fluorescence [2]. Since there are neighbouring modulatory binding sites for ATP other than the catalytic one, it is believed that the overall effect of quercetin could be multimodal yet always connected to the binding of ATP. This is supported by the increase of K_m for ATP (E1 state) in the presence of quercetin. The inhibition of SERCA1a by CPQ and CHNQ is likely associated with the binding to Glu113 (CPQ) and Glu243 together with Asp245 (CHNQ) in the E2 state, as those residues are involved in the initial interactions before Ca^{2+}-binding (Musgaard et al. 2012).

In conclusion, these findings suggest that quercetin and its derivatives can modulate SERCA1a activity through different modes of inhibition, highlighting their potential as agents for managing diseases associated with SERCA.

Acknowledgement
This work was supported by GrantName, GrantNumber. This work was supported by the Slovak Grant Agency VEGA 2/0113/21, VEGA 2/0063/22, VEGA 2/0103/22, and by the Slovak Research and Development Agency under the contract No. APVV-20-0543.

References

[1] P. Rezbarikova, J. Viskupicova, M. Majekova and L. Horakova, Gen Physiol Biophys., 5 (2023), 457-468.
[2] P. Zizkova, D. Blaskovic, M. Majekova; et al., Mol. Cell. Biochem., 386 (2014), 1-14.
[3] M. Musgaard, L. Thogersen, B. Schiott and E. Tajkhorshid, Biophys. J., 102 (2012), 268-277.

PO16

Determination of tryptophan metabolites in blood and urine of patients with depressive disorder

D. Masarovičová[1], L. Šikurová[1], I. Mikolášková[2], Ľ. Hunáková[2], B. Kollárik[3] and M. Zvarík[1]

[1] *Department of Nuclear Physics and Biophysics, Faculty of Mathematics, Physics and Computer Science, Comenius University in Bratislava, Mlynska dolina, 842 48 Bratislava 4, Slovakia.*
[2] *Institute of Immunology, Faculty of Medicine, Comenius University in Bratislava, Odborarske namestie 14, 811 08, Bratislava, Slovakia.*
[3] *Department of Urology, Saints Cyril and Methodius Hospital, University Hospital Bratislava, Antolská 11, 851 07 Bratislava, Slovakia.*

e-mail: masarovicova5@uniba.sk

Depressive disorder is currently becoming a significant public health issue, with a considerable impact on the quality of life of individuals and society as a whole. Despite intensive research in this area, the exact causes and mechanisms underlying the onset and development of this disorder are still not fully understood. In addition to genetic predispositions, it seems that metabolic dysfunctions of neurotransmitters, as well as oxidative stress and inflammatory processes, may play an important role in its pathogenesis. One of the main interests in this area is the imbalance in the catabolism of the amino acid tryptophan, which is a key precursor of the neurotransmitter serotonin. Reduced serotonin levels are often associated with symptoms of depressive disorder. Inadequate protein intake in the diet or increased tryptophan catabolism into the kynurenine pathway may lead to disruption of serotonin levels and worsen the patient's condition [1-2].

The aim of the presented study is to examine and identify tryptophan metabolites in bodily fluids, specifically in urine and blood plasma, in patients suffering from depressive disorder. Part of the objective is also to compare these levels with concentrations in healthy individuals. To achieve this goal, we utilized the highly efficient method of high-performance liquid chromatography (HPLC) with both absorbance and fluorescence detection, which allows for precise separation, identification, and quantification of individual metabolites. For the measurement of urine and plasma samples, we employed a reverse-phase HPLC system. The mobile phase consisted of a solution of 10 mmol/l KH_2PO_4 with 4% methanol at pH 7.0. A result was considered significant in statistical tests if the value of $p < 0.05$.

The study included adult patients taking psychotropic medication. There were a smaller number of samples; thus, we had 5 patients in blood plasma and 6 patients in urine. Through our experiments, we found that levels of tryptophan and serotonin did not change in the blood or urine of patients with depression. In plasma, we observed a significantly reduced ratio of 5-HTP/TRP (TPH) ($p < 0.05$), reflected in the decreased concentration of 5-HTP (Fig. 1A). In urine, we noted an increased concentration of kynurenine, as well as an increased ratio of KYN/TRP (IDO) (Fig. 1B).

Increased concentrations of 5-HTP/TRP (TPH) in blood plasma suggest increased tryptophan catabolism via the kynurenine pathway, which corresponds to our previous observations [3]. The decrease in the levels of 5-HIAA in urine and tryptophan in plasma in depression reported in studies [4-5] was not observed in our observations. The concentration of IDO is determined by the ratio of tryptophan to kynurenine, with a significant increase observed in depressive patients, as confirmed by our research [6].

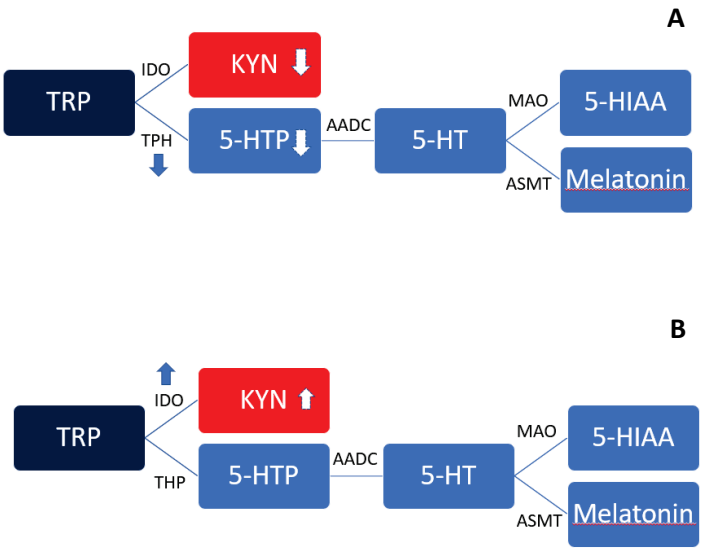

Fig. 2. Scheme of tryptophan metabolism in blood plasma (A) and urine (B).

TRP-Tryptophan, KYN-kynurenine, 5-HTP-5-hydroxytryptophan, 5-HT-serotonine, 5-HIAA-5-hydroxyindoleacetic acid, IDO-indoleamine 2,3-dioxygenase, TPH-tryptophanhydroxylase, AADC-decarboxylase of aromatic acids, MAO-monoamine oxidase, ASMT-N-acetylserotonin O-methyltransferase. Arrows indicate concentration change of metabolites (or ratio) in patients with depression compared to healthy controls.

Our analysis could provide important insights into the role of tryptophan metabolites in the pathogenesis of depressive disorder and their potential value as biomarkers for diagnosis and monitoring of patient status.

Acknowledgement
The study was conducted according to the guidelines of the Declaration of Helsinki, and approved by the Ethics Committee of UNB Saints Cyril and Methodius Hospital in Bratislava (EK 10/11/2013, date of approval 21 November 2013). This research was supported by grants from VEGA 2/0016/23 and APVV-22-0264.

References

[1] Y. Higuchi, T. Soga and I. S. Parhar, Frontiers in Neuroscience, 11 (2017), 604.
[2] J. Zhao, H. Chen, P. Ni, B. Xu, X. Luo, Y. Zhan, P. Gao and D. Zhu, Journal of chromatography B, 879(26) (2011), 2720-5.
[3] M. Öztürk, Ş. Y. Sapmaz, H. Kandemir, F. Taneli and Ö. Aydemir, International Journal of Clinical Practice, 75(4) (2021) e13739.
[4] H. Jayamohananan; et al., Adv. Pharm. Bull., (2019).
[5] C. Kohl; et al, J. Affect Disord., (2005).
[6] M. Maes, W. Rief, Psychiatry Res., (2012).

Allosteric Modulation of 14-3-3 Proteins: Implications for Adipogenesis and Obesity Treatment

S. Müller[1], L. Rivera[1], L.I. Fontana[1], M. Uhart[1], and D.M. Bustos[1,2]

[1]Laboratorio de Integración de Señales Celulares, IHEM (CONICET-UNCuyo), Mendoza, Argentina.
[2] FCEN, UNCuyo, Mendoza, Argentina.

e-mail: diegombustos@gm.fcen.uncu.edu.ar

The 14-3-3 proteins, an evolutionarily conserved family ubiquitous across eukaryotes, play a crucial role in cellular signalling by selectively binding to phosphorylated serine or threonine residues (pS/T) on a plethora of proteins [1]. Over 400 interacting proteins have been identified, underscoring the intricate involvement of 14-3-3 proteins in diverse biological processes, including differentiation, apoptosis, vesicular trafficking, cell cycle regulation, and lipid metabolism [2, 3, 4].

In the context of adipogenesis, the process wherein precursor cells differentiate into lipid-storing mature adipocytes [5], our laboratory had revealed different contributions of 14-3-3 paralogs [6]. Understanding the regulatory mechanisms orchestrated by 14-3-3 proteins in adipogenesis is imperative for addressing metabolic disorders such as obesity and type II diabetes [7], thereby highlighting the significance of identifying modulators of their activity for therapeutic intervention. Accordingly, our research has shifted towards the discovery of small molecules capable of modulating 14-3-3 protein activity via a distinct allosteric site.
Through virtual screening of $2x10^6$ compounds utilizing the ZINC database, we identified members of the β-carboline family as potential ligands capable of binding to an allosteric site on 14-3-3 proteins. This binding induces conformational changes in the protein, altering its interaction with partner molecules.

To elucidate the impact of these newly identified 14-3-3 ligands on adipogenesis, we investigated their effects on murine 3T3-L1 pre-adipocyte differentiation. Culturing 3T3-L1 cells in the presence of norharmane (a member of the β-carboline family) at non-cytotoxic concentrations, with DMSO as a control, allowed us to assess its influence on adipogenic differentiation. We employed mass spectrometry to analyze the protein profiles and Oil Red O staining to evaluate lipid droplet accumulation.

Our results demonstrate that after 5 days of adipogenic induction, norharmane-treated cultures exhibited reduced cellular differentiation, evidenced by decreased expression of adipogenic markers such as FABP4 and diminished lipid droplet accumulation. These findings suggest that norharmane affects adipogenic differentiation of 3T3-L1 cells. Moving forward, we aim to explore whether norharmane's effects are specific to particular 14-3-3 paralogs or if it modulates the activity of multiple 14-3-3 proteins simultaneously. Elucidating the precise mechanisms underlying norharmane-induced disruption of adipogenesis through 14-3-3 modulation positions it as a promising therapeutic target for obesity-related disorders.

Acknowledgement
This work was supported by Grant number 873127 InterTAU (Marie Sklodowska-Curie Action Research and Innovation Staff Exchange Grant Agreement).

References

[1] In Seminars in cancer biology, A. Aitken, Academic Press, 16 (2006), 162-172.
[2] D. M. Bustos, Molecular BioSystems, 8 (2012), 178-184.
[3] M. Uhart & D. M. Bustos, Frontiers in genetics, 5 (2014).
[4] S. A. Rial, R. Shishani, B. P. Cummings & G. E. Lim, Diabetes, 72 (2023), 1045-1054.
[5] T. C. Otto & M. D. Lane, Critical reviews in biochemistry and molecular biology, 40 (2005), 229-242.
[6] A. D. Gojanovich, D. M. Bustos & M. Uhart, Biochemistry and Biophysics Reports, 7 (2016), 106-112.
[7] D. Moseti, A. Regassa & W. K. Kim, International journal of molecular sciences, 17 (2016), 124.

11th Slovak Biophysical Symposium, High Tatras, June 12 – 14, 2024

Exploration of disordered tau protein's conformational space by metadynamics simulations

S. Njemoga[1], V. Spiwok[2], E.E. Barrera[3] and O. Cehlár[1]

[1] *Institute of Neuroimmunology, Slovak Academy of Sciences, Bratislava, Slovakia.*
[2] *Department of Biochemistry and Microbiology, University of Chemistry and Technology, Prague, Czech Republic.*
[3] *IHEM, Universidad Nacional de Cuyo, CONICET, Mendoza, Argentina.*

e-mail: stefana.njemoga@savba.sk

Intrinsically disordered protein (IDP) tau is neuronal protein that regulates the stability and dynamics of microtubules. On the other hand, because of the intrinsic disorder encoded in its high content of polar and charged amino acids in primary sequence, tau is often subjected to abundant posttranslational modifications that induce conformational shift of tau towards pathological structures. Misfolding of tau leads to accumulation of insoluble tau filaments in the brain of Alzheimer´s disease patients [1]. Turning IDPs into druggable targets provides a great opportunity to extend the druggable target-space for novel drug discovery. Thanks to its structural heterogeneity, the ability to explore the conformational space of tau and other IDPs is particularly important for producing the relevant conformational ensemble, as the most accurate way of describing the IDPs. Therefore, new drug design strategies to target IDPs include the first step of producing a conformational ensemble and then conducting a potential binding site analysis for non-specific binding by small molecules. To this day, ensemble generators (ENSEMBLE, ASTEROIDS) or molecular dynamics (MD) simulations are primarily chosen for production the initial set of protein conformers.

A common undesirable result of MD simulation is conformation trapping in specific local energetic minimum, leading to insufficient conformation sampling. One way for accelerating classical MD simulation and thus enhance the protein sampling is using simplified coarse-grain representation of protein residues. We produced three 750 ns long trajectories of truncated tau (321-391) using SIRAH force field and WT4 water model in three replicas starting from the conformers predicted by AlphaFold. No folding event was observed from the produced trajectories. Biasing MD simulations by altering the potential energy function can help protein to overcome energetic barrier and efficiently explore conformational space. With this aim, we employed metadynamics simulations with two sets of collective variables (CVs), with the first set being CVs derived from AlphaFold [2], and second set of CVs describing the protein's secondary structural properties by stimulation of α-helix and anti-β structure formation [3]. The metadynamics simulations were performed using GROMACS 2021.4 patched by plumed 2.9.0. Simulations guided by secondary structure CVs were run in all-atom representation with the CHARMm36 force field and TIP3P water model. Alphafold CVs were obtained from the AlphaFold output describing the distribution of inter-residual distances. For AlphaFold-guided MD simulations, coarse-grained representation of protein residues was chosen, using SIRAH force field and WT4 water model. Both trajectories are 100 ns long.

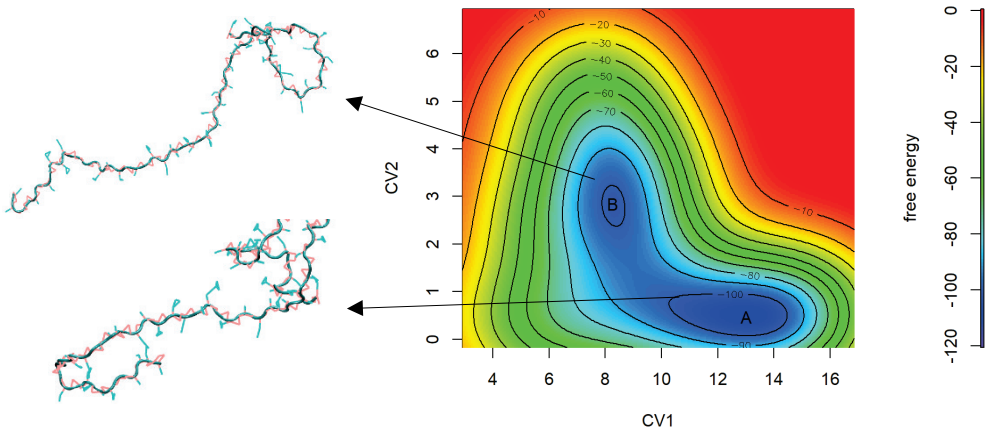

Fig. 1. The analysis of the free energy landscape of protein tau from metadynamics simulation guided by an AlphaFold-derived collective variables and the two corresponding global minimum energy conformations of protein tau [4].

By applying secondary structure stimulating CVs, we successfully induced formation of three helices, but only weak indications of beta structure have been observed. Alphafold-CVs simulations yielded mainly coil-like conformations of tau with the two energetic minima within the explored free energy landscape (Fig. 1).

After extending the previous MD simulations, results will be validated by NMR chemical shifts, secondary chemical shifts reporting on secondary structural propensities, and SAXS results.

Acknowledgement
This work was supported by COST (European Cooperation in Science and Technology, COST Action CA21160), APVV 21-0479, VEGA 2/0125/23 and MSCA-RISE 873127 funded by the Horizon 2020 program of the European Commission.

References

[1] H. Braak; et al., Journal of Neuropath. Exp. Neur., 70 (2011), 960-969.
[2] V. Spiwok; et al., Frontiers in Mol. Biosc., (2022), p. 9.
[3] The PLUMED consortium. Nat. Methods, 16 (2019), 670.
[4] D. Trapl & V. Spiwok, The R Journal, 14(3) (2022), 46-58.

11th Slovak Biophysical Symposium, High Tatras, June 12 – 14, 2024

Uncovering the structure of unstructured protein tau and its involvement in aggregation

A. Polák, S. Njemoga, K. Mešková, O. Cehlár and R. Škrabana

Institute of Neuroimmunology, Slovak Academy of Sciences; Bratislava, 845 10, Slovakia.

email: adam.polak@savba.sk

Aggregation of protein tau and accumulation of tau neurofibrillary tangles are characteristic features of Alzheimer's disease [1]. The study of tau structure is limited by the fact that tau is disordered in its full length; its conformation in complexes depends on binding partners [2]. Small structural motifs may significantly impact the conformation and function of disordered proteins. The motifs mostly depend on the weak interactions such as hydrogen bonds [3]. Our ultimate aim is to investigate transient structural motifs on tau, specifically those involved in tau aggregation. Primary screening for these motifs may be performed by structure determination of tau protein in complexes with Fabs (fragment antigen-binding regions) of monoclonal antibodies. To achieve this goal, our work consists of preparation of tau-Fabs complexes and protein crystallography, combined with computational tools.

We produced several Fabs, crystallized their complexes with tau proteins (Fab epitopes are highlighted in Fig. 1 and collected diffraction data [4]. We also crystallized complex of DC25Fab with tau peptide encompassing DC25 epitope (^{341}SEKLDFKDRVQSKIGSLDNI^{360}). All complexes were isolated using size-exclusion chromatography. By in-silico approach, we performed molecular dynamics simulations of free tau341-360 to assess tau motifs and corroborate X-ray crystallography analysis.

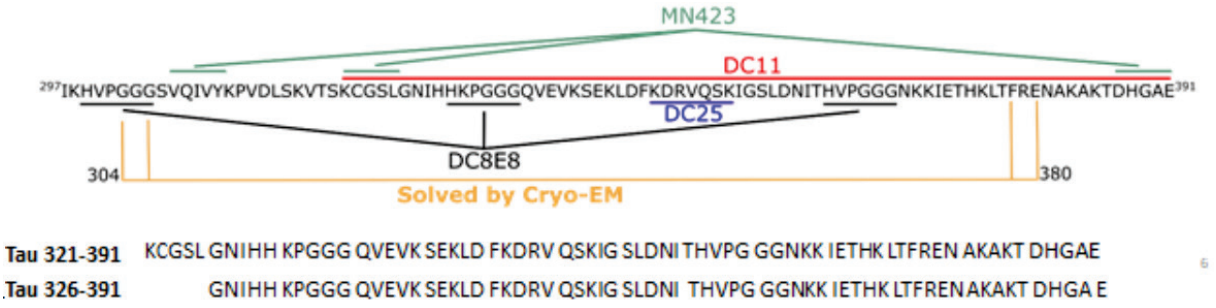

Fig. 1. Binding epitopes of MN423, DC11, DC25 and DC8E8 on the sequence of tau protein. Part of tau visualized by cryo-electron microscopy is highlighted in yellow.

In the next steps, we will use site-directed mutagenesis of tau residues in identified motifs and study their role in tau aggregation. Our experimental approach consisting in combination of crystallography experiments with computer simulations might help to gain insight into aggregation of tau protein and therefore to help in drug development targeting Alzheimer's disease.

Acknowledgement:
This project is supported by APVV-21-0479, VEGA 2/0141/23, 2/0125/23 and EU Grants ADDIT-CE, InterTau.

References:

[1] Athanasios Metaxas and Stefan J. Kempf. Neural regeneration research, 11.10 (2016), 1579-1581.
[2] Marco D. Mukrasch; et al, PLoS biology, 7.2 (2009), e34.
[3] E. N. Baker and R. E. Hubbard, Progress in biophysics and molecular biology, 44.2 (1984), 97-179.
[4] Antibodies, K. Meskova; et al, Basel, 12.3 51. (2023).

11th Slovak Biophysical Symposium, High Tatras, June 12 – 14, 2024

Comparison of biophysical properties of selected natural variants of staphylokinase

M. Štulajterová[1], M. Tomková[2], Ľ. Ambro[2], E. Sedlák[2,3]

[1] *Department of Biophysics, Faculty of Science, P. J. Šafárik University, Jesenná 5, 040 01 Košice, Slovakia.*
[2] *Center for Interdisciplinary Biosciences, Technology and Innovation Park, P. J. Šafárik University, Jesenná 5, 040 01 Košice, Slovakia.*
[3] *Department of Biochemistry, Faculty of Science, P. J. Šafárik University, Moyzesova 11, 040 01 Košice, Slovakia.*

e-mail: monika.stulajterova@student.upjs.sk

Thrombosis represents one of the leading causes of mortality in developed countries [1]. Thrombolytic therapy employs medications to dissolve intravascular clots [2]. Prompt treatment with thrombolytic drugs can restore blood flow before major brain damage and improve recovery after stroke [3]. Ideally, thrombolytic agents should have high fibrin specificity, require low dosages, prevent bleeding complications and re-occlusions, and be non-antigenic [4]. Yet, current drugs have limited efficacy and significant hemorrhagic risks, suggesting room for improvement.

Staphylokinase (SAK) is a 136 amino acid protein originating from lysogenic strains of *Staphylococcus aureus* [5]. SAK has a high tendency to turn inactive fibrin-bound plasminogeninto its active form plasmin through formation of equimolar (1:1) complex with plasmin. SAKis a promising thrombolytic agent with properties of cost-effective production and negligible side effects [6].

Currently, three natural variants SAK 42D, SAK φC and SAK STAR have been characterized. These variants have a similar potential to activate plasminogen, but differ in thermostability [7]. We purified two variants SAK 42D and SAK STAR and performed their conformational and functional characterization by applying of circular dichroism, differential scanning calorimetry and chromogenic activity assay. We further analyzed a role of His-tag onthe studied biophysical properties.

Keywords: thrombosis, thrombolytics, staphylokinase, ribosome display

Acknowledgement

This work was supported by the Slovak Research and Development Agency (project APVV-20-0340) and Agencyof Ministry of education, research, development and youth of the Slovak republic (VEGA 1/0074/22).

References

[1] Treasure Island. D. Ashorobi, M. A. Ameer, R. Fernandez (Eds.), StatPearls Publishing, FL (2019).
[2] Treasure Island. M. U. Baig, J. Bodle (Eds.), StatPearls Publishing, FL (2020).
[3] J. M. Wardlaw, V. Murray, E. Berge, G. J. Del Zoppo, Cochrane database of systematic reviews, 7 (2014).
[4] D. Nikitin, S. Choi, J. Mican, M. Toul, W. S. Ryu, J. Damborsky, D. E. Kim, Journal of Stroke, 23 (2021).
[5] L. T. Nguyen, H. J. Vogel, H. J., Scientific reports, 6 (2016).
[6] R. Nedaeinia, H. Faraji, S. H. Javanmard, G. A. Ferns, M. Ghayour-Mobarhan, M. Goli, M. Ranjbar, Molecular Biology Reports, 47 (2020), 819-841.
[7] S. Vanderschueren, F. Van de Werf, D. Collen, Fibrinolysis and Proteolysis, 11 (1997), 39-44.

Multimodal application of polymeric nanoparticles based on poly(2-oxazoline) *in vitro* and *in vivo*

Ľ. Timuľáková[1], S. Datta[2], J. Kronek[3], M. Máčajová[4], J. Levík[4], V. Huntošová[2,4]

[1]Department of Biophysics, Institute of Physics, Faculty of Science, P. J. Šafárik University in Košice, Jesenná 5, 041 54 Košic, Slovakia.
[2] Center for Interdisciplinary Biosciences, TIP, P. J. Šafárik University in Košice, Jesenná 5, 041 54 Košice, Slovakia.
[3] Department for Biomaterials Research, Polymer Institute of the Slovak Academy of Sciences, Dúbravská cesta 9, 84541 Bratislava, Slovakia.
[4] Institute of Animal Biochemistry and Genetics, Centre of Biosciences, Slovak Academy of Sciences, Dúbravská cesta 9, 840 05 Bratislava, Slovakia.

e-mail: ludmila.timulakova@student.upjs.sk

Biomedical engineering has excelled in recent decades through the collaboration of physicians and engineers in the development of biomaterials and medical devices. This field specifically focuses on polymers, particularly poly(2-oxazoline) s (POx) [1]. POx, commonly referred to as 'pseudopeptides', are biocompatible polymers known for their chemical flexibility and straightforward synthesis, making them ideal candidates for advancing polymer therapeutics into the next era. Variants of POx with methyl or ethyl side-groups can be water-soluble, non-ionic, and display stealth characteristics. Polymeric nanoparticles based on POx are considered as a promising alternative transport system for hydrophobic molecules as it was the case of hypericin [2].

Hypericin, a natural naphthodianthrone obtained from Hypericum perforatum L., also known as St. John's wort, stands out for its promising activity against cancer cells, high singlet oxygen quantum yield, remarkable fluorescence quantum yield and low toxicity in the absence of light [3]. Hypericin is a hydrophobic molecule that has suitable properties for photodynamic therapy and photodiagnostics. Hypericin is insoluble in aqueous solutions, but completely soluble in various organic solvents where emits bright fluorescence with a maximum intensity at 600 nm [4].

In this study, we compared the ability of two synthesized gradient poly(2-oxazolines) to create polymeric nanoparticles and entrap hypericin. These polymeric nanoparticles contain 2-ethyl-2-oxazoline (EtOx) and 2-phenyl-2-oxazoline (PhOx) in different ratios of hydrophobic and hydrophilic parts. With the aim to test low therapeutic concentration of hypericin in cancer cells, the loading of hypericin in the nanoparticles was small.

The size of hypericin-encapsulating self-assembled nanoparticles was measured using the dynamic light scattering method. The stability and release of hypericin from these formulations was monitored using fluorescence spectroscopy in the presence of serum proteins: low density lipoproteins (LDL) and fetal bovine serum (FBS). Fast and slow kinetics were observed with the promise of a gradual release application.

The uptake of hypericin and the particles by glioblastoma cells was observed using flow-cytometry and confocal fluorescence microscopy. We have noticed significant differences between two formulations that were prepared. In further, this uptake highly influenced photodynamic efficacy of the treatment.

Biocompatibility of POx encapsulated high concentration of hypericin suitable for bioimaging was tested on chorioallantoic membrane model (CAM) of quail embryo. High biocompatibility of the

formulations were denoted. Bright fluorescence of hypericin with gradual release was detected with fluorescence bioimaging of the CAM.

In the future study, POx will be functionalized and the specificity of such transport system towards receptors of cancer cells will be studied in the cells immobilized in the photoresist microstructures.

Acknowledgement
This work was supported by VEGA 2/0042/21 and APVV-21-0333.

References

[1] A. Zahoranová, R. Luxenhofer, Online Wiley Library, (2021).
[2] S. Jana, M. Uchman, Prog. Polym. Sci. 106 (2020), 101252.
[3] N. Nakajima & N. Kawashima, Photodiagnosis and photodynamic therapy, 9(3) (2012), 196-203.
[4] A. Kamuhabwa, P. Agostinis, B. Ahmed, W. Landuyt, B. Van Cleynenbreugel, H. Van Poppel, P. de Witte, Photochem. Photobiol. Sci., 3 (2004), 772-780.

11th Slovak Biophysical Symposium, High Tatras, June 12 – 14, 2024

Determination of the lifetime of radical in the P-type ferryl intermediate of cytochrome c oxidase

A. Tomkova[1], M. Fabian[2], D. Jancura[1]

[1]Department of Biophysics, Faculty of Science, P. J. Šafárik University, Jesenná 5, 040 01 Košice, Slovakia.
[2] Center for Interdisciplinary Biosciences, Technology and Innovation Park, P. J. Šafárik University, Jesenná 5, 040 01 Košice, Slovakia.

e-mail: adriana.tomkova1@student.upjs.sk

Respiratory cytochrome c oxidase (CcO) catalyzes the reduction of molecular dioxygen to water by electrons supplied by ferrocytochrome c. Four electrons, required for the full reduction of O_2 to H_2O, are transferred sequentially from cytochrome c via four metal centers, copper A (Cu_A), heme *a*, heme a_3 and copper B (Cu_B). Cu_A is the first electron acceptor from cytochrome *c*. The electron flow then continues in CcO to heme *a* and finally to the catalytic heme a_3-Cu_B center. At this heme a_3-Cu_B center the reduction of dioxygen takes place. Reduction of O_2 proceeds through a sequence of several oxy intermediates of the heme a_3-Cu_B center. These intermediates are determined by the number of electrons and protons delivered into the catalytic center [1]. In one of them, produced by the reaction of two-electron reduced CcO with O_2, the free radical at the catalytic center is also formed. In this state, the iron of heme a_3 is in the ferryl state and very likely Tyr244 (bovine CcO numbering), located in the proximity of the center, is oxidized to a neutral radical [Fe_{a3}^{4+}=O Cu_B^{2+} YO•]. For historical reasons this ferryl intermediate is called P_M state.

However, several published studies indicated that this radical migrates the large distances from the catalytic center of CcO. The result of this migration is oxidative damage of the enzyme. In spite of importance of this radical in catalysis of respiratory oxidases the lifetime of this radical has not been established [2, 3, 4]. To answer this question, we have developed a protocol to estimate its lifetime in the P_M form. This method is based on one-electron reduction of the P_M form. In case that radical is present, the product of this reduction is spectrally different second ferryl form (F type). However, if the radical already migrated from the catalytic center, then reduction of this intermediate results in the formation of fully oxidized CcO. Consequently, if this one-electron reduction is performed at different times after the formation of the P_M the generated fraction of the F form represents population in which the radical is still present.

This kind of measurements have been performed on purified bovine CcO at pH 8.0 and at 10 and 20 °C. At both temperatures, the loss of the radical from the catalytic center occurs on time scale of minutes. The time constant of migration increases with the rise of the temperature from 15 minutes at 10 °C to 7 minutes at 20 °C. Data also indicated that at 37 °C, the time constant should be about 100 seconds. This relatively long lifetime indicates that under physiological turnover conditions, the escape of the radical from this catalytic center is very unlikely. It can only occur if there is a very limited access of external electron donors.

Acknowledgement
This work was supported by VEGA, 0028/22.

References

[1] M. Wikstrom, K. Krab, and V. Sharma, Chem. Rev., 118 (2018), 2469-2490.
[2] A. Musatov, E. Hebert, C. A. Carroll, S. T. Weintraub, and N. C. Robinson, Biochemistry, 43 (2004), 1003-1009.
[3] A. Musatov, and N. C. Robinson, Free Radic. Res., 46 (2012), 1313-1326.
[4] P. Lemma-Gray, S. T. Weintraub, C. A. Carroll, A. Musatov, and N. C. Robinson, FEBS Lett., 581 (2007), 437-442.

11th Slovak Biophysical Symposium, High Tatras, June 12 – 14, 2024

Raman and SERS microspectroscopy studies on DNA and cells

B. G. Varchol[1], D. Horváth[2], V. Huntošová[2], Z. Jurašeková[1]

[1] *Department of Biophysics, Faculty of Science, P. J. Šafárik University, Jesenná 5, 040 01 Košice, Slovakia*
[2] *Center for Interdisciplinary Biosciences, Technology and Innovation Park, P. J. Šafárik University, Jesenná 5, 040 01 Košice, Slovakia.*

e-mail: bianka.varcholova@upjs.student.sk

Raman spectroscopy (RS) provides a structural fingerprint by which molecules can be identified. Typically, it does not require any or minimal sample preparation and can be used in aqueous solutions, which is important for biomedical applications. Moreover, when coupled with optical microscopy, it is possible to obtain high-spatial-resolution chemical maps and multispectral images even of such complex samples as cells, tissues, or organelles. However, the application of this technique can be significantly limited by two main drawbacks: in general, the very low Raman signal and the intense fluorescence emission. Surface-enhanced Raman scattering (SERS) can overcome the above disadvantages because of the fluorescence quenching of the analyte as well as the high sensitivity provided by the giant intensification of the radiation intensity in the presence of metal nanoparticles (NPs). In this context, we are exploring how to use Raman and SERS microspectroscopy and imaging to effectively study biological systems, particularly living cells. Specifically, our focus is on examining the structural and morphological alterations in cells as a result of various physical and chemical factors. Nevertheless, to detect and study such complex systems as living cells requires, first of all, a good knowledge and expertise of both the methodology itself and the much simpler systems that they consist of.

In the present work, we resume the preliminary results of our study focused on detecting selected biomacromolecules (primarily nucleic acids) using Raman and SERS spectroscopy. We measured DNA SERS spectra directly using positively charged silver NPs, whereas the recorded spectra were of good quality, demonstrated good reproducibility, and could be obtained even at low DNA concentrations (~ 10^{-6} M). Consequently, we conducted Raman/SERS studies on both cell cultures grown in monolayers and a spheroidal model of U87MG cells (designed to mimic superficial tumor tissue) to optimize the methodology and investigate aspects related to the cell response to photodynamic therapy (PDT). Further, we have also been exploring the use of the Raman imaging technique to obtain specific chemical images and distinguish between PDT-treated and non-treated cells. Finally, we have also been employing complementary optical spectroscopy and imaging techniques, along with chemometric methods, to ensure accurate data analysis.

Acknowledgement
The work was supported by the Ministry of Education, Science, Research and Sport of the Slovak Republic projects APVV-21-0333 and APVV-19-0580; and by the grant of Faculty of Science, P. J. Šafárik University in Košice (VVGS-2024-3101).

Incorporation of the conazole fungicide epoxiconazole into the DNA monitored by thermodynamic and hydrodynamic methods

V. Verebová[1], J. Staničová[1,2]

[1] *University of Veterinary Medicine & Pharmacy, Komenského 73, 040 01 Košice, Slovakia.*
[2] *First Faculty of Medicine, Charles University, Kateřinská 1, Prague, Czechia.*

e-mail: jana.stanicova@uvlf.sk

Pesticide application is an essential part of modern managed agriculture, contributing to food security and maintaining high-quality products. They are characterized as a heterogeneous group of substances with varying degrees of toxicity to non-target organisms, including humans. Most pesticides applied today are acutely toxic to humans. Exposure to pesticides is linked to chronic health effects such as neurological and reproductive disorders, developmental problems, and cancer [1]. We have concentrated our work on one group of pesticides, the conazole fungicides. Triazole epoxiconazole (EPX) represents conazole group of fungicides. Its adverse effects include developmental toxicity, hepatotoxicity, endocrine disruption, and DNA damage [2, 3]. Therefore, there is now a great need to study its effect on DNA structure and stability.

We have studied the interaction EPX with calf thymus DNA using the absorption spectroscopy with the Peltier module. Measurement of the complex (EPX/DNA) thermodynamic properties enables a determination of the DNA helix-loop transition. The obtained thermodynamic parameters (T_m, ΔH, ΔT) indicated that epoxiconazole destabilizes DNA, and its interaction causes a decrease in thermodynamic parameters characterizing DNA denaturation. This conclusion can be made since it is known that destabilization of DNA structure is associated with ligand interaction into the DNA groove [4]. Epoxiconazole by its interaction with DNA affects the length of DNA, there is a shortening of the length of the DNA double helix, which was confirmed by one of the hydrodynamic methods - measurement of kinematic viscosity. All performed experiments indicate that the conazole fungicide epoxiconazole is incorporated into the DNA groove with its triazole heterocycle. This incorporation is realized via hydrophobic or hydrogen bonds. The above observation can be predicted since it is well known from the literature that the interaction of small ligands with DNA in a non-specific manner by binding to the DNA groove is realized by hydrophobic or hydrogen bonds [5].

Our results could contribute to a better understanding of the influence and mechanism of action of epoxiconazole, as well as other conazole fungicides used in practice, on the DNA biomacromolecule.

Acknowledgement
This work was supported by a grant from the Slovak Research Grant Agency VEGA No. 1/0242/19. The authors thank the student Katarína Kozlovská for participation in the experiments.

References
[1] A. Tsaboula; et al., Environment International, 91 (2016), 78-93.
[2] J. A. Ross; et al., Mutagenesis, 27 (2012), 541-549.
[3] K. Grote; et al., Environmental Toxicology and Chemistry, 27 (2008), 2368-2374.
[4] S. Bi; et al., Spectrochimica Acta Part A: Molecular and Biomolecular Spectroscopy, 69 (2008), 123-129.

[5] Comprehensive Supramolecular Chemistry II. J. Gonzalez-Garcia and R. Vilar (Eds.), Elsevier, Amsterdam (2017), 39-70.

11th Slovak Biophysical Symposium, High Tatras, June 12 – 14, 2024

Allosteric inactivation of the ryanodine receptor channel

I. Zahradník, J. Pavelková, and A. Zahradníková

Dept. of Cellular Cardiology, Institute of Experimental Endocrinology, Biomedical Research Center, Slovak Academy of Sciences, Dúbravská cesta 9, 845 05 Bratislava, Slovakia.

e-mail: ivan.zahradnik@savba.sk

Calcium signalling and contractility of striated muscle cells depend on the ryanodine receptor (RyR) channels of the sarcoplasmic reticulum. These homo-tetrameric channels are regulated in a complex manner, which ensures dynamic control of the cytosolic concentration of Ca^{2+} ions during the contraction-relaxation cycle. The RyR1 isoform of skeletal muscle cells is activated by mechanical coupling to the voltage-operated DHPR channels of the plasmalemma. Intriguingly, it can be also activated by intracellular factors, namely, Ca^{2+}, ATP, and xanthines (XAN), and inactivated by high concentrations of divalent cations (M^{2+}: Ca^{2+} and Mg^{2+}). Each activator has its binding pocket at each RyR monomer, as was identified by methods of structural biology (Fig. 1). The M^{2+} inhibitory binding site was hypothesized to be located at the EF-hand region but the mechanism of how it may induce the inactivation has not been determined yet.

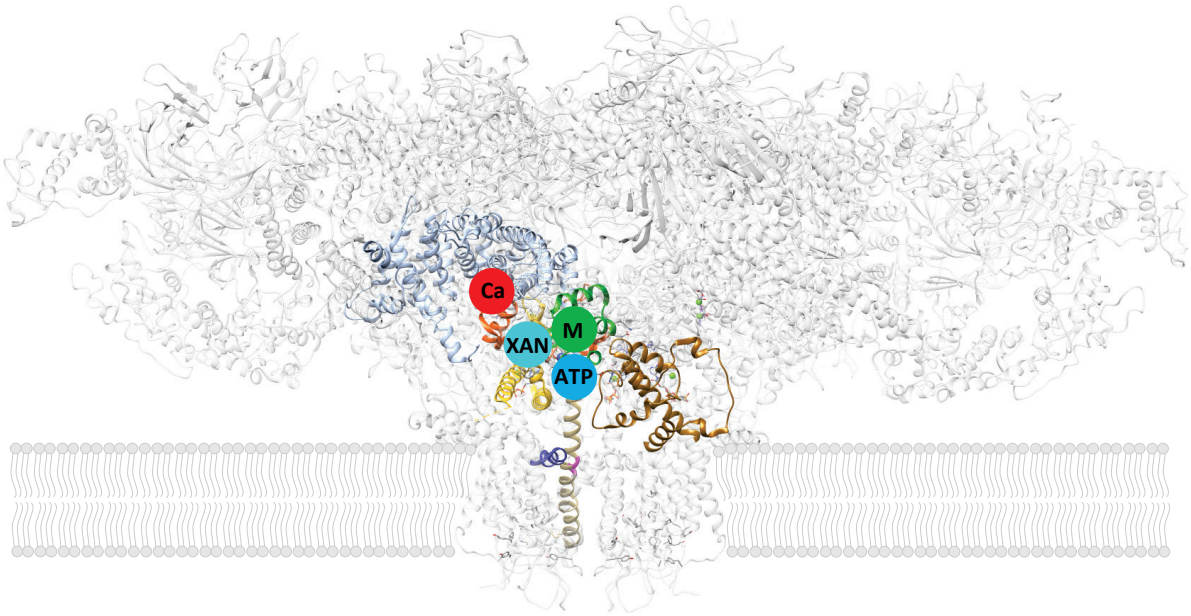

Fig. 1. Molecular structure of RyR1. The side view of the RyR tetramer in the membrane. Important structures of the RyR core are in color: light blue – central domain; orange – C-terminal domain; green – EF-hand region; yellow – U-motif; dark blue – S45 segment; magenta – Gate of S6 segment (beige); brown – S23* segment of the neighbor monomer. Ca, XAN, ATP, and M mark positions of the respective binding sites.

The aim of this work was to investigate the allosteric pathways leading from the M^{2+} inhibition site of RyR1 to the channel gate and to build a corresponding model of RyR1 operation.

We used *in silico* methods of structural biology to analyze regions relevant to M^{2+} inactivation in the published RyR1 structures. The structures were taken from the RCSB protein data bank (26

structures of rabbit RyR1 [1-4]). The RyR1 core monomer (residues 3667-5037) was edited and optimized in Chimera Ver. 1.17. The missing parts were added using the program MODELLER [5]. Two copies of the resulting core monomers were aligned to 2 neighbor monomers of the original structures and optimized. Allosteric pathways were traced using the server OHM [6].

It has been previously observed that in the inactivated RyR1 channel, salt bridges or hydrogen bonds form connections between the putative inhibitory site at the EF-hand region and the S23 segment of the neighbouring monomer [4] but it was not clear how this interaction is related to the inactivation. Analysis of RyR1 structures found the distances between the Cα atoms of the interacting residues (Fig. 2A) to be sufficiently small to allow interaction in open, primed, and inhibited RyR1 states, but not in the closed state. Altogether 7 different interactions are possible between monomers (Fig. 2B).

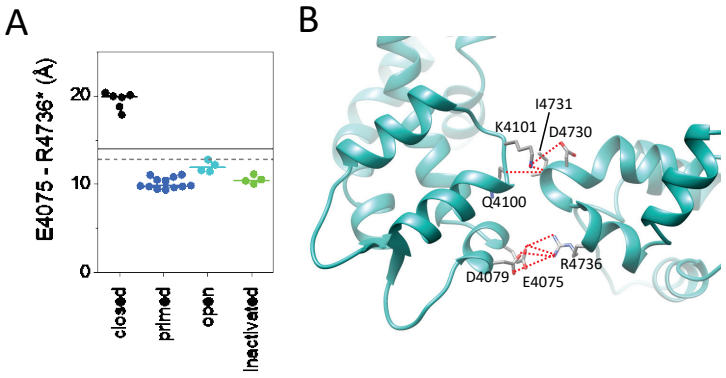

Fig. 2. Electrostatic interactions between the EF-hand region and the S23* segment. A - Separation distances between Cα atoms of E4075 and R4736* of the EF-hand domain and S23* segment, measured in RyR1 structures of defined states: closed (black); primed (blue); open (cyan); inactivated (green). Solid line – the maximal theoretical distance allowing H-bond formation; dashed line – the maximal measured distance allowing H-bond formation. B – Possible spatial interactions between residues of the EF-hand region (left) and S23* segment (right) in the open RyR1 structure.

The allosteric network between the EF-hand region and the gating site consisted of two major pathways (Fig. 3). First, the dominant intra-monomeric pathway connected the EF-hand ion-binding loops with the U-motif and continued *via* the ATP binding site. The pathway reached the channel gate *via* the S6 segment. This intra-monomeric inactivation pathway has the potential to affect and be affected by the Ca^{2+}/ATP modulation of RyR channel activity. Surprisingly, it is shared with the Ca^{2+}-activation pathway. Second, the inter-monomeric pathway connected the EF-hand loops with the S23* segment of the neighbor monomer *via* the interaction bridges. It was present in primed, open, and inactivated RyR1 structures. This inter-monomeric pathway used the S45 segment and the U-motif to reach the S6 segment with the channel gate. The existence of two inactivation pathways means that the binding of M^{2+} ion to the inhibition site at the RyR EF-hands leads to the channel inactivation by a direct effect on the channel

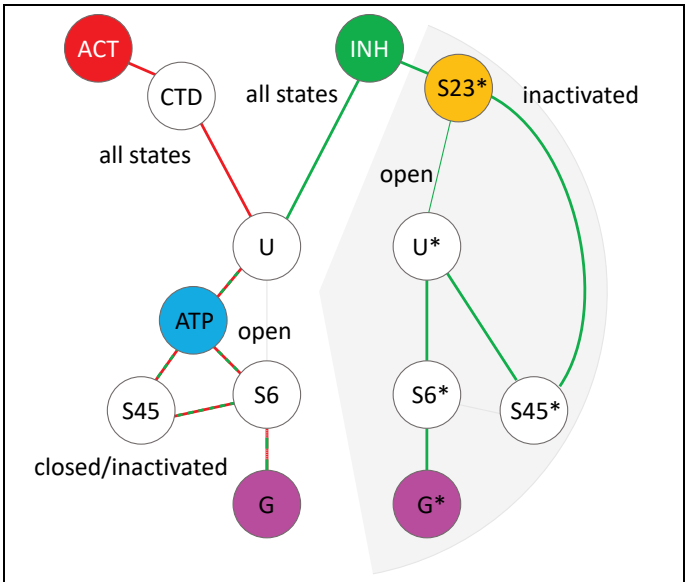

Fig. 3. The allosteric pathways of the RyR1 channel. Green - inhibition pathway; red – activation pathway. ACT – Ca^{2+} binding activation site; INH – M^{2+} binding inhibition site; CTD – C-terminal domain; U – U-motif; ATP – ATP binding site; S45 – the helix connecting S4 and S5 segments; S6 – gate-bearing segment; G – gate; * marks a neighbor monomer.

gate (i.e., directly decreasing the free energy of the inactivated state) and also by an interaction with the calcium activation pathway (i.e., decreasing the free energy of the inactivated state when Ca^{2+} is bound to the activation site)

In conclusion, we propose an allosteric mechanism of Ca^{2+}/Mg^{2+}-dependent activation/inactivation of RyR1. Our findings provide a deeper understanding of the control of RyR1 channels in calcium signalling of skeletal muscle cells.

Acknowledgments
This work was supported by the projects VEGA 2/0182/21 from the Scientific Grant Agency of the Slovak Academy of Sciences and APVV-21-0473 from the Slovak Research and Development Agency.

References
[1] A. des Georges, O. B. Clarke, R. Zalk; et al, Cell, 167 (2016), 145-157.
[2] Z. Melville, K. Kim, O. B. Clarke, A. R. Marks, Structure, 30 (2022) 172-180.
[3] Z. Melville, H. Dridi, Q. Yuan; et al, Structure, 30 (2022), 1025-1034.
[4] A. R. Nayak, M. Samso, eLife, 11 (2022), e75568.
[5] A. Sali, T. L. Blundell, J. Mol. Biol., 234 (1993), 779-815.
[6] J. Wang, A. Jain, L. R. McDonald; et al, Nat. Commun. 11 (2020), 3862.

11th Slovak Biophysical Symposium, High Tatras, June 12 – 14, 2024

Application of Raman microspectroscopy for the chemical analysis of fossilized tissues of the gigantic theropod Deinocheirus mirificus

G. Fabriciová[1], Z. Jurašeková[1] and M. Kundrát[2]

[1] *Department of Biophysics, Faculty of Science, P. J. Šafárik University, Jesenná 5, 040 01 Košice, Slovakia.*
[2] *Center for Interdisciplinary Biosciences, Technology and Innovation Park, P. J. Šafárik University, Jesenná 5, 040 01 Košice, Slovakia.*

e-mail: gabriela.fabricioval@upjs.sk

Raman microspectroscopy (RMS) is a nondestructive and noncontact analytical technique with the potential for noninvasive and in situ molecular identification in heterogeneous and rare samples, such as fossil tissues. RMS allows one to analyze the chemical composition and mineral arrangement affected by diagenetic processes in these tissues. In the present study, we have investigated the bone tissue and mineral residues found in the fossil bones of the giant ornithomimosaur Deinocheirus myrificus from the Upper Cretaceous of the Mongolian part of the Gobi basin.

The aim was to find some organic matter and identify mineral fillings in some Haversian canals of the cortical and cancellous tissue of the rib and tibia.

The measurements were performed with a Renishaw Raman inVia spectrometer equipped with a 785 nm laser line. The laser beam was focused through 20x and 50x microscope objectives.

The Raman spectra collected on the edge of the tibia reveal unexpected strong bands in the region of 1100–1700 cm-1 (Fig. 1a). In contrast, in the spectra collected closer to the center of the bone, only the apatite band is observed (Fig. 1b). This intriguing observation is likely due to diagenetic alteration during the fossilization process [1].

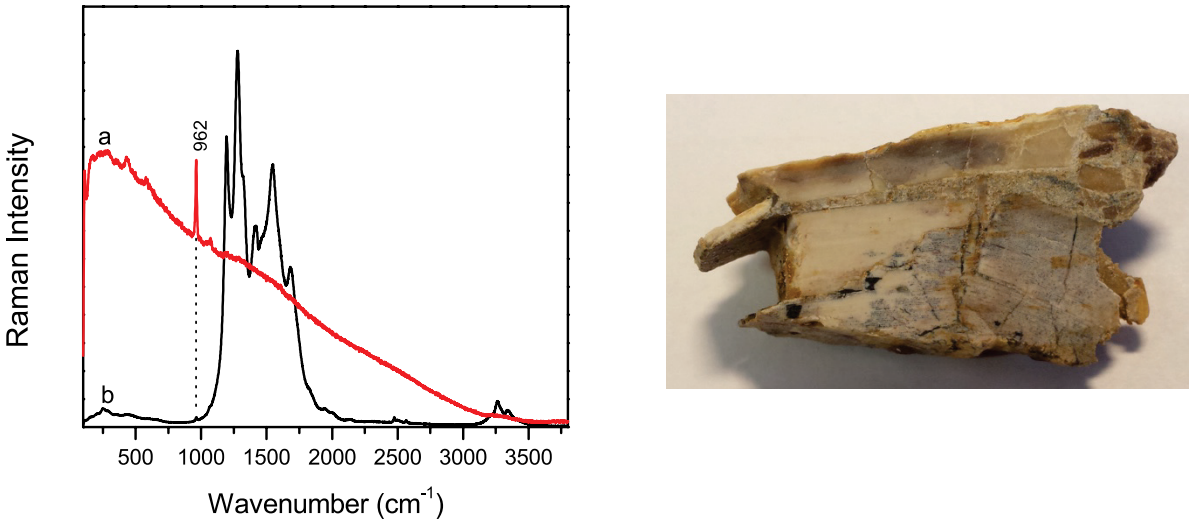

Fig. 1. The Raman spectra were collected (a) on the edge of the tibia and (b) closer to the center of the bone.

The Raman spectra were also obtained from the different infillings of the canals and cracks in the bones. Calcite was mainly present in the vascular canals of the bones (Fig. 2a). The Raman spectra taken from the dark brown infillings of vascular canals contain typical Raman bands of hematite (225, 294, 409, 612 cm-1) (Fig. 2b, c). The Raman spectra taken from the orange-brown infillings revealed the presence of goethite at 302, 394, and 551 cm-1) (Fig. 2c, d). The shapes and positions of the bands in the Raman spectra obtained from the black infillings of the canals and cracks of the bones indicate the presence of the manganese oxides, predominantly manganese oxides with structures similar to rancieite (Fig. 2e) and romanechite (Fig. 2f).

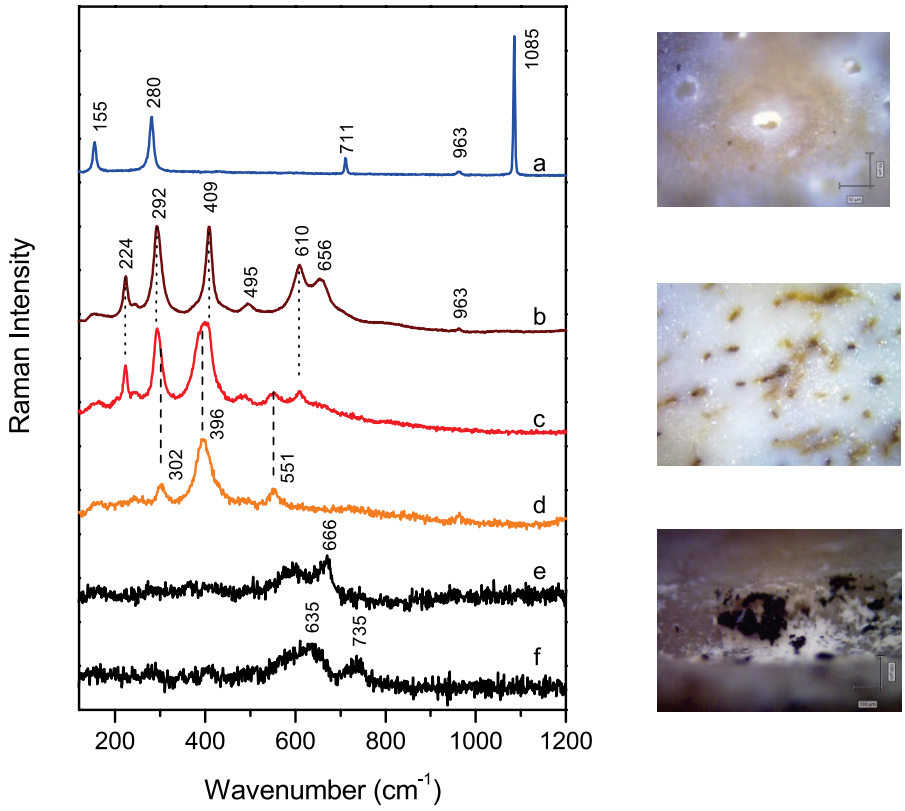

Fig. 2. Representative Raman spectra obtained from the different infillings of the vascular canals of Deinocheirus's tibia.

With the help of Raman microspectroscopy, it was possible to identify the minerals found in the Haversian canals and cracks in the bones. These minerals probably got into the bones during fossilization from the surrounding sediment.

Acknowledgement

This work was supported by APVV-21-0319 and VEGA 1/0075/22.

References

[1] Z. Jurašeková, G. Fabriciová, L. F. Silveira, Y.-N. Lee, J. M. Gutak, M. M. Ataabadi, M. Kundrát, International Journal of Molecular Science, 23 (2022), 10689.

11th Slovak Biophysical Symposium, High Tatras, June 12 – 14, 2024

Insulin Amyloid Aggregation: Effect of protein concentration

H. Kareem Abdul, Z. Bednáriková and Z. Gažová

Institute of Experimental Physics, Slovak Academy of Sciences, Watsonova 47, 040 01 Kosice, Slovakia.

e-mail: kareem@saske.sk

Insulin, a crucial peptide hormone for regulating blood sugar levels and treating diabetes, exhibits a propensity to form insoluble amyloid fibrils under various conditions, posing challenges in both industrial production and therapeutic administration.

This study investigates the aggregation dynamics of insulin at different protein concentrations under specific experimental conditions using half-volume 96-well plate design in a plate reader ClarioStar: 100 mM NaCl-HCl buffer (pH 1.6), elevated temperature (65°C), shaking at 700 rpm with two fluorescence reading intervals of 3 min and 10 min. The concentration of insulin varied from 10 to 300 μM. Using a combination of techniques including thioflavin T (ThT) fluorescence assay, atomic force microscopy (AFM), and circular dichroism (CD), we identified the conditions leading to amyloid fibril formation with high reproducibility and specific fibrils morphology.

Our findings confirmed relationship between insulin concentration and aggregation kinetics. Higher insulin concentrations formed critical nuclei more quickly, accelerating the fibrillization characterizing shorter lag phases. While the secondary structure content of fibrils remains approximately similar across all concentrations, increasing insulin concentrations result in longer and higher number of fibrils compared to lower concentration. We analysed the effect of shaking on aggregation by setting up fluorescence reading time intervals to 3 min and 10 min. The 10 min interval did not yield sufficient time points for kinetic curves analysis, leading us to repeat the experiment with a 3 min fluorescence reading interval. The 3 min interval provided enough data in elongation phase enhancing the accuracy and consistency of the sigmoidal growth curve. We have observed that different time of shaking significantly influenced the lag phase and half-time of the growth curves, with the 3 min interval resulting in a longer lag phase and half-time compared to the 10 min interval. These observations are important and must be taken in the account when setting up experimental conditions in the study of insulin amyloid fibrillization.

Based on the data obtained for different insulin concentration and shaking interval we can conclude that insulin with concentrations exceeding 50 μM consistently produced longer amyloid fibrils with high accuracy and reproducibility. For the kinetic experiments the most optimal insulin concentration is 75 μM at 3 min shaking (Fig. 1).

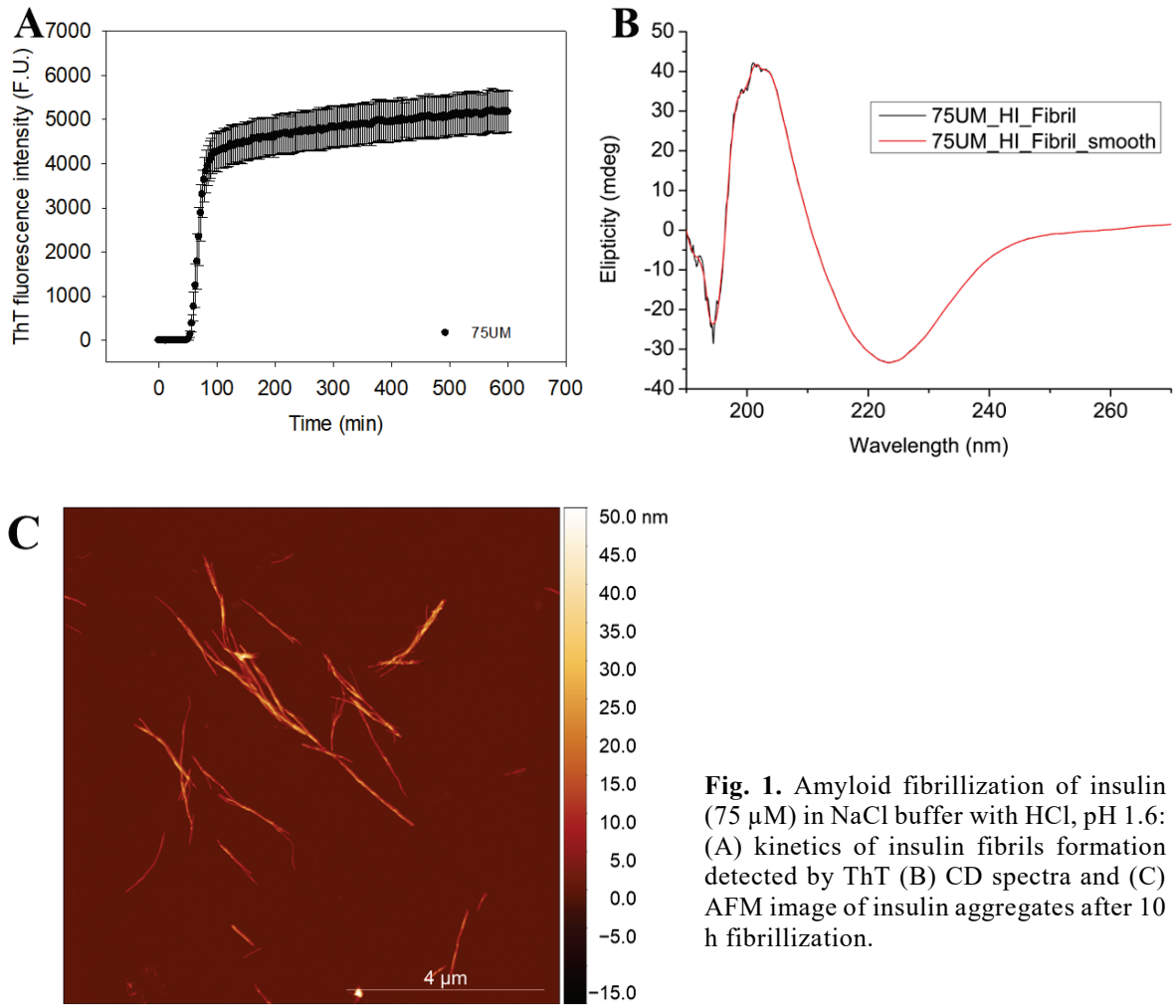

Fig. 1. Amyloid fibrillization of insulin (75 µM) in NaCl buffer with HCl, pH 1.6: (A) kinetics of insulin fibrils formation detected by ThT (B) CD spectra and (C) AFM image of insulin aggregates after 10 h fibrillization.

Acknowledgement
This work was supported by the Slovak Research and Development Agency under the contract No. APVV-22-0598; the Science Grant Agency VEGA 2/0176/21 and project from the call Plán obnovy R1-00039.

11th Slovak Biophysical Symposium, High Tatras, June 12 – 14, 2024

Correlation analysis of factors influencing blood flow and viscosity upon in vitro addition of dendron-based nanoparticles

P. Mydla[1], S. Suty[1], M. Ionov[2], K. Milowska[2], D. Shcharbin[3], J.-P. Majoral[4,5] M. Bryszewska[2] and I. Waczulikova[1]

[1] Department of Nuclear Physics and Biophysics, Faculty of Mathematics, Physics and Infomatics, Comenius University Bratislava, Mlynska dolina F1, 842 48 Bratislava, Slovakia .
[2] Department of General Biophysics, Faculty of Biology and Environmental Protection, University of Lodz, Narutowicza 68, 90-136 Lodz, Poland.
[3] Institute of Biophysics and Cell Engineering of the National Academy of Sciences of Belarus, Academicheskaya 27, 220072 Minsk, Belarus.
[4] Laboratoire de Chimie de Coordination du CNRS, 205 Route de Narbonne, CEDEX 4, 31077 Toulouse, France.
[5] Université Toulouse, 118 Route de Narbonne, CEDEX 4, 31077 Toulouse, France.

e-mail: patrick.mydla@fmph.uniba.sk

Nanoparticles are currently one of the intensively researched areas for medical applications. Several of them are already used in clinical practice, e. g. as carriers for drugs with high toxicity or as selective cytostatics themselves. For administration into the body, they must be encapsulated in liposomes or surface-modified, thereby controlling their interactions with their surroundings.

Nanoparticles can interact with other substances by specific and non-specific interactions. Non-specific physical interactions may be desirable - they are involved in passive targeting to the target cell or tissue, passage across barriers (e. g. successful gene transfer into the cell), and selective accumulation of nanoparticles in tumour tissue. However, non-specific interactions with tissues may also be the cause of adverse effects and toxicity of nanoparticles, which may be manifested e. g. after premature release of the nanomedicine from the complexes during transport through the blood.

In this context, it is important to evaluate the safety of nanoparticles/nanocomplexes in order to achieve hemocompatibility and desired activity. We have performed in vitro blood rheological studies coupled with the measurement of haematological and coagulation parameters. We designed an experimental model for intravenous administration of self-assembling dendron nanoparticles and dendrimers with pyrrolidine and piperidine end groups by adding them to a blood sample of healthy volunteers aged between 20 and 30 years. Simultaneous measurements of haematological and coagulation parameters, as well as rheometric measurements at different shear rates, were performed on these samples to simulate blood flow in different types of blood vessels in the body. In addition to the effect of shear rate, the experimental setup allowed us to observe the influence of three other factors - sex, concentration of nanoparticles applied, and generation (size) of the dendron (dendrimer) molecule.

Previous results [1, 2] show that the influence of dendrons leads to changes in the average values of platelet counts, clotting times and blood viscosity. In this work, using correlation analysis and modelling, we investigated the correlation between changes in a range of haematological and coagulation parameters and blood rheological properties as a function of the main factors (predictors).

By analysing heat maps, we observed changes in correlation coefficients between viscosity and coagulation parameters of blood. This suggests that the influence of individual experimental factors on the measured characteristics may not be independent and there may be an interaction between them. For sex, although we confirmed the additivity of the effect on viscosity, we do not exclude a more complex picture of the influence of haematological and coagulation parameters, which may modify the influence of factors on viscosity. The increase in blood viscosity may be due to two effects: a) the observed platelet clumps, b) changes in hematologic-coagulation parameters

that indicate activation of some links of the coagulation cascade. We observed a non-linear dependence of the viscosity increase on dendron (dendrimer) concentration, which may be due to the interaction between concentration, generation and type of dendritic nanoparticles. All factors influence the self-assembly of dendrons in polar (aqueous) environments into micellar formations of different shapes and sizes. Thus, it can be explained that stronger effects were observed for dendrons than for dendrimers, since dendrimers are purposefully prepared molecules with a known structure.

The most pronounced changes in viscosity were observed at low shear rates and in males; however, based on expert judgment by an experienced haematologist, the observed changes did not reach clinical significance. Areas predicting significant increases in viscosity were also observed when modelling the interrelationships between viscosity and coagulation factors in the experimental subgroups using surface and contour plots. This highlights the possibility that some combinations of input factors may lead to a more complex picture of changes in haematological, coagulation and rheological parameters and influence blood function and flow properties.

The correlation analysis can improve our understanding of the complex interplay between blood counts, coagulation indices, viscosity and flow properties after adding nanoparticles. Based on our results, we conclude that the dendrons and dendrimers in the concentrations used by us have sufficient blood tolerability. However, the nonlinearity and non-monotonicity of the correlations between haematological, coagulation and rheological parameters after simulated intravenous administration of nanoparticles may complicate the prediction of adverse effects at higher concentrations. These effects need to be further investigated.

Acknowledgement

The research was supported by NAWA Europartner PPI/APM/2018/1/00007/U/001, APVV-SK-BY-RD-19-0019, APVV-22-0154 and UK/1175/2024 projects.

References

[1] S. Suty, V. Oravczova, Z. Garaiova, V. Subjakova, M. Ionov, D. Shcharbin, Z. Simonikova, P. Bartek, M. Zvarik, X. Shi, S. Mignani, J.-P. Majoral, M. Bryszewska, T. Hianik, I. Waczulikova, Biomedicines, 11 (2021), 1672.

[2] M. Veliskova, M. Zvarik, S. Suty, J. Jacko, P. Mydla, K. Cechova, D. Dzubinska, M. Morvova, M. Ionov, M. Terehova, J.-P. Majoral, M. Bryszewska, I. Waczulikova, Pharmaceutics, 8 (2022), 1596.

In silico peptide design to disable the p53 pathway.

Exequiel E. Barrera

Instituto de Histología y Embriología Mendoza (CONICET), Av. Del Libertador 80, Mendoza, Argentina.

e-mail: ebarrera@mendoza-conicet.gob.ar

See page 45.

AUTHOR INDEX

Abdul Kareem H.	PO27	Grman M.	PO11, PO12
Ambro Ľ.	PO20	Horák D.	SC10
Antošová A.	SC6	Horáková L.	PO15
Baglaeva I.	PO3	Horváth A.	PO12
Balážová M.	PO13	Horváth D.	PO23
Barrera E. E.	SC7, PO18, PO29	Hovan A.	AW2, SC5, PO1
Bánó G.	AW2, SC10, PO1, PO14	Hovanová V.	SC5
Bednáriková Z.	SC8, PO2, PO27	Hovengen O.J.	SC2
Belous A.	PO10	Humenik M.	SC5, PO5
Beriková D.	SC2	Hunáková Ľ.	PO16
Bitter Fialová S.	PO9	Huntošová V.	SC1, PO21, PO23
Bryszewska M.	PO28	Chorvát D.	SC9
Bustos D.M.	PO17	Iaparov B.	PO3
Cagalinec M.	PO3	Ionov M.	PO28
Cehlár O.	PO2, PO18, PO19	Jacko J.	PO13
Cibulková L.	SC14	Jancura D.	PO7, PO22
Černík M.	CP1	Jurašeková Z.	SC10, PO7, PO23, PO26
Datta S.	PO4, PO21	Jutková A.	PO1
Dokupilová S.	PO9	Kania P.	CP3
Drajnová M.	PO10	Klacsová M.	SC12
Eliaš D.	PO13	Kollárik B.	PO16
Fabián M.	PO22	Králiková O.	SC14
Fabriciová G.	PO26	Krejčíová E.	PO8
Fedorová V.	PO5	Kronek J.	PO4, PO21
Fedunová D.	PO6	Kubacková J.	PO14
Felčíková K.	AW2	Kundrát M.	PO26
Fontana L.I.	PO17	Kurin E.	PO9
Fuenzalida F. Belén	PO7	Lermak I.	CP1
Gaburjáková J.	SC3, PO8	Levík J.	PO21
Gaburjáková M.	SC3, PO8	Majoral J.-P.	PO28
Gančár M.	SC6, PO9	Marček Chorvátová A.	SC9
Garčárova I.	PO10	Marek J.	SC6
Gažová Z.	SC6, PO2, PO6, PO9, PO27	Marrabini R.	CP2
Gbelská Y.	PO13	Martvoň L.	SC1, SC2

LIST OF CONTRIBUTORS

1	Abdul Kareem Hanan	Department of Biophysics, Institute of Experimental Physics, Slovak Academy of Sciences, Watsonova 47, 040 01 Košice, Slovakia.
2	Ambro Ľuboš	Center for Interdisciplinary Biosciences, Technology and Innovation Park, P. J. Šafárik University, Jesenná 5, 040 01 Košice, Slovakia.
3	Antošová Andrea	Department of Biophysics, Institute of Experimental Physics, Slovak Academy of Sciences, Watsonova 47, 040 01 Košice, Slovakia.
4	Baglaeva Iuliia	Department of Cellular Cardiology, Institute of Experimental Endocrinology, Biomedical Research Center, Slovak Academy of Sciences, Dúbravská cesta 9, 845 05 Bratislava, Slovakia.
5	Balážová Mária	Institute of Animal Biochemistry and Genetics, Centre of Biosciences, Slovak Academy of Sciences, Dúbravská cesta 9, P.O.BOX 63, 840 05 Bratislava, Slovakia.
6	Barrera Exequiel Ernesto	Institute of Histology and Embryology of Mendoza "Dr. Mario H. Burgos", CONICET – National University of Cuyo, Av. Del Libertador 80, Mendoza, Argentina.
7	Bánó Gregor	Department of Biophysics, Faculty of Science, P. J. Šafárik University, Jesenná 5, 040 01 Košice, Slovakia.
8	Bednáriková Zuzana	Department of Biophysics, Institute of Experimental Physics, Slovak Academy of Sciences, Watsonova 47, 040 01 Košice, Slovakia.
9	Belous Anatolii	V. I. Vernadsky Institute of General & Inorganic Chemistry, NAS of Ukraine, Kyiv, Ukraine.
10	Beriková Denisa	Department of Medical Biophysics, Jessenius Faculty of Medicine in Martin, Comenius University in Bratislava, Mala Hora 4, 036 01 Bratislava, Slovakia.
11	Bernátová Soňa	Merck LifeScience spol.s r.o., Dvořákovo nábrežie 4, 810 06 Bratislava, Slovakia.
12	Bitter Filaová Silvia	Faculty of Pharmacy, Comenius University Bratislava, Odbojárov 10, 832 32 Bratislava, Slovakia.

13	Bryszewska Maria	Department of General Biophysics, Faculty of Biology and Environmental Protection, University of Lodz, Narutowicza 68, 90-136 Lodz, Poland.
14	Bustos Diego Martín	Laboratorio de Integración de Señales Celulares, IHEM, CONICET – National University of Cuyo, Mendosa, Argentina.. FCEN, National University of Cuyo, Mendoza, Argentina.
15	Cagalinec Michal	Department of Cellular Cardiology, Institute of Experimental Endocrinology, Biomedical Research Center, Slovak Academy of Sciences, Dúbravská cesta 9, 845 05 Bratislava, Slovakia. Centre of Excellence for Advanced Material Application, Slovak Academy of Sciences, Štefánikova 49, 811 04 Bratislava, Slovakia.
16	Cehlár Ondrej	Institute of Neuroimmunology, Slovak Academy of Sciences, Dúbravská cesta 9, 845 10 Bratislava, Slovakia.
17	Cibulková Lucia	Department of Medical Biophysics, Jessenius Faculty of Medicine in Martin, Comenius University in Bratislava, Malá Hora 4, 036 01 Bratislava, Slovakia.
18	Černík Marek	Uni-Export Instruments, s.r.o., Šultysova 15, 169 00 Prague 6 Czech Republic.
19	Datta Shubhashis	Center for Interdisciplinary Biosciences, Technology and Innovation Park, P. J. Šafárik University, Jesenná 5, 040 01 Košice, Slovakia.
20	Dokupilová Svetlana	Faculty of Pharmacy, Comenius University Bratislava, Odbojárov 10, 832 32 Bratislava, Slovakia.
21	Drajnová Michaela	Department of Biophysics, Institute of Experimental Physics, Slovak Academy of Sciences, Watsonova 47, 040 01 Košice, Slovakia. Department of Biochemistry, Institute of Chemistry, Faculty of Science, P. J. Šafárik University, Jesenná 5, 040 01 Košice, Slovakia.
22	Eliaš Daniel	Faculty of Natural sciences, Comenius University, Ilkovičova 6, 842 48 Bratislava, Slovakia.

23	Fabián Marián	Center for Interdisciplinary Biosciences, Technology and Innovation Park, P. J. Šafárik University, Jesenná 5, 040 01 Košice, Slovakia.
24	Fabriciová Gabriela	Department of Biophysics, Faculty of Science, P. J. Šafárik University, Jesenná 5, 040 01 Košice, Slovakia.
25	Fedorová Viktória	Department of Biophysics, Institute of Experimental Physics, Slovak Academy of Sciences, Watsonova 47, 040 01 Košice, Slovakia.
26	Fedunová Diana	Department of Biophysics, Institute of Experimental Physics, Slovak Academy of Sciences, Watsonova 47, 040 01 Košice, Slovakia.
27	Felčíková Kristína	Department of Biophysics, Faculty of Science, P. J. Šafárik University, Jesenná 5, 040 01 Košice, Slovakia.
28	Fontana Lorena Ines	Laboratorio de Integración de Señales Celulares, IHEM, CONICET – National University of Cuyo, Mendosa, Argentina.
29	Fuenzalida Sandoval Francisca Belén	Department of Biophysics, Faculty of Science, P. J. Šafárik University, Jesenná 5, 040 01 Košice, Slovakia.
30	Gaburjáková Jana	Institute of Molecular Physiology and Genetics, Centre of Biosciences, Slovak Academy of Sciences, Dúbravská cesta 9, 840 05 Bratislava, Slovakia.
31	Gaburjáková Marta	Institute of Molecular Physiology and Genetics, Centre of Biosciences, Slovak Academy of Sciences, Dúbravská cesta 9, 840 05 Bratislava, Slovakia.
32	Gančár Miroslav	Department of Biophysics, Institute of Experimental Physics, Slovak Academy of Sciences, Watsonova 47, 040 01 Košice, Slovakia.
33	Garčárová Ivana	Department of Biophysics, Institute of Experimental Physics, Slovak Academy of Sciences, Watsonova 47, 040 01 Košice, Slovakia.
34	Gažová Zuzana	Department of Biophysics, Institute of Experimental Physics, Slovak Academy of Sciences, Watsonova 47, 040 01 Košice, Slovakia.
35	Gbelská Yvetta	Faculty of Natural sciences, Comenius University, Ilkovičova 6, 842 48 Bratislava, Slovakia.

36	Grman Marián	Biomedical Research Center, Slovak Academy of Sciences, Dúbravská cesta 9, 845 05 Bratislava, Slovakia.
37	Horáková Ľubica	Centre of Experimental Medicine Institute of Experimental Pharmacology and Toxicology, Slovak Academy of Sciences, Dúbravská cesta 9, 841 04 Bratislava, Slovakia.
38	Horák Daniel	Institute of Macromolecular Chemistry, Czech Academy of Sciences, Heyrovského nám. 2, 162 06 Prague, Czech Republic.
39	Horváth Anton	Faculty of Natural Sciences Comenius University, Ilkovičova 6, 842 48 Bratislava, Slovakia.
40	Horváth Denis	Center for Interdisciplinary Biosciences, Technology and Innovation Park, P. J. Šafárik University, Jesenná 5, 040 01 Košice, Slovakia.
41	Hovan Andrej	Department of Biophysics, Faculty of Science, P. J. Šafárik University, Jesenná 5, 040 01 Košice, Slovakia.
42	Hovanová Veronika	Center for Interdisciplinary Biosciences, Technology and Innovation Park, P. J. Šafárik University, Jesenná 5, 040 01 Košice, Slovakia. Department of Biophysics, Faculty of Science, P. J. Šafárik University, Jesenná 5, 040 01 Košice, Slovakia.
43	Hovengen Ole Jacob	Department of Medical Biophysics, Jessenius Faculty of Medicine in Martin, Comenius University in Bratislava, Malá Hora 4, 036 01 Bratislava, Slovakia.
44	Humenik Martin	Department of Biomaterials, Faculty of Engineering Science, University of Bayreuth, Germany.
45	Hunáková Ľuba	Institute of Immunology, Faculty of Medicine, Comenius University, Odborárske námestie 14, 811 08 Bratislava, Slovakia.
46	Huntošová Veronika	Center for Interdisciplinary Biosciences, Technology and Innovation Park, P. J. Šafárik University, Jesenná 5, 040 01 Košice, Slovakia. Institute of Animal Biochemistry and Genetics, Centre of Biosciences, Slovak Academy of Sciences, Dúbravská cesta 9, 840 05 Bratislava, Slovakia.

47	Chorvát Dušan	Department of Biophotonics, International Laser Center, Slovak Centre of Scientific and Technical Information, Ilkovičova 3, 814 04 Bratislava, Slovakia.
48	Iaparov Bogdan	Department of Cellular Cardiology, Institute of Experimental Endocrinology, Biomedical Research Center, Slovak Academy of Sciences, Dúbravská cesta 9, 845 05 Bratislava, Slovakia.
49	Ionov Maksim	Department of General Biophysics, Faculty of Biology and Environmental Protection, University of Lodz, Narutowicza 68, 90-136 Lodz, Poland.
50	Iermak Ievgeniia	WITec GmbH, Oxford Instruments Group, Lise-Meitner-Str. 6, Ulm, Germany.
51	Jacko Juraj	Department of Nuclear Physics and Biophysics, Faculty of Mathematics, Physics and Informatics, Comenius University, Mlynská dolina F1, 842 48 Bratislava, Slovakia.
52	Jancura Daniel	Department of Biophysics, Faculty of Science, P. J. Šafárik University, Jesenná 5, 040 01 Košice, Slovakia.
53	Jurašeková Zuzana	Department of Biophysics, Faculty of Science, P. J. Šafárik University, Jesenná 5, 040 01 Košice, Slovakia.
54	Jutková Annamária	SAFTRA Photonics Ltd., Moldavská 51, 040 11 Košice, Slovakia.
55	Kania Pawel	NanoTemper Technologies spzoo, Bobrzynskiego 14, 30-348 Krakow, Poland.
56	Klacsová Mária	Department of Physical Chemistry of Drugs, Faculty of Pharmacy, Comenius University, Odbojárov 10, 832 32 Bratislava, Slovakia.
57	Kollárik Boris	Department of Urology, Saints Cyril and Methodius Hospital, University Hospital Bratislava, Antolská 11, 851 07 Bratislava, Slovakia.
58	Králiková Oľga	Department of Medical Biophysics, Jessenius Faculty of Medicine in Martin, Comenius University in Bratislava, Mala Hora 4, 036 01 Bratislava, Slovakia.
59	Krejčíová Eva	Institute of Molecular Physiology and Genetics, Centre of Biosciences, Slovak Academy of Sciences, Dúbravská cesta 9, 840 05 Bratislava, Slovakia.

60	Kronek Juraj	Department for Biomaterials Research, Polymer Institute, Slovak Academy of Sciences, Dúbravska cesta 9, 845 41 Bratislava, Slovakia.
61	Kubacková Jana	Department of Biophysics, Institute of Experimental Physics, Slovak Academy of Sciences, Watsonova 47, 040 01 Košice, Slovakia.
62	Kundrát Martin	Center for Interdisciplinary Biosciences, Technology and Innovation Park, P. J. Šafárik University, Jesenná 5, 040 01 Košice, Slovakia.
63	Kurin Elena	Faculty of Pharmacy, Comenius University Bratislava, Odbojárov 10, 832 32 Bratislava, Slovakia.
64	Levík Jaroslav	Institute of Animal Biochemistry and Genetics, Centre of Biosciences, Slovak Academy of Sciences, Dúbravská cesta 9, 840 05 Bratislava, Slovakia.
65	Majoral Jean-Pierre	Laboratoire de Chimie de Coordination du CNRS, 205 Route de Narbonne, CEDEX 4, 31077 Toulouse, France. Université Toulouse, 118 Route de Narbonne, CEDEX 4, 31077 Toulouse, France.
66	Marček Chorvátová Alžbeta	Department of Biophotonics, International Laser Center SCSTI, Slovak Centre of Scientific and Technical Information, Ilkovičova 3, 814 04 Bratislava, Slovakia.
67	Májeková Magdaléna	Centre of Experimental Medicine Institute of Experimental Pharmacology and Toxicology, Slovak Academy of Sciences, Dúbravská cesta 9, 841 04 Bratislava, Slovakia.
68	Marek Jozef	Department of Biophysics, Institute of Experimental Physics, Slovak Academy of Sciences, Watsonova 47, 040 01 Košice, Slovakia.
69	Marrabini Riccardo	FIDA biosystems ApS, Generatorvej 6, 2860 Søborg, Denmark.
70	Martvoň Lukáš	Medical Education Support Center, Jessenius Faculty of Medicine in Martin, Comenius University in Bratislava, L. Novomeského 7A, 036 01 Martin, Slovakia.
71	Masarovičová Dominika	Department of Nuclear Physics and Biophysics, Faculty of Mathematics, Physics and Informatics, Comenius University, Mlynská dolina F1, 842 48 Bratislava, Slovakia.

72	Mateašík Anton	Department of Biophotonics, International Laser Center, Slovak Centre of Scientific and Technical Information, Ilkovičova 3, 814 04 Bratislava, Slovakia.
73	Máčajová Mariana	Institute of Animal Biochemistry and Genetics, Centre of Biosciences, Slovak Academy of Sciences, Dúbravská cesta 9, 840 05 Bratislava, Slovakia.
74	Mešková Klaudia	Institute of Neuroimmunology, Slovak Academy of Sciences, Dúbravská cesta 9, 845 10 Bratislava, Slovakia.
75	Mikolášková Iveta	Institute of Immunology, Faculty of Medicine, Comenius University, Odborárske námestie 14, 811 08 Bratislava, Slovakia.
76	Miłowska Katarzyna	Department of General Biophysics, Faculty of Biology and Environmental Protection, University of Lodz, Narutowicza 68, 90-136 Lodz, Poland.
77	Mirza Nadia	FIDA biosystems ApS, Generatorvej 6, 2860 Søborg, Denmark.
78	Misek Jakub	Department of Medical Biophysics, Jessenius Faculty of Medicine in Martin, Comenius University in Bratislava, Mala Hora 4, 036 01 Bratislava, Slovakia.
79	Mišák Anton	Biomedical Research Center, Slovak Academy of Sciences, Dúbravská cesta 9, 845 05 Bratislava, Slovakia.
80	Miškovský Pavol	Center for Interdisciplinary Biosciences, Technology and Innovation Park, P. J. Šafárik University, Jesenná 5, 040 01 Košice, Slovakia. SAFTRA Photonics Ltd., Moldavská 51, 040 11 Košice, Slovakia.
81	Morvová Marcela ml.	Department of Nuclear Physics and Biophysics, Faculty of Mathematics, Physics and Informatics, Comenius University, Mlynská dolina F1, 842 48 Bratislava, Slovakia.
82	Musatov Andrej	Department of Biophysics, Institute of Experimental Physics, Slovak Academy of Sciences, Watsonova 47, 040 01 Košice, Slovakia.
83	Müller Sergio	Laboratorio de Integración de Señales Celulares, IHEM, CONICET – National University of Cuyo, Mendosa, Argentina..

84	Mydla Patrick	Department of Nuclear Physics and Biophysics, Faculty of Mathematics, Physics and Informatics, Comenius University, Mlynská dolina F1, 842 48 Bratislava, Slovakia.
85	Naďová Zuzana	Department of Biophysics, Faculty of Science, P. J. Šafárik University, Jesenná 5, 040 01 Košice, Slovakia.
86	Nagy Milan	Faculty of Pharmacy, Comenius University Bratislava, Odbojárov 10, 832 32 Bratislava, Slovakia.
87	Njemoga Stefana	Institute of Neuroimmunology, Slovak Academy of Sciences, Dúbravská cesta 9, 845 10 Bratislava, Slovakia. Faculty of Natural sciences, Comenius University, Ilkovičova 6, 842 48 Bratislava, Slovakia.
88	Olejárová Soňa	Department of Biophysics, Faculty of Science, P. J. Šafárik University, Jesenná 5, 040 01 Košice, Slovakia.
89	Ondáčová Katarína	Centre of Biosciences, Slovak Academy of Sciences, Dúbravská cesta 9, 840 05 Bratislava, Slovakia.
90	Ondriaš Karol	Biomedical Research Center, Slovak Academy of Sciences, Dúbravská cesta 9, 845 05 Bratislava, Slovakia.
91	Patsula Vitalii	Institute of Macromolecular Chemistry, Czech Academy of Sciences, Heyrovského nám. 2, 162 06 Prague, Czech Republic.
92	Pavelková Jana	Department of Cellular Cardiology, Institute of Experimental Endocrinology, Biomedical Research Center, Slovak Academy of Sciences, Dúbravská cesta 9, 845 05 Bratislava, Slovakia.
93	Polák Adam	Institute of Neuroimmunology, Slovak Academy of Sciences, Dúbravská cesta 9, 845 10 Bratislava, Slovakia.
94	Polčicová Katarína	Biomedical Research Center, Slovak Academy of Sciences, Dúbravská cesta 9, 845 05 Bratislava, Slovakia.
95	Poliaček Ivan	Department of Medical Biophysics, Jessenius Faculty of Medicine in Martin, Comenius University in Bratislava, Malá Hora 4, 036 01 Bratislava, Slovakia.
96	Repovská Mária	SAFTRA Photonics Ltd., Moldavská 51, 040 11 Košice, Slovakia.

97	Rezbáriková Petronela	Centre of Experimental Medicine, Institute of Experimental Pharmacology and Toxicology, Slovak Academy of Sciences, Dúbravská cesta 9, 841 04 Bratislava, Slovakia.
98	Rivera Lautaro	Laboratorio de Integración de Señales Celulares, IHEM, CONICET – National University of Cuyo, Mendosa, Argentina..
99	Sánchez-Cortés Santiago	Institute of the Structure of Matter, IEM-CSIC, Serrano 121, 28006 Madrid, Spain.
100	Sedlák Erik	Center for Interdisciplinary Biosciences, Technology and Innovation Park, P. J. Šafárik University, Jesenná 5, 040 01 Košice, Slovakia. Department of Biochemistry, Faculty of Science, P. J. Šafárik University, Moyzesova 11, 040 01 Košice,Slovakia.
101	Shlapa Yuliia	V.I. Vernadsky Institute of General & Inorganic Chemistry of the NAS of Ukraine, Kyiv, Ukraine.
102	Shcharbin D.	Institute of Biophysics and Cell Engineering of the National Academy of Sciences of Belarus, Academicheskaya 27, 220072 Minsk, Belarus.
103	Slabý Cyril	Department of Biophysics, Faculty of Science, P. J. Šafárik University, Jesenná 5, 040 01 Košice, Slovakia.
104	Slepčíková Paulína	SAFTRA Photonics Ltd., Moldavská 51, 040 11 Košice, Slovakia.
105	Spiwok Vojtěch	Department of Biochemistry and Microbiology, University of Chemistry and Technology, Technická 1903/3, 160 00 Prague, Czech Republic.
106	Staničová Jana	Department of Chemistry, Biochemistry and Biophysics, University of Veterinary Medicine and Pharmacy, Komenského 73, 041 81 Košice, Slovakia. Institute of Biophysics and Informatics, First Faculty of Medicine, Charles University, Salmovská 1, 120 00 Prague, Czech Republic.
107	Sutý Šimon	Department of Nuclear Physics and Biophysics, Faculty of Mathematics, Physics and Informatics, Comenius University, Mlynská dolina F1, 842 48 Bratislava, Slovakia.

108	Štepanovský Jakub	Faculty of Chemical and Food Technology STU, Radlinského 9, 812 37 Bratislava, Slovakia.
109	Strejčková Alena	Department of Chemistry, Biochemistry and Biophysics, University of Veterinary Medicine and Pharmacy, Komenského 73, 041 81 Košice, Slovakia.
110	Ševčíková Tomášková Zuzana	Centre of Biosciences, Slovak Academy of Sciences, Dúbravská cesta 9, 845 05 Bratislava, Slovakia.
111	Šikurová Libuša	Department of Nuclear Physics and Biophysics, Faculty of Mathematics, Physics and Informatics, Comenius University, Mlynská dolina F1, 842 48 Bratislava, Slovakia.
112	Šimera Michal	Department of Medical Biophysics, Jessenius Faculty of Medicine in Martin, Comenius University in Bratislava, Malá Hora 4, 036 01 Bratislava, Slovakia.
113	Šipošová Katarína	Department of Biophysics, Institute of Experimental Physics, Slovak Academy of Sciences, Watsonova 47, 040 01 Košice, Slovakia.
114	Škrabana Rostislav	Institute of Neuroimmunology, Slovak Academy of Sciences, Dúbravská cesta 9, 845 10 Bratislava, Slovakia.
115	Štroffeková Katarína	Department of Biophysics, Faculty of Science, P. J. Šafárik University, Jesenná 5, 040 01 Košice, Slovakia.
116	Štulajterová Monika	Department of Biophysics, Faculty of Science, P. J. Šafárik University, Jesenná 5, 040 01 Košice, Slovakia.
117	Timuľáková Ľudmila	Department of Biophysics, Faculty of Science, P. J. Šafárik University, Jesenná 5, 040 01 Košice, Slovakia.
118	Tomášová Lenka	Biomedical Research Center, Slovak Academy of Sciences, Dúbravská cesta 9, 845 05 Bratislava, Slovakia.
119	Tomková Adriána	Department of Biophysics, Institute of Experimental Physics Slovak Academy of Sciences, Watsonova 47, 040 01, Košice, Slovakia.
120	Tomková Mária	Center for Interdisciplinary Biosciences, Technology and Innovation Park, P. J. Šafárik University, Jesenná 5, 040 01 Košice, Slovakia.

121	Tomori Zoltán	Department of Biophysics, Institute of Experimental Physics, Slovak Academy of Sciences, Watsonova 47, 040 01 Košice, Slovakia.
122	Tóth-Hervay Nora	Faculty of Natural sciences, Comenius University, Ilkovičova 6, 842 48 Bratislava, Slovakia.
123	Uhart Marina	Laboratorio de Integración de Señales Celulares, IHEM, CONICET – National University of Cuyo, Mendosa, Argentina..
124	Uherek Martin	Department of Biophotonics, International Laser Center, Slovak Centre of Scientific and Technical Information, Ilkovičova 3, 814 04 Bratislava, Slovakia.
125	Uhríková Daniela	Department of Physical Chemistry of Drugs, Faculty of Pharmacy, Comenius University, Odbojárov 10, 832 32 Bratislava, Slovakia.
126	Uskoba Jozef	BioTech a.s., Služeb 4, 108 00 Prague 10, Czech Republic.
127	Vaník Vladimír	Department of Biophysics, Institute of Experimental Physics, Slovak Academy of Sciences, Watsonova 47, 040 01 Košice, Slovakia.
128	Varchol Bianka Gizela	Department of Biophysics, Faculty of Science, P. J. Šafárik University, Jesenná 5, 040 01 Košice, Slovakia.
129	Vasylyshyn Taras	Institute of Macromolecular Chemistry, Czech Academy of Sciences, Heyrovského nám. 2, 162 06 Prague, Czech Republic.
130	Velísková Martina	Department of Nuclear Physics and Biophysics, Faculty of Mathematics, Physics and Informatics, Comenius University, Mlynská dolina F1, 842 48 Bratislava, Slovakia.
131	Verebová Valéria	Department of Chemistry, Biochemistry and Biophysics, University of Veterinary Medicine and Pharmacy, Komenského 73, 041 81 Košice, Slovakia.
132	Veterník Marcel	Department of Medical Biophysics, Jessenius Faculty of Medicine in Martin, Comenius University in Bratislava, Malá Hora 4, 036 01 Bratislava, Slovakia.
133	Viskupičová Jana	Centre of Experimental Medicine Institute of Experimental Pharmacology and Toxicology, Slovak Academy of Sciences, Dúbravská cesta 9, 841 04 Bratislava, Slovakia.

134	Višňovcová Nadežda	Department of Medical Biophysics, Jessenius Faculty of Medicine in Martin, Comenius University in Bratislava, Malá Hora 4, 036 01 Bratislava, Slovakia.
135	Zahradník Ivan	Department of Cellular Cardiology, Institute of Experimental Endocrinology, Biomedical Research Center, Slovak Academy of Sciences, Dúbravská cesta 9, 845 05 Bratislava, Slovakia.
136	Zahradníková ml. Alexandra	Department of Cellular Cardiology, Institute of Experimental Endocrinology, Biomedical Research Center, Slovak Academy of Sciences, Dúbravská cesta 9, 845 05 Bratislava, Slovakia.
137	Zahradníková Alexandra	Department of Cellular Cardiology, Institute of Experimental Endocrinology, Biomedical Research Center, Slovak Academy of Sciences, Dúbravská cesta 9, 845 05 Bratislava, Slovakia.
138	Zvarík Milan	Department of Nuclear Physics and Biophysics, Faculty of Mathematics, Physics and Informatics, Comenius University, Mlynská dolina F1, 842 48 Bratislava, Slovakia.
139	Žoldák Gabriel	Center for Interdisciplinary Biosciences, Technology and Innovation Park, P. J. Šafárik University, Jesenná 5, 040 01 Košice, Slovakia.
140	Waczulikova Iveta	Department of Nuclear Physics and Biophysics, Faculty of Mathematics, Physics and Informatics, Comenius University, Mlynská dolina F1, 842 48 Bratislava, Slovakia.
141	Wardega Piotr	NanoTemper Technologies spzoo, Bobrzynskiego 14, 30-348 Krakow, Poland.

Book of Contributions, 11th Slovak Biophysical Symposium, June 12 – 14, 2024, High Tatras, Slovakia

Editors: Z. Gažová, A. Antošová, J. Kubacková
Reviewers: M. Fabián, D. Fedunová, D. Jancura, I. Poliaček, J. Staničová
Number of pages: 131

ISBN: 978-80-973719-5-1
EAN: 9788097371951

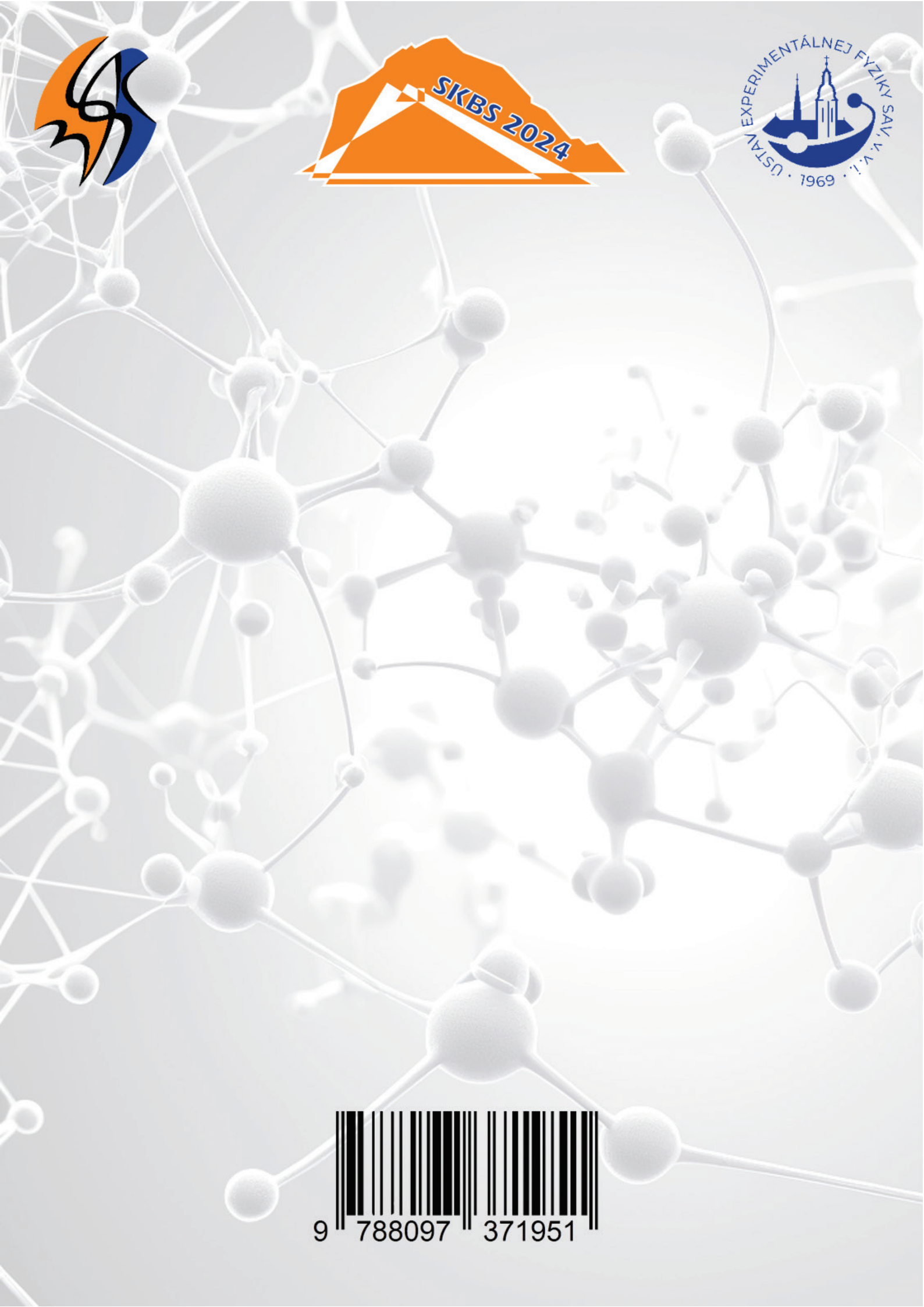

9 788097 371951